Preliminary Assessment of Seawater Intrusion in Phuket Island, Thailand

Sakanann VANN

A Thesis Submitted in Fulfillment of the Requirements for the Degree of Master of Science in Earth System Science

Prince of Songkla University

2018

Preliminary Assessment of Seawater Intrusion in Phuket Island, Thailand

Sakanann VANN

A Thesis Submitted in Fulfillment of the Requirements for the Degree of Master of Science in Earth System Science

Prince of Songkla University

2018

Thesis Title	Preliminary Assessment of Seawater Intrusion in Phuket Island, Thailand
Author	Mr. Sakanann VANN
Major Program	Earth System Science

Major Advisor

……
(Dr. Avirut Puttiwongrak)

Co-advisor

……
(Assoc. Prof. Dr. Pham Huy Giao)

Examining Committee:

……Chairperson
(Prof. Dr. Piti Sukontasukkul)

……Committee
(Dr. Avirut Puttiwongrak)

……Committee
(Assoc. Prof. Dr. Pham Huy Giao)

……Committee
(Dr. Kritana Prueksakon)

……Committee
(Dr. Tanwa Arpornthip)

The Graduate School, Prince of Songkla University, has approved this thesis as fulfillment of the requirements for the Master of Science Degree in Earth System Science

……
(Prof. Dr. Damrongsak Faroongsarng)
Dean of Graduate School

This is to certify that the work here submitted is the result of the candidate's own investigations. Due acknowledgment has been made of any assistance received.

.....Signature
(Dr. Avirut Puttiwongrak)
Major Advisor

.....Signature
(Mr. Sakanann VANN)
Candidate

I hereby certify that this work has not been accepted in substance for any degree, and is not being currently submitted in candidature for any degree.

.....Signature

(Mr. Sakanann VANN)

Candidate

Thesis Title Preliminary Assessment of Seawater Intrusion in Phuket Island, Thailand
Author Mr. Sakanann VANN
Major Program Earth System Science
Academic Year 2017

ABSTRACT

Seawater intrusion can gradually cause a severe problem by contaminating freshwater aquifers and causing a lack of fresh water. Coastal areas of Phuket Island are under risk of seawater intrusion due to many factors, e.g., sea level rise, over-use of groundwater, and so on. The main purpose of this study was to assess the seawater intrusion problem, which refers to the encroachment of seawater into underground freshwater aquifers, in the coastal area of Phuket. To map the seawater intrusion in the coastal areas of Phuket, an analysis of existing groundwater chemistry data (2003-2016), obtained from groundwater observation wells and network monitoring wells, was carried out. Chloride (Cl^-) and Total Dissolved Solids (TDS) concentration were the two main indicators of seawater intrusion. The average Cl^- and TDS concentration are highly correlated in a cross-plot in 8 districts (Chalong, Rawai, Karon, Kamala, Mai Khao, Choeng Thale, Sisunthon and Thep Krasitti) of Phuket, and the risk areas with seawater intrusion problem were identified by these levels exceeding threshold numbers (500 and 1,000 mg/L for Cl concentration and TDS, respectively). A map of Phuket seawater intrusion was created by GIS techniques, by overlaying the based maps for Cl concentration, TDS concentration, groundwater extraction, and transmissivity. The map indicates that the coastal areas in Mai-Khao sub-district has serious seawater intrusion, while the coastal areas of Kamala, Rawai, and Chalong sub-districts have only moderate seawater intrusion. To map the subsurface cross-section in the area seawater intrusion in those sub-districts, ten Electrical Resistivity Imaging (ERI) was successfully generated by using a Dipole-Dipole array and Werner Array. Then those data files were input in EarthImager2D and 3D software to do inversion

using smooth model in inversion method. In addition, four stations of Vertical Electrical Sounding (VES) using Schlumberger array were done near to the groundwater producing wells and monitoring wells in Kamala sub-district in the aim of verifying the correlation between groundwater salinity indicators- Cl^- and TDS- getting from groundwater producing and monitoring wells and apparent resistivity values obtaining from VES. A relationship between the resistivity and the seawater was demonstrated by laboratory testing to confirm that ERI is a feasible and efficient tool for delineating seawater intrusions, and an empirical model between resistivity and TDS and Cl concentrations in the study area was established. Seawater intrusion in the western part of Phuket, Kamala sub-district, can be seen to intrude in a freshwater aquifer with the expansion approximately 400 m inland and in the depth around 4 m below land surface. Similar to Kamala, Chalong sub-district, seawater intrude in a freshwater aquifer with the expansion approximately 150 m inland and in the depth around 3 m below land surface. In terms of Rawai, bedrock zone has been found in the shallow depth around 3 m above mean sea level and the saline zone has been found near the bedrock zone in shallow depth as well. Regarding Mai Khao, the area which is located around 500 m from the beach is completely covered by seawater intrusion. An empirical relationship between the resistivity and the seawater concentration (TDS and Cl) of the study area was established to identify fresh, brackish, and saline zones. Finally, the correlation of Cl^- and TDS with an apparent resistivity of soil, soil sample in laboratory testing and fence diagram of subsurface layers were presented to confirm that ERI is a feasible and an efficient tool for quantitative and qualitative studies of seawater intrusion.

ACKNOWLEDGMENT

First of all, I must express my very profound gratitude to my family for providing me with unfailing support and continuous encouragement throughout my years of study. This accomplishment would not have been possible without them.

I would like to extend many thanks to Prince of Songkla University (Phuket Campus) which offer me the 2-year research scholarship through the Royal Thai Princess Scholarship.

Also, I would like to address my honorable thank to my main advisor, Dr. Avirut Puttiwongrak for instructing me any steps of doing research.

I am grateful for the Interdisciplinary Graduate School of Earth System Science and Andaman Natural Disaster Management (ESSAND) for giving me an opportunity to study here.

I would like to acknowledge to Assoc. Prof. Dr. Pham Huy Giao, as the co-advisor of this thesis, and I am gratefully indebted to him for his very valuable comments on this thesis.

I would also like to acknowledge to Prof. Dr. Piti Sukotasukkul for serving as an external committee member of my thesis committee and to Dr. Kritana Prueksakorn and Dr. Tanwa Arpornthip for serving as internal committee members and giving me any useful lectures.

Many thanks go to Dr. Vipawee Dummee and Dr. Samkiat Khokiattiwong for their concerning and encouragement in the past years.

Finally, I am thankful to my friends, especially ESSAND students, and classmates, for support and motivation.

Sakanann VANN

CONTENTS

CONTENTS (cont.)

CONTENTS (cont.)

LIST OF FIGURES

LIST OF FIGURES (cont.)

LIST OF FIGURES (cont.)

LIST OF TABLES

CHAPTER 1

INTRODUCTION

1.1 Background of the Study

There are some main factors causing seawater intrusion, the movement of saline water into underground freshwater aquifers, along coastal areas such as rising of seawater level caused by global warming, high consumption of freshwater that can cause the shortage of freshwater, over-pumping from aquifer that can reduce water pressure and then let the seawater intrude to aquifer, agricultural process with requiring lots of amount of fresh water, and shortage of precipitation, oil-drilling, lack of knowledge as well. The salinization of water could be investigated by geophysical (resistivity and self- potential), geochemical and hydrological investigations. Using geophysical, geochemical, and groundwater level measurements defining the boundary between freshwater and seawater and monitoring seawater intrusion are needed to be set up.

1.2 Statement of Problem

While the seawater intrusion is the main topic of discussion in many parts of the world, it is also an issue that should be investigated in Phuket Island, Thailand. Phuket island is a well-known tourist attraction in Thailand, with around 9 million visitors in 2013 and growth rate of approximately 100,000 visitors/year (unpublished tourist data from the Department of Tourism, Thailand) (ISET, 2014). The rapid increases in population, tourism, and economic growth have severely increased water demands in the Phuket area. In Phuket, the water supply source is 68% groundwater and 32% surface water (DGR, 2015). Overuse of groundwater near the coast contributes to intrusion by seawater. Consequently, the groundwater close to the coast shows a relatively high salinity. Seawater intrusion is globally a common problem in the coastal areas by the sea. It is normally caused by prolonged changes in coastal groundwater levels, and seawater intrusion is the main cause of high groundwater

salinity, bringing with it also high TDS. In addition, the reduction in fresh groundwater of a coastal aquifer results in the freshwater-seawater interface moving inland, to previously freshwater areas (USGS, 2000; Chang *et al*., 2011; Ataie-Ashtiani *et al*., 1999). The balance between freshwater and seawater on Phuket island, with intrusion from the Andaman Sea, has been disturbed by excessive pumping to meet the water demands rapidly increased by tourism.

As mentioned above, Phuket is now experiencing with overpopulation; therefore, possible factors causing seawater intrusion in the coastal area can be caused by high extraction rate of groundwater due to highly requiring daily water supply for residents over last few decades (DGR, 2012). Whenever water in an aquifer containing or being near saline groundwater is pumped up, the zone of diffusion will move regarding this pumping. Any pumping might make a change of displacement in the contact between the freshwater and the surrounding seawater. If the boundary moves far enough, some wells become saline, thus contaminating the water supply. The location and magnitude of the groundwater withdrawals with respect to the location of the seawater determines how quickly and by how much the seawater moves. The individual wells located near the seawater/freshwater boundary can become saline as a result of significant local drawdowns that cause underlying seawater to “upcone” into the well (USGS, 2000). In addition, there have been a gradual rise of Andaman mean sea level from 1992 to 2016 with the trend of around 4.2 mm/year (NOAA, 2016). Therefore, two main factors which are possible to cause seawater intrusion in Phuket coastal areas are the high extraction of groundwater and mean sea level rise.

Above factors are just prediction based on previous studies and fact. Obtaining specific information related to seawater intrusion in Phuket coastal area, it is required to manage the relevant research teams. Then do a field-observation based on primary study and actual study, collect the relevant data, make an experiment by using scientifically methods, discuss the result from experimenting. Last, of all, point out the real cause and solution for that issues.

1.3 Research Objectives

- To assess seawater intrusion problem referring to the intrusion of the seawater into underground freshwater aquifers in Phuket coastal area.
- To map the risk areas of seawater intrusion in Phuket Island
- To delineate an extent and depth of seawater intrusion using groundwater data analysis and ERI

1.4 Research Scopes

Area:

- This research focuses mainly on the coastal areas of Phuket Island.

Method:

- An analysis of existed groundwater chemical data (2003-2016), obtained from groundwater producing and monitoring wells was carried out to map the seawater intrusion in the coastal areas of Phuket.
- Electrical Resistivity Survey was successfully conducted in the coastal areas of Phuket to delineate the extent and depth of seawater intrusion which was validated with the relationship between the resistivity and the seawater demonstrated by laboratory testing to confirm that ERI is a feasible and efficient tool for delineating seawater intrusions, and an empirical model between resistivity and groundwater salinity (TDS and Cl concentrations) in the study area was established.

Time:

- This research will conduct for 2 years. The existed data of 2000-2016 will be analyzed for identifying the risk areas, and the field survey (electrical resistivity survey) with chemical validation will operate from Jan 2017 – April 2018.

CHAPTER 2

LITERATURE REVIEW

2.1 Introduction to Seawater Intrusion

A seawater intrusion, the movement of saline water into underground freshwater aquifers, as shown in Figure 2.1 and 2.2, is surprisingly considered as one of the most serious either natural or environmental impacts since four-fifths of the world's population resides along the coast and exceedingly consume local groundwater for their daily water supply. Under hydrological cycle conditions, precipitation event plays the main role in recharging the freshwater in a coastal aquifer, and the recharged water migrating towards the sea would be a barrier to prevent seawater not to move to freshwater zone. Otherwise, over-pumping of groundwater in coastal aquifers has resulted in decreasing groundwater levels and has led to severe seawater intrusion (Chang *et al*., 2011).

Groundwater sustainability refers to improving and utilizing groundwater in an effective way that can be maintained permanently without contaminating environmental, economic, or social consequences. In many world's regions, the future ground-water sustainability is risk from over-pumping and careless control. Consisting of the high level of salinity or nutrient concentrations might let groundwater unsuitable for public consumption. A long-term investigation should be conducted to govern this precious resource because ground freshwater process generally responds slowly to human activities (USGS, 2000)

Seawater intrusion is a global impact since most parts of the world are experiencing with it. Groundwater has been widely consumed by some main sectors such as agricultural processes, industrial, municipal purposes and so on; therefore, groundwater has been pumped from the aquifer abruptly than it can be reclaimed by precipitation like snow, healing, especially rainfall. The over-pumping of the groundwater has led those areas to encounter the seawater intrusion now (Shammas and Jacks, 2007).

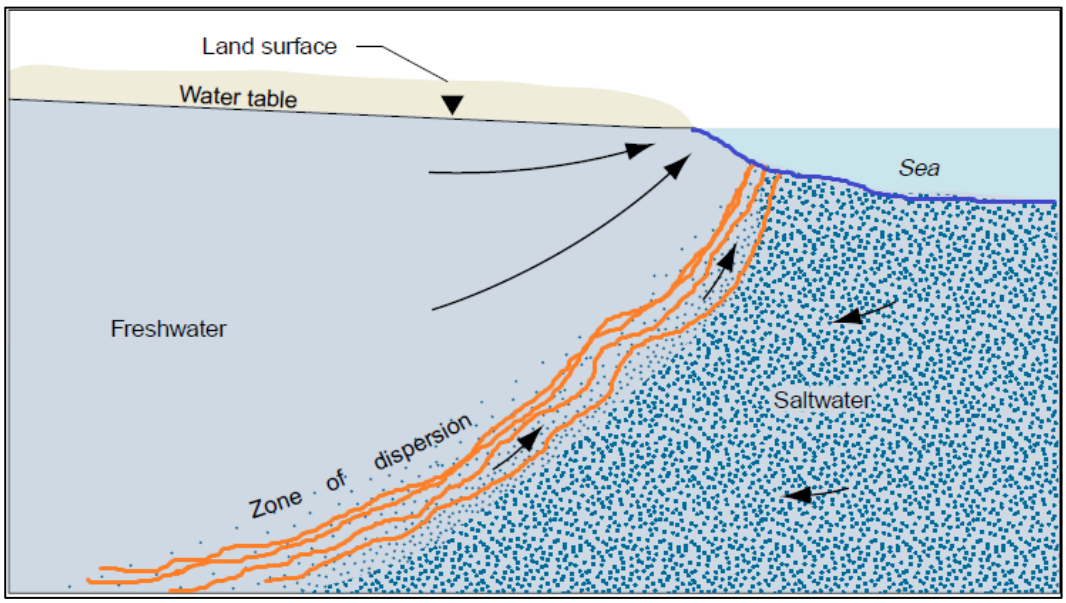

Figure 2.1 Flow Patterns of Groundwater and the Dispersion Zone in Coastal Aquifer. (USGS, 2000)

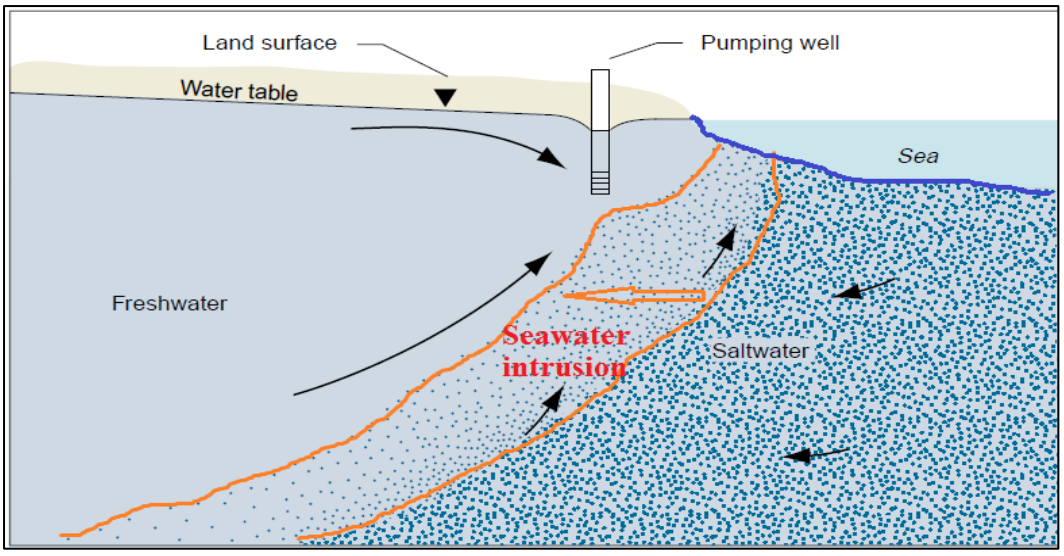

Figure 2.2 Flow Patterns of Groundwater Near A Pumping Well in Coastal Aquifer. (USGS, 2000)

2.1.1 Seawater Intrusion Characterization

The consequences are then applied to elaborate a concept for seawater intrusion dynamics, which are able to assist an effective judgment and take into account the long lasting impacts of rising of sea-level on coastal aquifers. Ataie-Ashtiani *et al*.

(1999) have, furthermore, specifically clarified tidal fluctuation effect on seawater contamination in an unconfined aquifer and the results of this factor for the groundwater table and zone of dispersion. In addition, it is identified that the large inflow of seawater that was deposited during the Tsunami can affect many coastal wetlands. In addition to increasing the magnitude of seawater intrusion, it can significantly affect these nutrient pollution problems.

2.1.1.1 Groundwater Quality and Pollution

Seawater composition around the world remains stationary; otherwise, the fresh groundwater composition in aquifers probably seasonally change. Some chemical water characteristics frequently accumulate in the coastal aquifer because of the chemical reactions between the host material and groundwater occurring when intruded fresh groundwater and seawater interface or when the others are substituted by another one. Furthermore, because of the variation in fresh groundwater and seawater chemical composition, different hydro-chemical processes are possibly able to accompany seawater intrusion driving to not only importantly contaminate in water quality but might also change the hydraulic properties of the subsurface. It is proved that the dissolution of carbonate is considered as a crucial process in the dispersion zone forming even the sea-freshwater end members are at chemical equilibrium with the carbonate mineral. Cation exchange caused by variety in dominance of cation in both fresh groundwater and seawater is also listed in one of many factors which influence to groundwater quality (Werner *et al*., 2013). Seawater is slightly dissolved with fresh groundwater even far below the fresh-saline water interface. This dilution of seawater naturally forms the cation exchange process enhancing saline groundwater with Calcium (Ca^{+2}) and Strontium (Sr^{+2}). Chemical data from the research express that cation exchange formed by seawater dilution in the aquifer is such an important impact common to the coastal region aquifers in most parts of the world and can lead those aquifers to encounter with contamination (Sivan *et al*., 2005).

2.1.1.2 Mechanisms of Seawater Intrusion

There are numerous processes and factors which should be discussed in detail in the mechanism of seawater intrusion. Those are closely related to mixing of zone dispersion, tidal effects, effects of density-surface hydrology and paleo-

hydrogeology- human activities and structural geology that effect to the change of aquifer hydraulic and mitigation processes. The relationship between these and other factors such as geochemical evolution, giant wave as well as beach morphology on coastline water table conditions reliably contribute to other settings in which seawater intrusion possibly take place.

Dispersive processes are the key parameters for discussing the seawater intrusion mechanism. Due to both molecular diffusion and mechanical dispersion, the concentration of salt and fluid density change along the freshwater-saline water interfaces (mixing zones). In the steady state of equilibrium, uniform systems, the mechanical dispersion, molecular diffusion, the discharged rate of freshwater, and the density contrast between groundwater and seawater, those factors possibly drive the change of mixing zone thickness in the groundwater aquifer.

It is identified that the variance of the mixing zone in the aquifers are the result of migration processes provoked by density contrast, both diffusion and dispersion of molecular and mechanic respectively, and kinetic mass transfer (mass exchange processes between mobile and relatively immobile zones due to low-permeability zone) which are affected by a large number of mechanisms and aquifer characteristics. Owing to the variations in discharge and recharge rates, it can make dispersive zones vary based on both location and time (Werner *et al*., 2013).

2.1.1.3 Factors of Seawater Intrusion

In term of steady-state conditions in a coastal aquifer, an equilibrium is maintained between seawater and fresh water. Otherwise, groundwater may be subjected to over-exploitation due to increasing water demand, thus natural state of equilibrium is exacerbated. This approaches seawater intrusion to severely intrude inland aquifers. The estimation of zone dispersion movement regarding groundwater discharge and recharge should be observed through potential design and management on the system of coastal groundwater (Mahesha, 1996). In fact, besides of over-exploitation which is the main factor to cause seawater contamination in many coastal areas, other factors developing seawater intrusion should be proposed such as:

• Lack of rainfall

Lack of rainfall causes replacement of fresh water consumption was slow while the uses are increased in this case, it will reduce the amount of fresh water in the ground and it will be replaced by seawater (Mahesha, 1996). It is possible that intrusion-affected and abandoned aquifers can be reclaimed over a period of a few years in areas receiving moderate to heavy rainfall. It means that high rainfall, high reduction of seawater intrusion.

• Over-pumping

When the recharge rate is less than the discharge rate in aquifers, seawater intrusion can be produced (USGS, 2000). Moreover, USGS identified that pumping of groundwater lowers water levels and can cause seawater to be drawn toward the areas of stress. Moreover, pumping groundwater from an aquifer can decrease the water pressure which migrates seawater into new areas. When fresh water levels fall, seawater intrusion can proceed inland and reach the pumped well.

• Rising of seawater level

Typically, sea level rise which made by global warming has become the main cause of the rise in the quantity of seawater that many will try to enter the freshwater aquifer. Rising of sea level can lift the entire aquifer and this lifting process would help alleviate the overall long-term impacts of seawater intrusion (Giambastiani *et al*., 2007).

• Tidal effect

Tides was found to be made mixing zone change. Relationships between seawater intrusion and sea stresses are accompanied by many factors: hydraulic properties of coastal aquifer, shoreline morphology (i.e., the slope of the beach) and the characteristics of the ocean fluctuations themselves. Storm phenomenon is possible to produce the persistent salinity conditions of aquifer, driving much more impact on dispersive zone improvement than oscillation of tidal and other events. It is proposed that tidal fluctuations caused minimal movements of interface relating to the response caused by a modest storm event; for example, 4.5 m significant wave height induced interface movements of several meters (Werner *et al*., 2013). Due to the variation in the velocity and flow pattern of the groundwater near the shoreline, a tidal effect leads the seawater to intrude further inland and also makes a thicker dispersion

zone (Ataie-Ashtiani *et al*., 1999). The changes of chloride concentration contours, moreover, driven by the variation of tidal oscillations are more remarkable at the upper layer of the aquifer, near to the groundwater level than the bottom of the aquifer because of the penetration of seawater into the top aquifer at higher tidal level and therefore a flatter beach slope intensity this phenomenon. The tidal fluctuation effects are more noticeable for a sloping beach because salt water intrudes further inland for the sloping case. Even though tidal activity can affect to the seawater intrusion at coastal areas, the tidal fluctuation has a very minimal influence on how far the seawater intrudes into the aquifer if the depth of aquifer is much bigger than amplitudes of tidal.

• Geological aspect

Typically, seawater intrusion is not only triggered by decreasing of recharge rate, over-pumping, and sea level rise and so on, but it is also affected by geological property of aquifers as well. Some coastal areas over-exploited groundwater but the rate of seawater intrusion remains less than some areas with less consumption. This is because of the difference of geological effect of those zones. Such a rapid reaction to both contamination and washing of the aquifer (groundwater flow into the sea) is not simple way in seawater intrusion process (Calvache *et al*., 1997). The unexpectedly rapid washing of the aquifer is because of the very high transmissivity of sediments, which permits rapid flow, and the scarcity of clayey sediments that would retain salt. The preferential route for washing of the aquifer moves through the high permeability, high porosity and high transmissive materials in the aquifer. Geological effect on seawater intrusion, two main parameters, i.e., hydraulic conductivity and specific storage should not be neglected for making discussion because it plays a very important role for the change of seawater intrusion state in the aquifer along the coastal areas. Basically, seawater intrusion will easily intrude to freshwater aquifer if that aquifer has a high hydraulic conductivity (Werner *et al*., 2009). One more thing, the maximum level of intrusion was more sensitive to variation in specific storage values than the duration of intrusion. It was claimed that if the aquifer consists of the small specific storage, the expansion of seawater intruding to inland is also small compared to the aquifers with higher specific storage (Chang *et al*., 2011).

2.1.2 Seawater Intrusion Observation

Geophysical methods are composed of 4 main methods: 1) seismic, 2) gravity, 3) magnetic and 4) electrical methods (e.g. resistivity, induced polarization, self-potential, electromagnetic and radar as well). That electrical methods are really popular for applying on groundwater supply exploration. Typically, the resistivity values of seawater and freshwater are not a universal standard. Due to the contrast of electrical resistivity between freshwater and seawater, more than 5 Ω.m and around 0.2 Ω.m respectively, the electrical resistivity can be used to delineate groundwater salinity distribution in subsurface using electrical methods (Werner *et al*., 2013). Electrical resistivity tomography (ERT) used to recover an extensive mixing zone and infiltrated rainwater is indicated in 2D or 3D visualization of the subsurface resistivity distribution. The combination of borehole data and surface-based geophysics was, moreover, the crucial parameter to accurately interpret the electrical visualizations However, the proportion of salinity obtained from an investigation of geophysical is approximate since there are two main errors in geophysical measurement processes: 1) the observation model relating to the measurement signal to the salinity is not exact and 2) the measurement signal can be affected by other variation besides salinity, such as the presence of clay layers.

Werner *et al*. (2013) provided that there have been lots of researches and case studies having mentioned about applying the groundwater chemical analysis in coastal areas as a material to prove the formation of salt dissolutions. He reviewed some case studies relating to using the chemical and isotope characteristics to analyze the groundwater properties such as:

- Br^- concentrations and isotopes have been used to distinguish origins of contamination in a coastal aquifer in Spain letting seawater to be differentiated from industrial wastewater sources.
- Cl^-/Br^- ratio was utilized as a tool to differentiate between the non-synthetic source (i.e. seawater and potassium halite) and artificial source (i.e. wastewater, solid waste, and pesticides).
- The Sr^{2+} ratio of groundwater was used to determine a contribution of the water source to the mixing zone in a near-surface aquifer.

- H^+ and C^- isotopes were applied to identify the movement of seawater into inland over the times.

2.1.3 Seawater Intrusion Hazards

The submarine fresh groundwater discharge (SFGD), defined as the discharge of freshwater to the sea, mixes in the coastal aquifer with recirculated seawater forming saline groundwater discharge. The hazard of seawater intrusion linked to SFGD through connections between groundwater flow and interface location; for instance, it is expressed that a decreased risk of seawater was assisted by improvement of SFGD. The site investigation and numerical modelling can reveal the salinity of submarine groundwater discharge (SGD) increase when the interface increases. Moreover, seawater intrusion can cause the nutrient discharge through geochemical processes taking place at the mixing zone.

As above mention, seawater intrusion concerns can cause the reduction of freshwater resources, pollute wells of water supply and directly exacerbate the ecological issues. Environmental contamination formed by seawater intrusion relates to the application of high salinity groundwater in crop production processes, which modifies soil chemistry and contaminates soil fertility. Geochemical and hydrochemical reactions are produced by seawater intrusion based on the subsurface environment characteristics. A large number of the synthesized factors making seawater intrusion: over-pumping of groundwater or the construction of surface drainage systems in coastal areas influence both water chemistry and rate of SFGD. Moreover, seawater intrusion is also realized to emit and migrate other pollutants such as arsenic and heavy metals and it is likely to destroy ecosystems through SFGD delivery mechanisms. Regarding the tidal system, it is also explained that seawater intrusion can impart more considerable ecosystem stress compared to non-tidal system, especially where vegetation and other biological substance in the coastal setting are dependent on fresh groundwater conditions.

2.1.4 Seawater Intrusion Mitigations

To solve the seawater intrusion problem, a network of sewers- pipe for pumping wastewater- can be used, and a sewage treatment plant should be operated. An artificial recharge system has, one more thing, been employed to create a barrier

against intrusion of seawater. Typically, artificial recharge of the treated wastewater is beneficial to prevent intrusion of seawater from the sea and it also stabilizes water table in the aquifer. New water sources and additional conservation measures should take into account to ensure the preservation of freshwater resources for coming generations. Even though government makes effort to solve this problem through setting up injection of recharge system of the treated wastewater, water quality is still threatened by contamination of seawater and other pollutants (Shammas and Jacks, 2007). Artificial recharge, as shown in Figure 2.3, mitigates seawater intrusion through the abstracting of brackish water from the saline zone and then desalinating of the abstracted brackish water using reverse osmosis (RO) treatment process. Finally, they injected of that treated water into the aquifer. Undoubtedly, the reason they decided to pump the brackish water from the coastal aquifer for the treatment process because they aimed to decrease the volume of saline water. The combination of injection of freshwater and extraction of saline water can reduce the volume of saltwater and increase the volume of freshwater. Moreover, injecting treated wastewater is to act as a barrier to seawater intrusion, to elevate the piezometric head and to provide a source of water. As discussed above, the main factors that potentially led to seawater intrusion were pumping a large

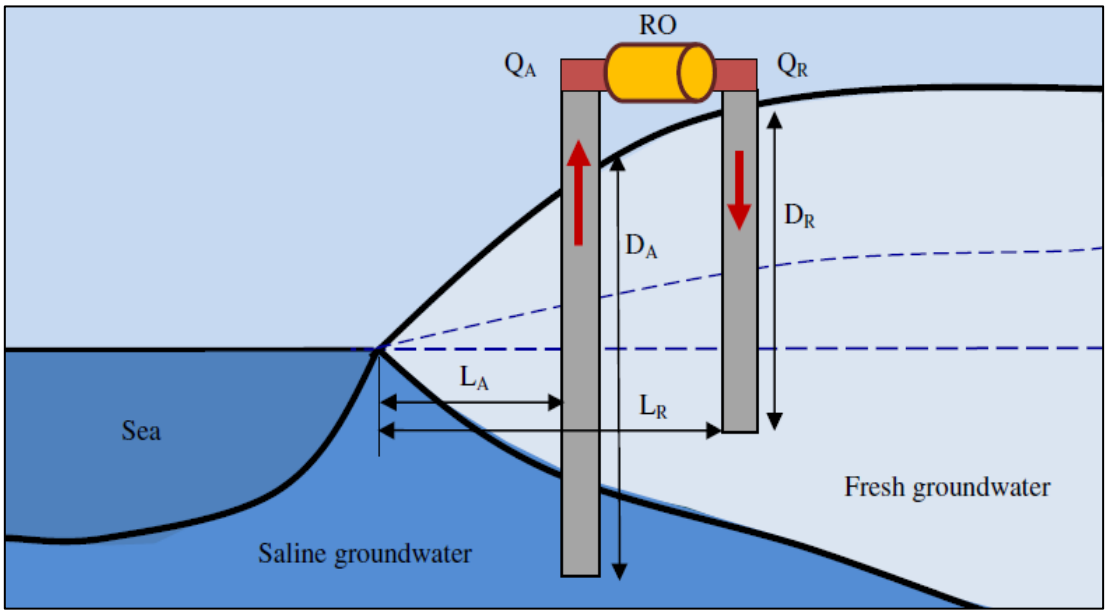

Figure 2.3 Diagram of the ADR (Abstraction, Desalinization and Recharge) Methodology. (Abd-Elhamid and Javadi, 2011)

Amount of groundwater for agriculture processes, using fertilizer for improving their crops and leakage of nitrate concentration from septic tank system; therefore, other mitigations such as restricting water demand on agricultural process, restricting on using fertilizer on resident's crops and checking frequently and properly on septic tank system set up should be discussed.

Moreover, USGS has already provided a summary of the contamination of seawater into freshwater and various mitigation techniques. It is mentioned that groundwater is the significant natural resources providing usable water to both rural and urban sectors, supporting either irrigation or industry, sustaining both flow of streams and rivers, and maintaining ecosystems of wetland areas. To determine the boundary between freshwater and seawater and to monitor seawater intrusion, three evaluations: geochemical, geophysical and groundwater-level measurements are successfully utilized by USGS researchers working to get familiar with geologic, geochemical, and hydrological controls on seawater intrusion loading to coastal environments.

A numerical simulation on optimal schemes of groundwater exploitation in the three-aquifer system to determine some mitigations for solving seawater intrusion impact has been proposed. Based on the calculation, suggesting that groundwater pumping should not be pumped along the coast. Moreover, the location of the production wells in that area must be scattered. Some wells are not highly expected to pump any longer, especially wells along the coast boundary; otherwise, other wells in inland cells can be possible to pump groundwater at the certain pumping rates. These are very benefit in groundwater resource management and potentially preventing seawater contamination in the peninsula to the greatest degree possible (Zhou *et al*., 2003). In case of controlling groundwater pumping, it is recommended that installing the flow water meter is very useful to control the volume of groundwater pumped whether it matches with what the government allows or not. One more thing, pumping eagerly needs the electrical power to pump; therefore, implementation of electricity quota and pricing electricity are some kinds of other methods to reduce the groundwater pumping.

Another effective way of seawater intrusion mitigation is land reclamation, as shown in Figure 2.4, along with the shoreline because the fill materials

are regarded as an additional aquifer and it can gradually freshen the original brackish water in aquifer. However, the proportion of freshening relies on many factors such as aquifer permeability, the fill materials, the structure of aquifer and the recharges from the lateral flow and precipitation. The dispersion zone might have moved seaward that is significant process accountable for the gradual freshening (Chen and Jiao, 2007). Basically, effective approaches which have been applied to maintain the groundwater sustainability generally are relevant to consumption of aquifers as a main storage reservoir, conjunctive use of surface water and groundwater, synthesized recharge of water through wells or surface spreading, and the use of recycled or reclaimed water.

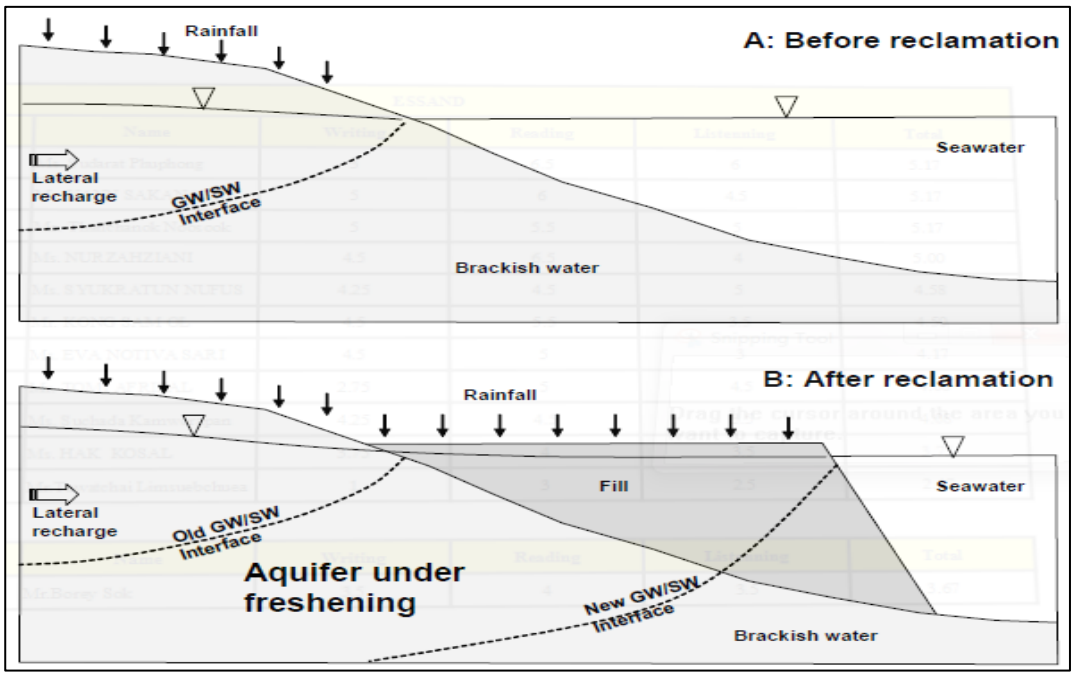

Figure 2.4 Setting up Land Reclamation for Mitigation Seawater Intrusion. (Chen *et al*., 2007)

2.2 Electrical Resistivity Survey (ERS)

The application of geophysics methods for engineering studies, groundwater exploration, and seawater intrusion, has been more commons over the last decade owing to the sudden improvement in computer software and the solutions of numerical modelling.

ERS is known as the detection of the surface effects produced by flow of electrical current beneath the subsurface. Typically, the electrical surveys have been utilized in various ways of observation such as mineral or geothermal exploration, engineering studies, archaeological studies, geological mapping and so on. Moreover, ERS is normally classed depending on the energy source, e.g., natural and synthesized source (Jatau *et al*., 2013). In terms of resistivity method, artificial electric currents are injected into the ground and the resulting potential differences are measured at the surface. Certain minerals (e.g. native metals and graphite) transmit electricity via the passage of electrons. However, most rock-forming minerals are insulators; therefore, electrical current is conducted through a rock mainly by the passage of ions in pore waters. Hence, the porosity is the major control of the resistivity of rocks and that resistivity normally increases as porosity decreases.

2.2.1 Vertical Electrical Sounding (VES)

VES is significantly applied in the investigation of horizontal interfaces. The estimation is done based on the measurement of the voltage of the electric field induced by the distant grounded electrodes (current electrodes). The potential and current electrodes are adjusted at the same relative spacing which is expanded about a fixed central point. The technique is extensively applied in geotechnical works to investigate overburden or subsurface thickness and also in hydrogeology to determine horizontal zones of porous strata (Kearey *et al*., 2002). Moreover, VES, one kind of electrical resistivity, has been applied powerfully with groundwater study because of the simplicity of the techniques.

2.2.2 Electrical Profiling (EP)

Electrical profiling (EP) is mainly applied to observe lateral resistivity data. The current and potential electrodes are maintained at a fixed separation and progressively moved along a profile. This technique is utilized in mineral exploration to detect faults or shear zones and localized bodies of anomalous conductivity. It is also employed in geotechnical surveys to recover variations in depth of basement or bedrock and the presence of steep discontinuities. Furthermore, it is applied to study groundwater mechanism and seawater intrusion along the coastal zone (Kearey *et al*., 2002).

2.2.3 Electrical Resistivity Imaging (ERI)

ERI, also known as electrical resistivity tomography (ERT), is a geophysical method for imaging sub-surface structures from electrical resistivity measurements made at the surface, or by electrodes in one or more boreholes. If the electrodes are suspended in the boreholes, deeper sections can be investigated. ERI provides information about the subsurface not only in the vertical but also in the lateral direction. ERI performed with different electrode configurations has proved to be very effective for illustrating with higher resolution near-surface resistivity anomalies for a wide range of environmental problems such as seawater contamination (Vafidis *et al*., 2014).

2.3 Phuket Water Situations

Phuket, the biggest island in Thailand with around 543 km^2 in area, located in the Andaman Sea of southern Thailand, is the place that has been developed significantly: economic improvement, social integration, industrialization, especially the expansion of tourism vision. This region is mostly covered by granite, which is hard and several meters deep, but it provides a good potential groundwater.

Typically, water is regarded as an essential resource for livelihood and tourism development as well in Phuket. Due to consisting of the mountain around 70% and being influenced by Monsoon, Phuket is one of the regions that account for a high rainfall level to promote those developments. Water source in Phuket is already divided to two main types: surface water source (32 %) and groundwater source (68 %) which are repeatedly produced from the presence of precipitation (ISET *et al*., 2013), especially rainfall, in many parts of Phuket, as shown in Figure 2.5.

The amount of rainfall falling in rainy season between April and November and summer season from September to March has so far different that leads water source in Phuket have been unstably changed also. The yearly water amount around 34.12 million m^3 flows into the reservoir and the sea. Precipitation moves through the layer of rock to accumulate the groundwater that is the main source for local consumption, especially for general pumping.

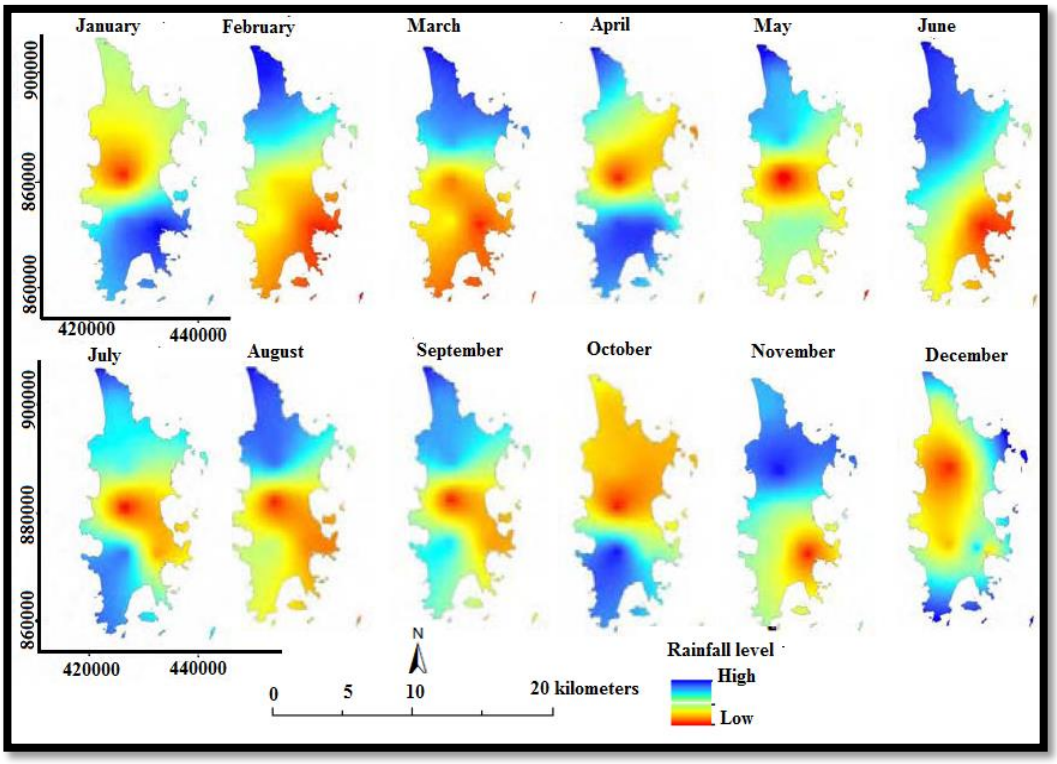

Figure 2.5 Distribution of Monthly Average Rainfall Level in Phuket from 2007 to 2011. (ISET *et al*., 2013)

According to the study of rainfall level over last 40 years from 1970 to 2010 (Figure 2.6), it is shown by (ISET *et al*., 2013) that there has been a change of rainfall level and season that May-March in 2010 accounted less rainfall level and longer dry season than in the past.

Up to now, all citizens depend on shallow wells and artesian wells for local consumption. Reported by (ISET *et al*., 2013), there was the highest rate of drilling wells for pumping groundwater in 2000 and then there has been a significant rise of drilling borehole year to year with around 1,290 wells in total spreading in Phuket in recently (Meung 363 wells, Kathu 168 wells).

Description of a number of groundwater wells and the allowed volume water consumption being shown in Table 2.1 and the distribution of wells in Phuket is illustrated in Figure 2.7. However, the observation of groundwater potential illustrated

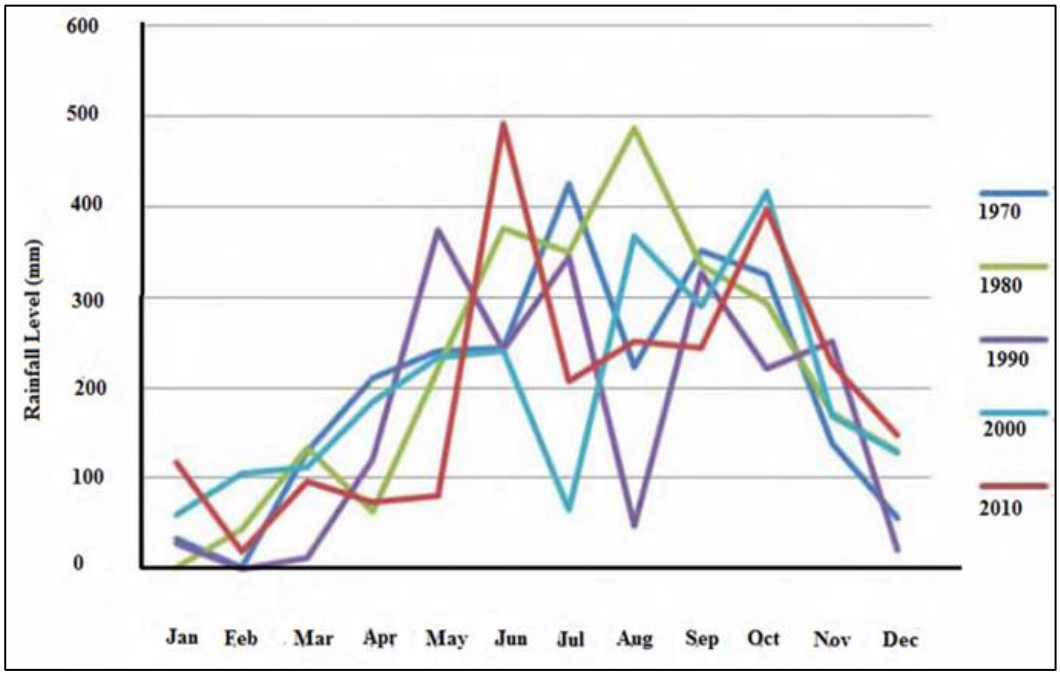

Figure 2.6 Distribution of Monthly Average Rainfall Level in Phuket from 1970 to 2010. (ISET *et al*., 2013)

Table 2.1 Number of Groundwater Wells and Amount of Allowed Water Consumption in Phuket in 2012. (ISET *et al*., 2013)

Activities	Number of wells	Amount of allowed water consumption(m^3/day)
Agriculture	6	325
Business	567	34,881
Business service	14	470
Industrie	2	220
Local	282	2,881

a region which has the potentiality of groundwater in the highest rate is Tepkrasattri subdistrict, Thalang district. The water quality of that researched area is usable because it is freshwater; on the other hand, the area near the coast along western and northern of Phuket has salty groundwater due to seawater intrusion or brackish water (ISET *et al*., 2013).

According to the graph of average groundwater level changes in Phuket from 2006 to 2016, it is seen that the trend seems to fluctuate for the whole period. The

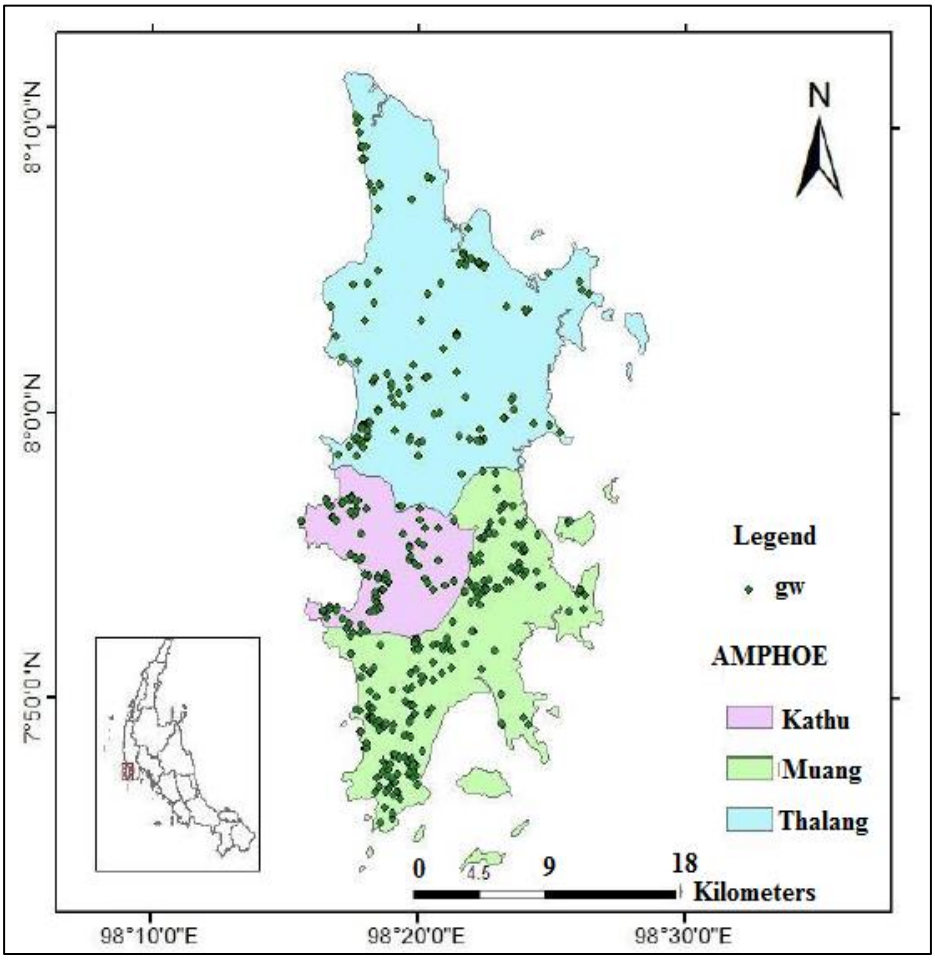

Figure 2.7 Distribution of Wells in Phuket Province, (Saowanee *et al*., 2012)

level of groundwater was approximately -6.5 m in 2006, followed by a gradual decrease to just under -7.5 m in 2009. The trend remained steady from 2006 to 2011. After that, it rose steeply to -4.5 m in 2013, followed by a slight fall to around -5 m at the end of the period, 2016, as shown in (Figure 2.8).

From 2006 to 2013, groundwater pumping rate in Phuket steadily increased at just over 3,000 m^3/day to 4,200 m^3/day; otherwise, there was a significant rise to approximately 19,000 m^3/day in 2014 and then still surprisingly jumped to over 40,000 m^3/day in 2015. It is expected to continue increasing for the next years, as shown in (Figure 2.9).

2.4 Phuket Groundwater Characterization

The aquifer is refers to a geologic formation which has sufficient interconnected porosity and permeability to store and transmit significant quantities of water under natural hydraulic gradients. It is identified that fresh, brackish or saline water in volume ranging from minor to a large amount to support the public water system is confined in the aquifer; moreover, it confines fresh groundwater sources for utilizing in urban areas and agriculture. It is pointed out that a potential aquifer for the well-screen installation is a kind of permeable layer below the groundwater table. The top layer of the aquifer is considered as the phreatic aquifer.

Typically, there are four fundamental aquifer materials such as sand and gravel, limestone, fractured and volcanic rock. Based on DGR (2010, 2012), It is undoubtedly mentioned that the aquifers of Thailand are regionally categorized into 6 hydrological zones: Northern Highland, Upper Central Plain, Lower Central Plain, Khorat Plateau, Eastern province and Southern Peninsula. The hydrogeological units of Phuket are mainly divided into 2 main aquifers: unconsolidated and consolidated aquifers. Major aquifers are in the unconsolidated aquifers referring to Rayong-Satoon aquifers including recent and old beach sand aquifer, floodplain deposit aquifers and colluvium aquifers.

In addition, the reduction of Phuket groundwater level and flow path variations is principally made due to both natural and anthropogenic factors, e.g., over-pumping of groundwater, the decrease of annual rainfall caused by climate change, urbanization which is the influential mechanism impact on climate contrast and land management disturbing the recharge and increasing the demand of water supply. Therefore, the coverage pertinent to the hydrological area- topography, stream network, land use- and hydrogeologies such as wells, subsurface topography relief, and potentiometric surface is essential to identify groundwater sources.

Thailand has estimated that it has 25 active river basins with approximately 1700 mm in an average of annual rainfall. Those 25 basins are located at a different location with its distinguished characteristics like Central, Northern, Northeastern, Eastern and Southern areas. Large numbers of short rivers, water reservoirs, and high annual rainfall are naturally presented in Southern part; however,

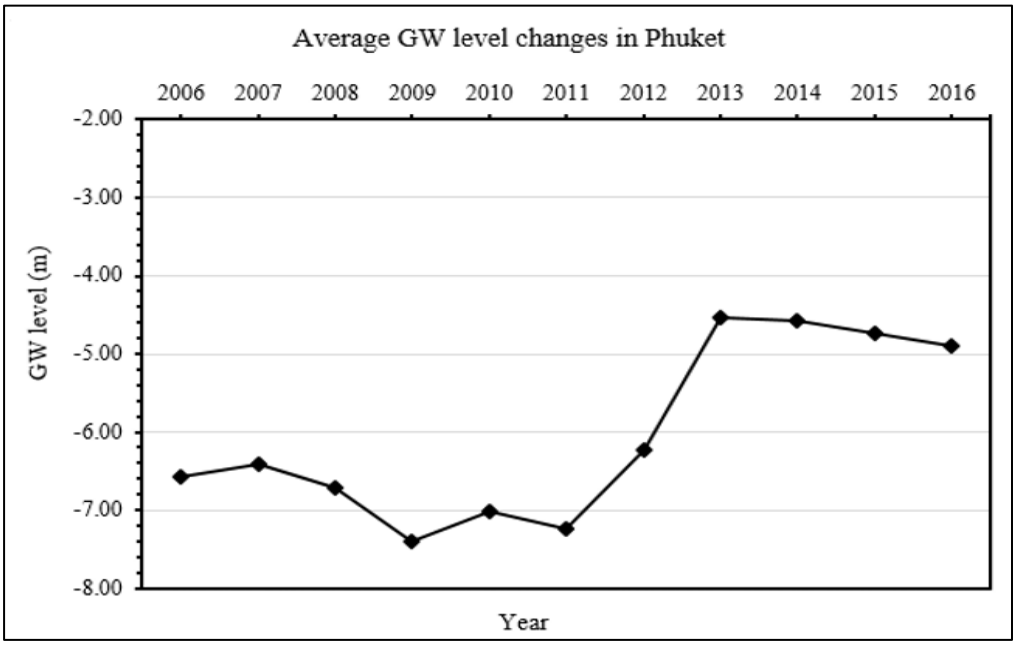

Figure 2.8 Groundwater Level Change in Phuket, 2006-2016. (DGR, 2016)

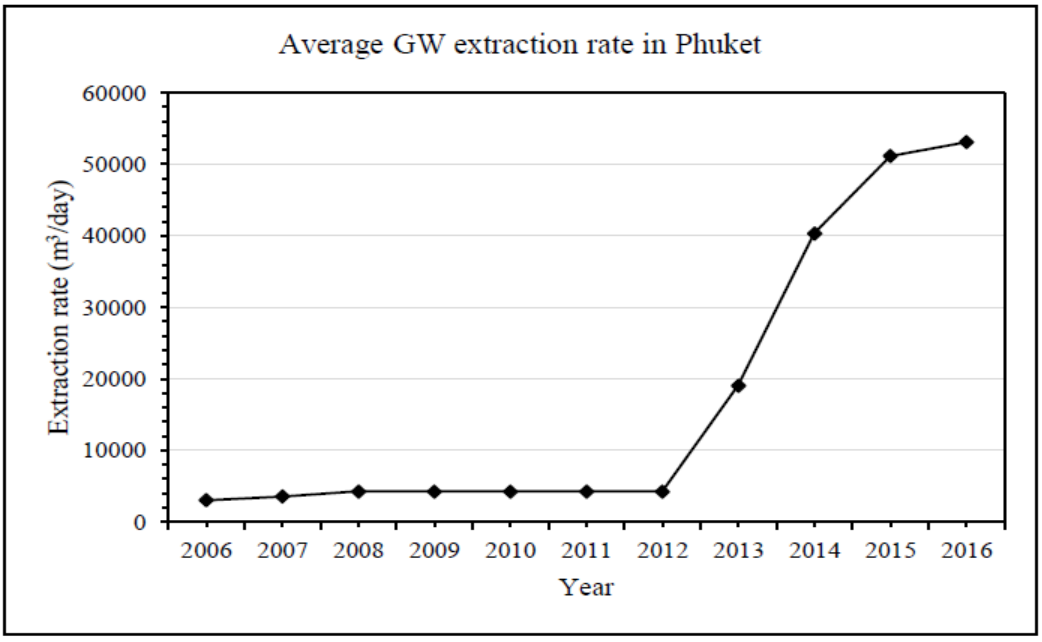

Figure 2.9 Groundwater Extraction Rate in Phuket, 2006-2016. (DGR, 2016)

the scarcity of water is unpredictably occurring in a few areas of that part. The total amount of rainfall in those 25 river basins is estimated at 800,000 million m^3.

Water supply sources, as shown in Figure 2.10, are normally obtained from two main sources: surface and subsurface. Typically, catchment regions are supposed to significant sources of surface water in Phuket which is estimated around 34.12 million m^3. The catchment raining area has 1,244 km^3 in an area categorized into 24 minor catchments and short 188 streams in the Eastern part, 63 streams in the Southern part and 9 main canals in the Western part. Phuket also has 113 mining ponds in total and two dams with the capacity of 59.00 million m^3. In addition, Phuket has recently constructed 6 main reservoirs with the storage capacity of approximately 27.51 million m^3.

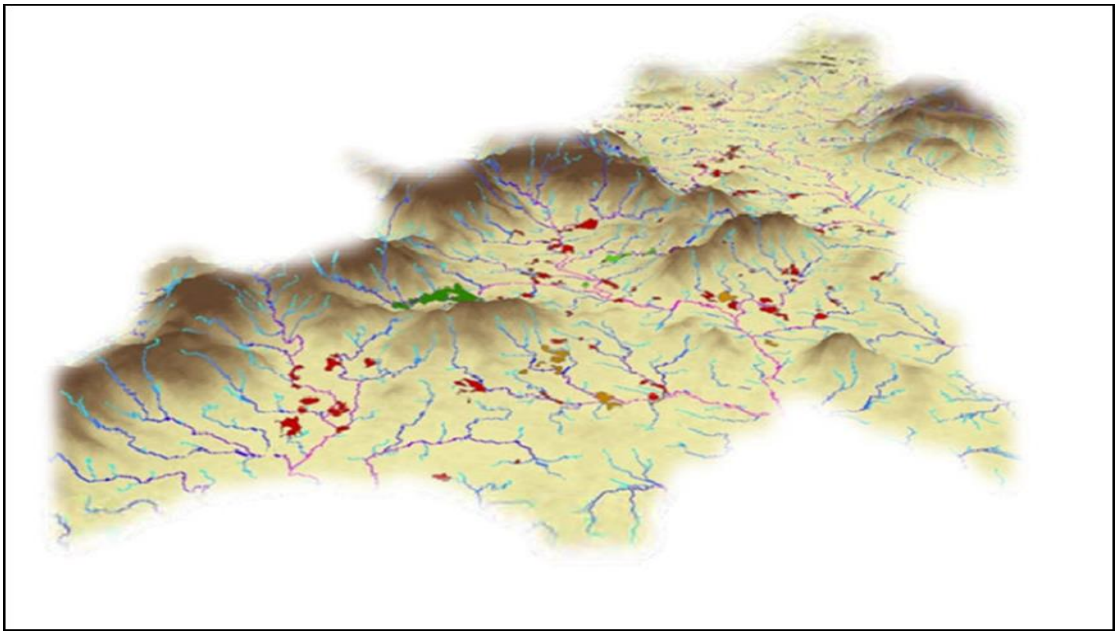

Figure 2.10 Surface Water Supply. (ISET *et al*., 2013)

2.5 Phuket Groundwater Over-exploitation Caused by Urbanization

Phuket's population is sharply increasing by years due to rapid development on many sectors: economic, social integration, industrialization, particularly tourism and so on. Steele *et al*. (2013) reported over five hundred and twenty thousand people were residing on the Phuket island, including one hundred and fifteen thousand foreigners, or 21.1% of the population in 2010 with approximately sixty-four thousand migrant workers from Burma, Laos, and Cambodia.

It was assumed that the number of tourists has been dramatically increased, approximately 2,500,000, around 9,000,000 and more than 12,000,000 in respectively 2009, 2013 and 2015 (ISET *et al*., 2014). These rapid increases have led to a significant growth of residents and a noticeable expansion of urbanization across the island as shown in Figure 2.11, 2.12 and 2.13. This growth has influenced existing pressures and created new vulnerabilities, especially relating to land use and water resources management. The land use or land cover, expanded as urbanization in the last decades, has been occurring in response to the demand of the tourist industry, hotel, housing estates and condominium projects, shopping malls, restaurants, shops, and other infrastructures. Recently, it is illustrated that some parts of the island have encountered water shortages because of climate vulnerability and the linkages of the urbanization. There is still no effective mechanism for generating the kind of comprehensive assessment of water balance in across the island to access the current and future vulnerabilities and risks due to the demand of water increasing (ISET *et al*., 2014).

The maximum of water demand reach to the water limitation around 120,000 m^3/day and the demand keeps increasing to more than 180,000 m^3/day. The maximum of daily water demand reached a peak of water limitation around 120,000

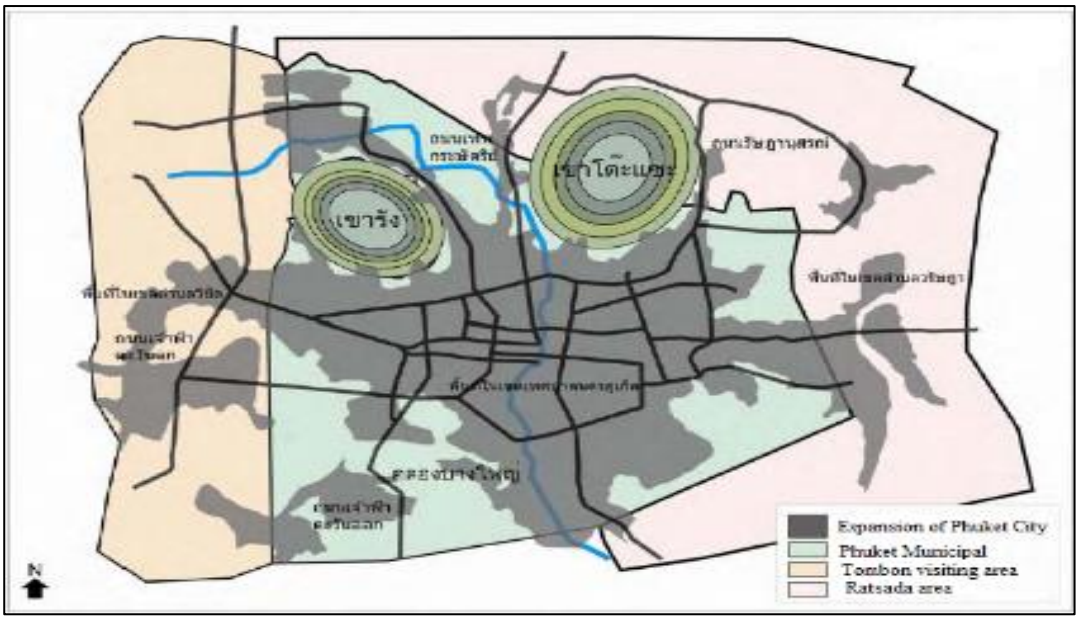

Figure 2.11 Phuket Urbanization in 1995. (ISET *et al*., 2013)

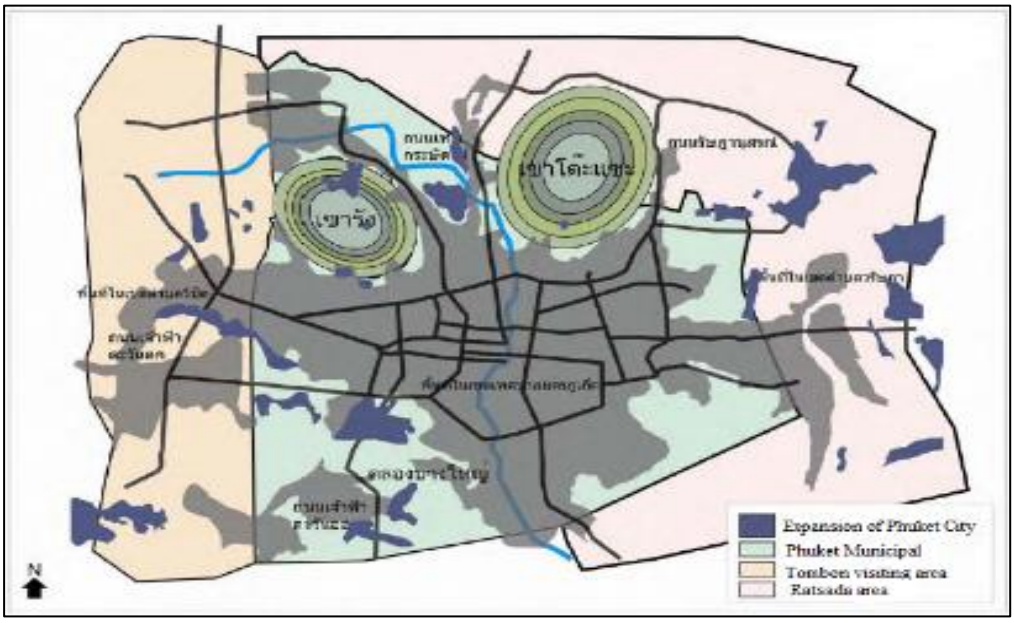

Figure 2.12 Phuket Urbanization in 2005. (ISET *et al*., 2013)

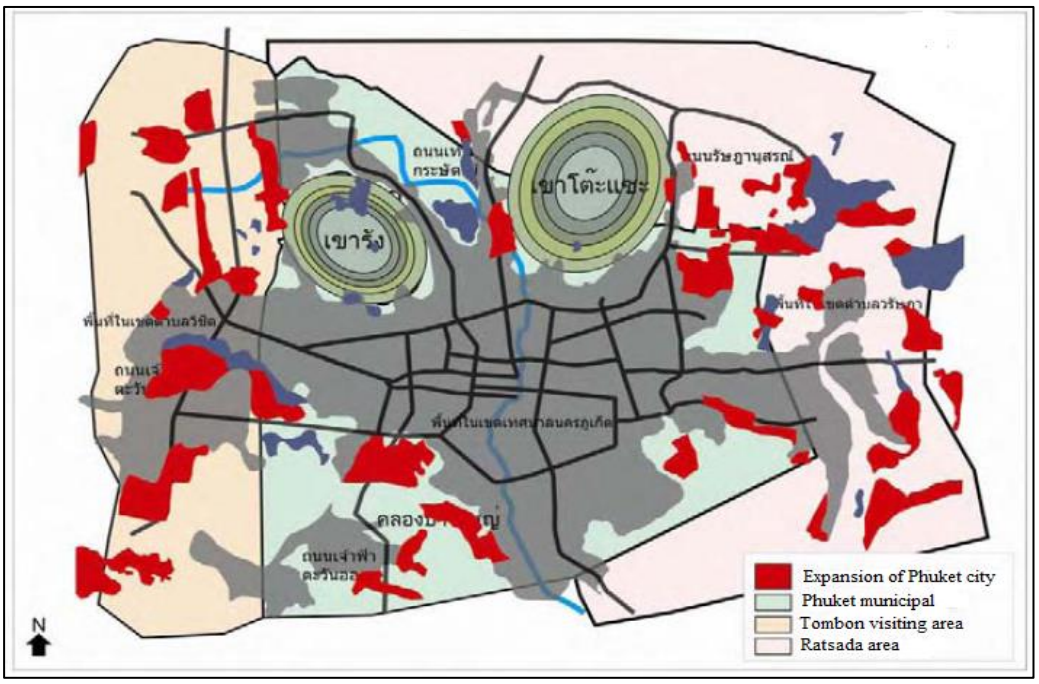

Figure 2.13 Expansion of Phuket Urbanization in 2009. (ISET *et al*., 2013)

m^3/day in 2015. It will keep steadily rising into just over 180,000 m^3/day in 2025. The high water demand for urbanization can reduce the groundwater level, around 100 m in depth, because most of the water supply in the Phuket area relies on pumping groundwater (ISET *et al*., 2014). ISET *et al* (2013) briefly reported that there was the

highest rate of drilling wells for pumping groundwater in 2000 and then there has been significantly increasing of drilling boreholes with around 1,290 wells in total in Phuket (Meung 363 wells, Kathu 168 wells, and Thalang 759 wells). The over-used of the groundwater is likely to induce the groundwater recharge of seawater intrusion because Phuket is an Island and located as coastal areas.

2.6 Geographic Information System (GIS) Software

The main objective of GIS using is for analysis, collection, storage, manipulation, retrieval and presentation on the set of the geodatabase. GIS is known as a computer-based program able to contribute sets of capabilities for users to manage georeferenced data, e.g., data manipulation and analysis, data management (storage and maintenance), data capture and presentation, and data presentation (Millett and Evans, 2009). The two distinct application capabilities of GIS have been known as- the first pertaining to querying and obtaining information and the second pertaining to in targeted analytical modelling. It was mentioned that designing and organizing a GIS database should be focused on different disciplines such as cartography and mapmaking, geography, GIS, databases etc. GIS software is typically considered as a concept of the geographic management system and geodatabase is directly applied to database management systems. GIS can be used to store geographic data, make maps, and perform spatial analysis tasks (Millett and Simon 2009). Therefore it is enabled database management system which is the best sophisticated geographic software. GIS database is the essential systems of database combination which is closely interrelated and need to be well structured for catering to the different needs of applications. Actually, there are two components of the GIS database, - namely spatial data and non-spatial data (Healey, 1991). In addition, GIS can be used to integrate with other models. For example, artificial recharge zones of Maknassy basin located in the southern central Atlas of Tunisia by using coupling of GIS and groundwater modelling method. The GIS-based model was developed for purpose of an artificial recharge, particularly. Data was used to generate a hydrogeological GIS model and maps were made for the conceptualization and the characterization of the aquifer system of the artificial recharge zones of the study area (Chenini *et al*., 2010).

2.7 Seawater Intrusion Observation Using Electrical Resistivity Survey

Irénée *et al* (2016) stated that VES is recognized as one of the most powerful methods to obtain the resistivity data in the field. When the resistivity is decreased with saltwater, seawater intrusion can be interpreted by using electrical resistivity methods. Furthermore, they applied ERT and GIS to identify seawater intrusion and contamination in the parts of the Pondicherry area, South-East coast of India. In their research, geo-electrical resistivity survey was carried out at 7 selected locations within the study area by practising Schlumberger array with an electrode spacing of 100 m in a maximum of the current electrode, (AB/2), with spreading up to 100 m was undertaken to justify complete lithology of the study area. Moreover, the electrical resistivity observation and GIS have been applied for investigating groundwater in various results, the top layer resistivity and thickness spatial distribution maps (Figure 2.14a) illustrates the surveyed site is classified into four classes: less than 20, 20-60, 60-100 and greater than 100 Ohm-m. The resistivity value of less than 20 Ω.m depicts the area is dominated by seawater intrusion in east, west and southern part of the study area, while the resistivity of 20 to 60 Ohm-m and 60 to 100 Ohm-m indicates the area is moderately affected by seawater contamination. Moreover, the resistivity value of the second layer is less than 20 Ohm-m dominated the west and southern part of the study area and their area coverage is 1.47 km^2 and indicates the area is under seawater intrusion, as shown in Figure 2.14b. Otherwise, the major area is not affected by seawater intrusion or geological setting and finding out the extent of seawater intrusion. Based on their salinization for the third layer as shown in Figure 2.14c. Finally, the resistivity value of the fourth layer expresses (Figure 2.14d) that less than 20 Ohm-m covered the west and northern part of the study area and their areal coverage is 0.57 km^2 and indicates the area is under seawater intrusion.

Jatau *et al*. (2013) applied VES by following Schlumberger array covering 15 stations to generate and fully interpret around Bomo area, Nigeria, aiming to successfully investigate the subsurface geological properties in order to determine the depth of basement or geological stratigraphy thickness. Normally the overburden in the bedrock region is supposed to be not as thick as to warrant large current electrode spacing for deeper penetration.

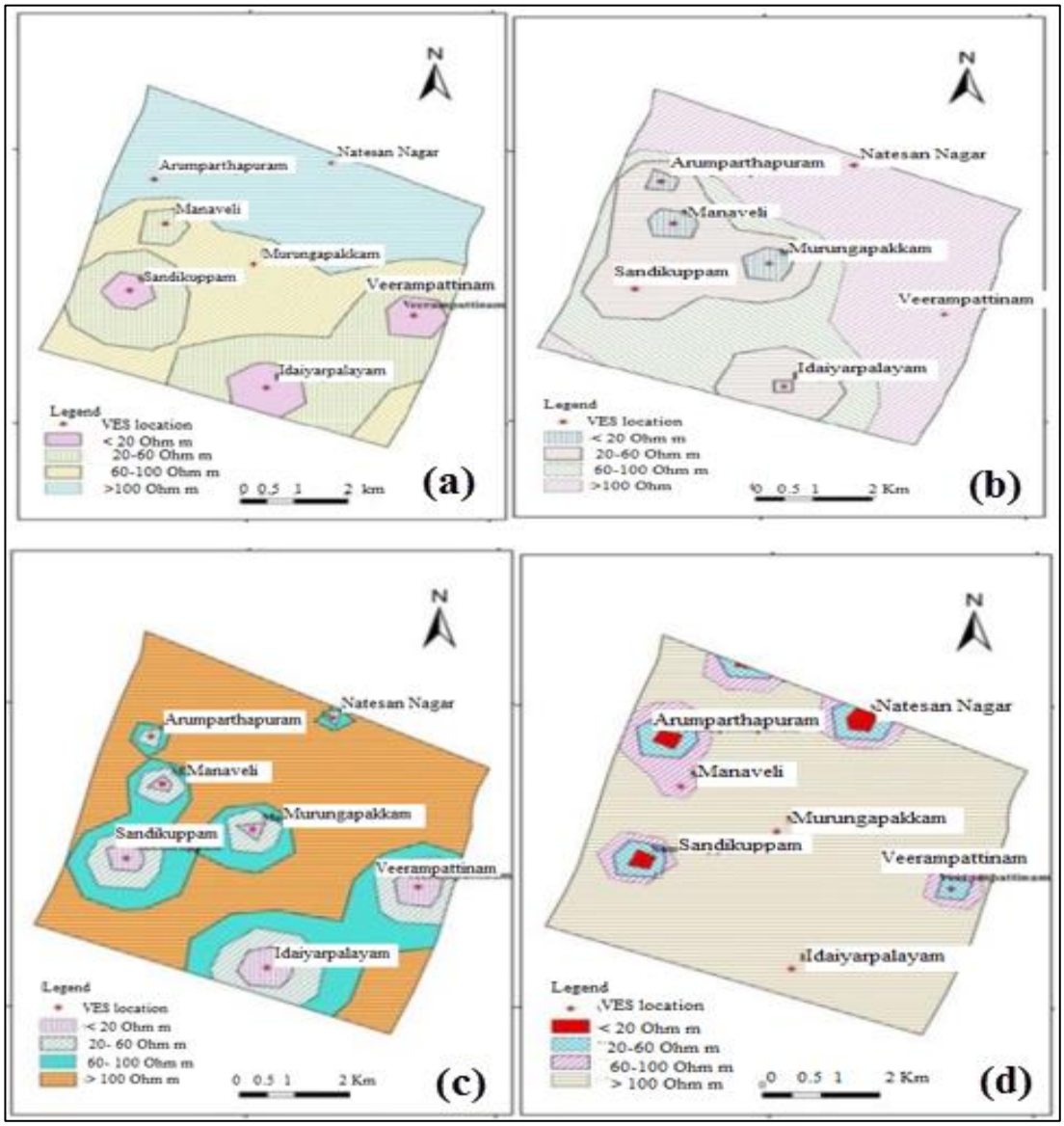

Figure 2.14 Resistivity Spatial Distribution (a) The First Layer, (b) The Second Layer, (c) The Third Layer and (d) the Fourth Layer. (Irénée *et al*., 2016)

Thus, the highest spacing AB which is utilized was around 200 m. They also pointed out the essentiality of using this method for studying civil engineering structures and groundwater prospecting. Three types of resistivity curve were shown in studied area such as H (ρ1>ρ2<ρ3), A (ρ1< ρ2<ρ3) and KH (ρ1>ρ2<ρ3>ρ4) type curves as shown in Figure 2.15, where ρ1,ρ2,ρ3, and ρ4 are the resistivity value of the first layer, second layer, third layer and fourth layer respectively.

According to Figure 2.16 and 2.17, there are mostly three strata under each VES point, and two-layer cases at three different VES points. The subsurface layer in the research site is structured by topsoil (sandy and clayey-lateritic hardpan), weathered bedrock, partly fractured bedrock and fresh bedrock. The resistivity of topsoil ranges from approximately 40 Ohm-m to 450 Ohm-m and the thickness ranges from 1.25 to 7.5 m. However, VES station 1, 2, 7 and 10 can be seen with low values of resistivity ranging from 40 Ohm-m to 90 Ohm-m recommending the clayey nature of the topsoil are high moisture content. The second layer is composed of the weathered basement with resistivity and thickness ranging from 50 Ohm-m and 593 Ohm-m and 1.37 to 20.1 m respectively, whereas the third layer (the partly weathered bedrock) has resistivity and thickness values between 218 Ohm-m to 520 Ohm-m and 12.9 to 26.3 m respectively. Unlike the second and third layer, the fourth layer is the fresh basement whose resistivity values vary from 1,215 Ohm-m to 2,150 Ohm-m with an infinite depth.

Martínez *et al* (2009) successfully used ERT to investigate the seawater intrusion in detrital aquifers, Southern Spain, as shown in Figure 2.18. ERT has provided 2D and 3D electrical images of the subsurface. In this observation, the Wenner–Schlumberger array was applied which apparent resistivity (ρa) for the array is given by

$$\rho_a = n\pi\ (n+1)aR \tag{2.2}$$

where R is the resistance, a is the spacing between the P1 and P2 potential electrodes and n is the ratio of the distances between the current and potential electrodes.

Integrated computer and features, 112 addressable connected through a single seven-core cable, were used with 250 W, 2.5 A and 880 V of the power source to analyze the results as shown in Figure 2.10. Electrodes were required for the spacing of 5 m and 475 m in total length. A total of 2,021 data points of resistivity were recorded, reaching 90.3 m of maximum investigated depth.

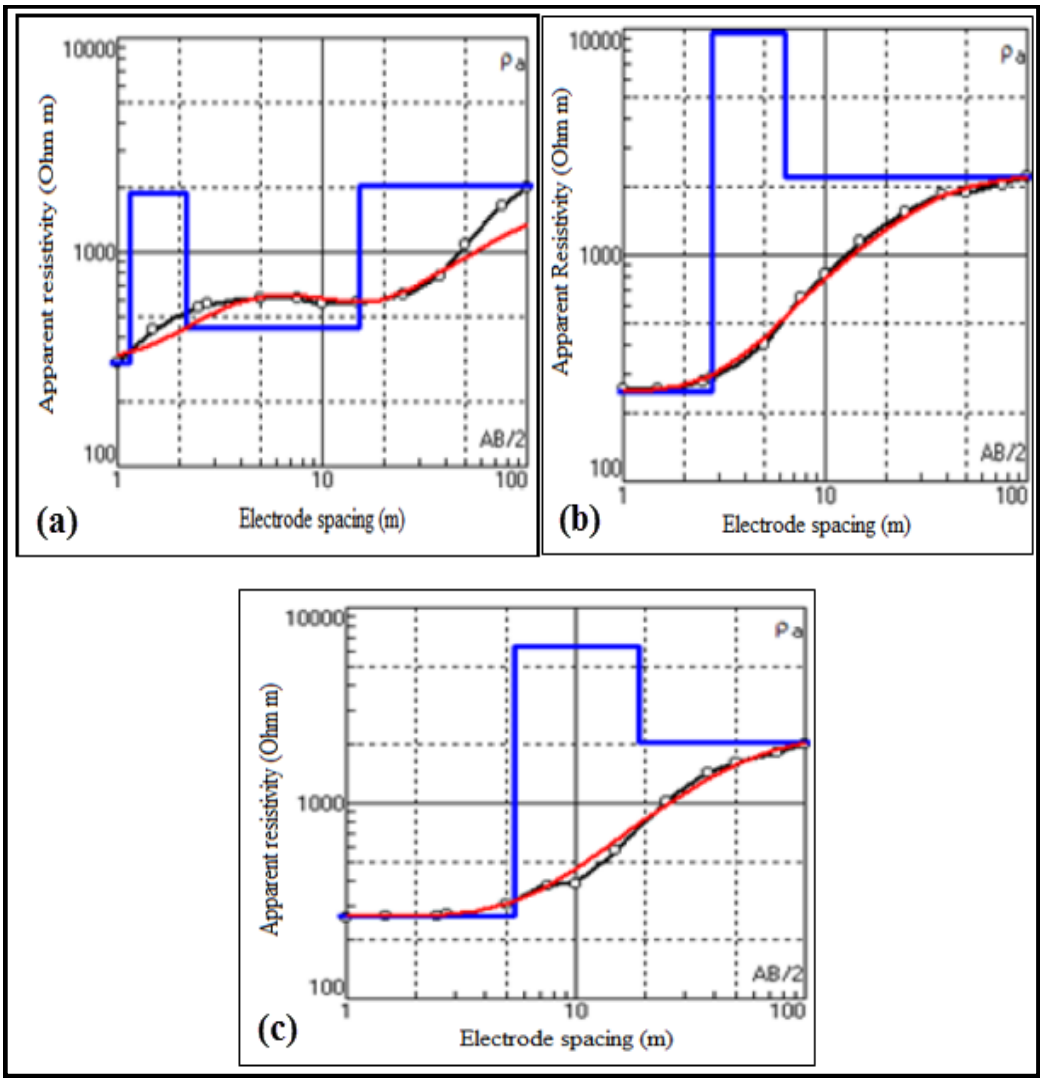

Figure 2.15 VES Curve Types: (a) KH curve- VES Station 5, (b) A curve- VES Station 6, (c) A Curve- VES Station 9. (Jatau *et al*., 2013)

Three levels, in the vertical observation, could be characterized by the degree of resistivity values obtained. There was, in the top layer, a superficial level from 3 to 15 m in thickness with high resistivity values ranging from 20 Ohm-m to 80 Ohm-m, compared to very low levels below 15 Ohm-m and even as low as 2 Ohm-m of the second level as shown in Figure 2.19. Finally, the resistivity values of the third level were characterized by a steady increase from 25 to more than 80 Ohm-m. Profile 1 in (Figure.2.19a) illustrated low resistivity section close to the shoreline (SE), which could

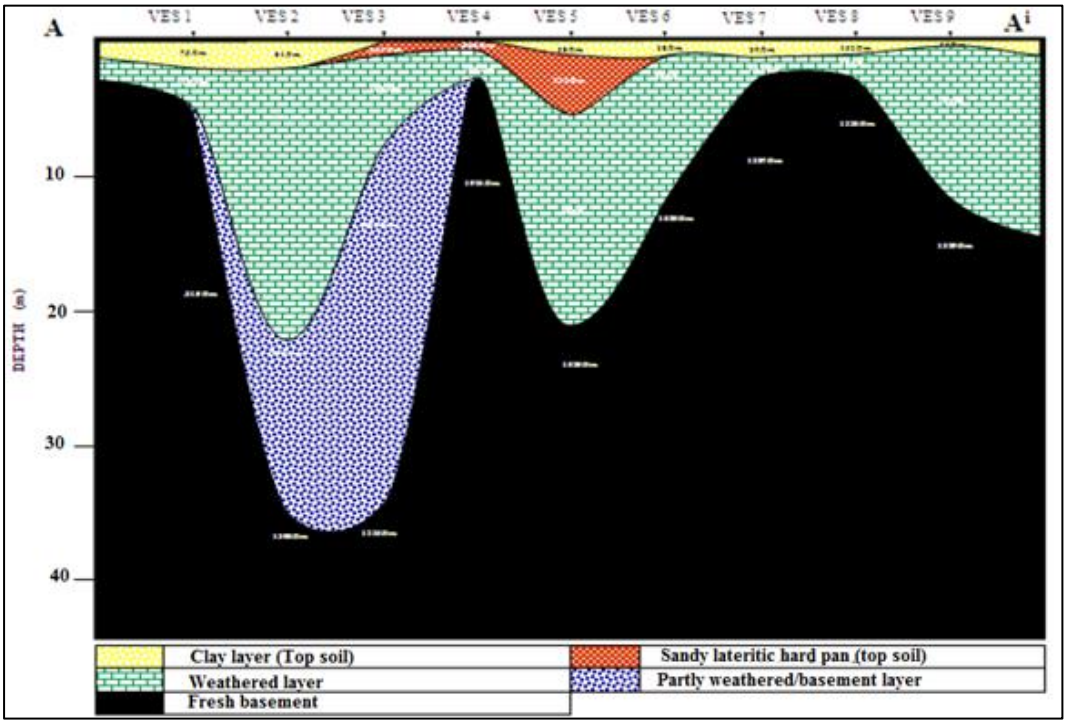

Figure 2.16 Geoelectric Section along Profile A-Ai (Jatau *et al*., 2013)

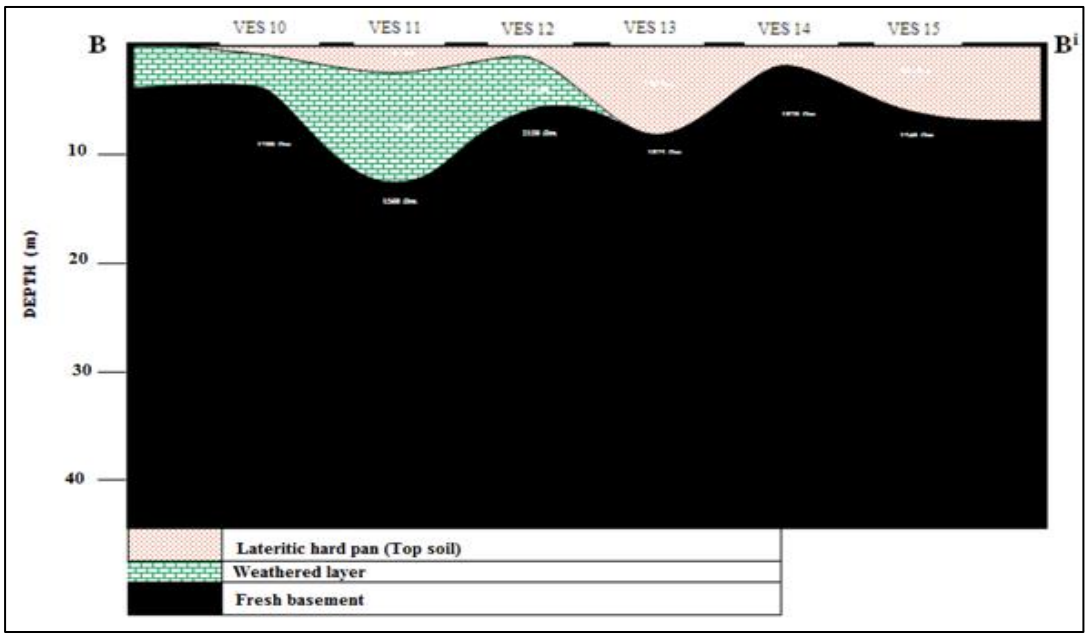

Figure 2.17 Geoelectric Section along Profile B-Bi. (Jatau *et al*., 2013)

be involved in seawater intrusion as in other sectors. The ERT profile 2 (Figure 2.19b) observed a saltwater wedge located near the shoreline which was expected as a consequence of freshwater seepage to the sea. The toe position of salt wedge remained

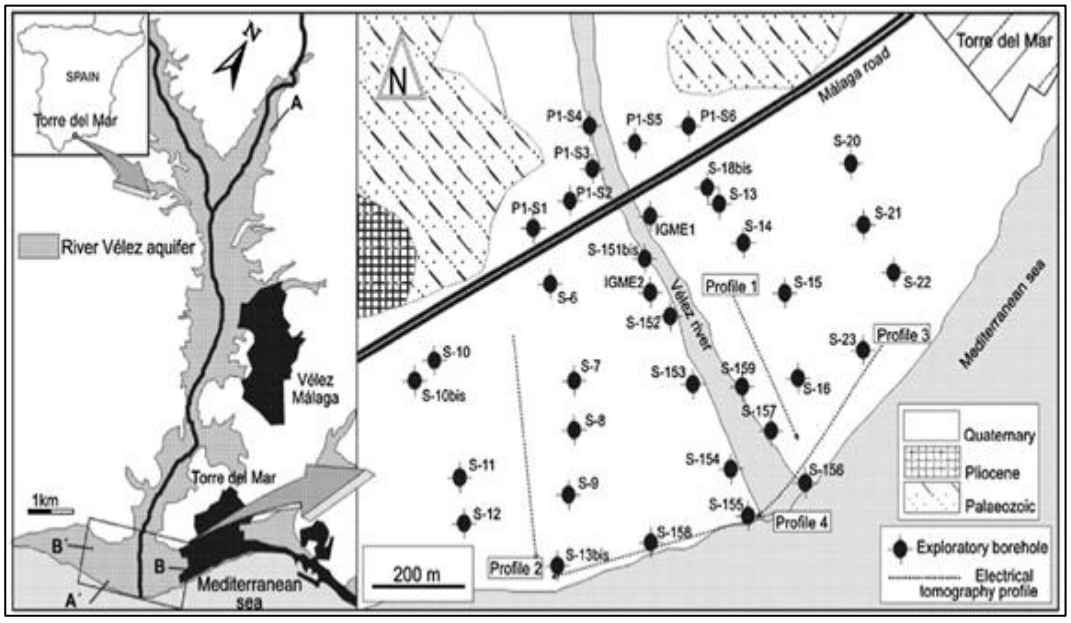

Figure 2.18 Map of Study Area. (Martinez *et al*., 2009

unchanged in Profiles 3 and 4 (Figure 2.19 c and d). The deepest level was the Palaeozoic substrate. The dramatic changes in the altitude of this section were because of faults which affect the basement of the profile. The geometry of the impervious basement deduced from the ERT profiles depicted an average thickness in the eastern sector of the delta higher than in the substrate (Martinez *et al*., 2009).

Moreover, ERM was successfully applied to identify soil layer by (Hazreek *et al*., 2015). His study was categorized into 3 phases: fieldwork, laboratory, and data processing. For fieldwork, ABEM SAS 400 was applied to measure 2D electrical resistivity survey (as called 2DERS) at two different sites representing two various types of soil investigation. Then, Schlumberger array was applied with two resistivity land cables, 41 electrodes, and 42 jumper cables, 0.05 m in spacing and 2.00 m in total length. After that, the soil sample taken from the field was brought to determine water content, particle size distribution (dry and wet sieve) and specific gravity test. Finally, RES2DINV software was utilized to invert raw data obtained from 2DERS in order to map the structure of subsurface as shown in Figure 2.20 and 2.21. Hazreek *et al*. (2016) successfully applied the ERI through using Schlumberger array to identify the small-scale study of detecting cubic concretes buried in the subsurface. It is stated that 3 phases (via laboratory, fieldwork, and data processing) were performed

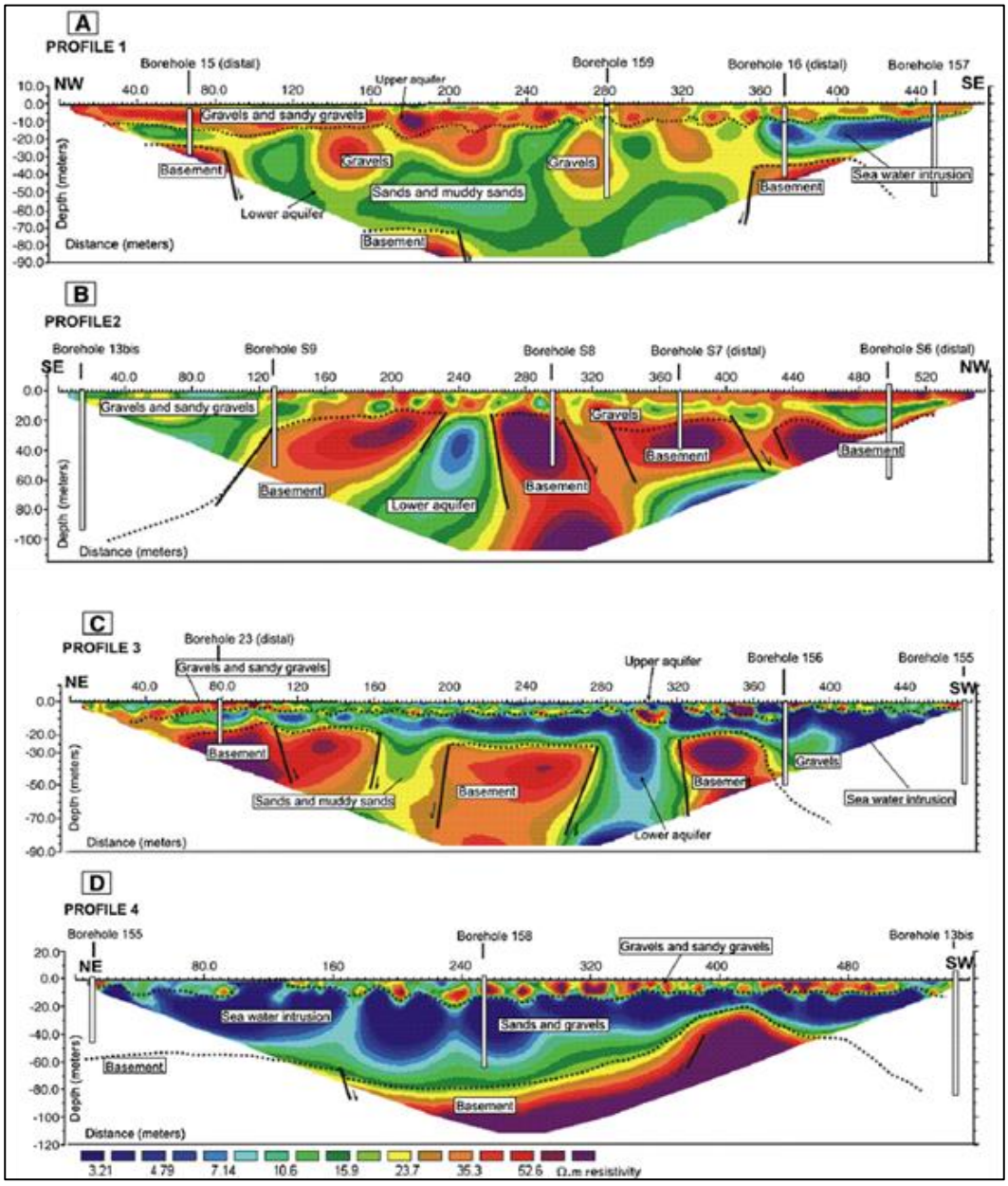

Figure 2.19 Obtained Electrical Resistivity Tomographic profiles. (Martinez *et al.*, 2009)

in their study which strength of 3 cubics concretes (20, 25, and 30 MPa) were tested in laboratory. The construction of lateritic soil model (3.5 m in length, 1 m in wide and 0.5 m in height), as shown in Figure 2.22, was built in the field. ABEM SAS4000 was used for data acquisition and RES2DINV was used to invert the data. Both results are presented in Figure 2.23 and 2.24 referring ERT section and its correlation because of the various strength of the concrete. Based on Figure 2.23 and 2.24, the Schlumberger

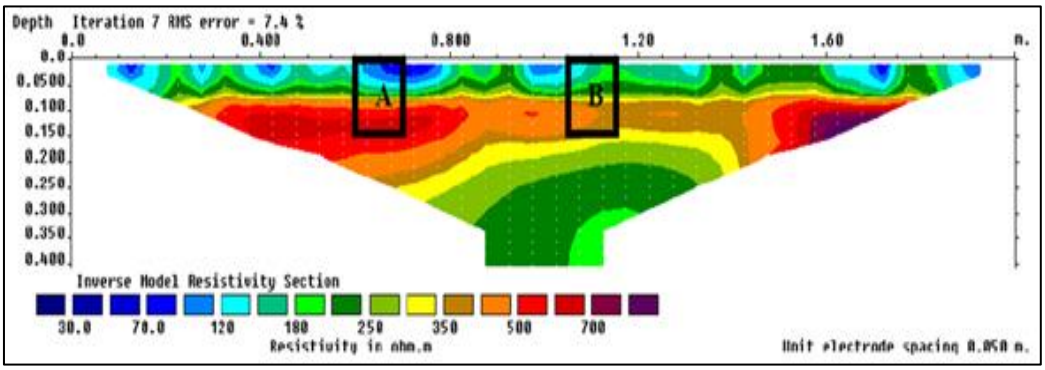

Figure 2.20 Inverted Electrical Resistivity Imaging and Localize Selected Point of ERV for Gravelly Sand. (Hazreek *et al*., 2015)

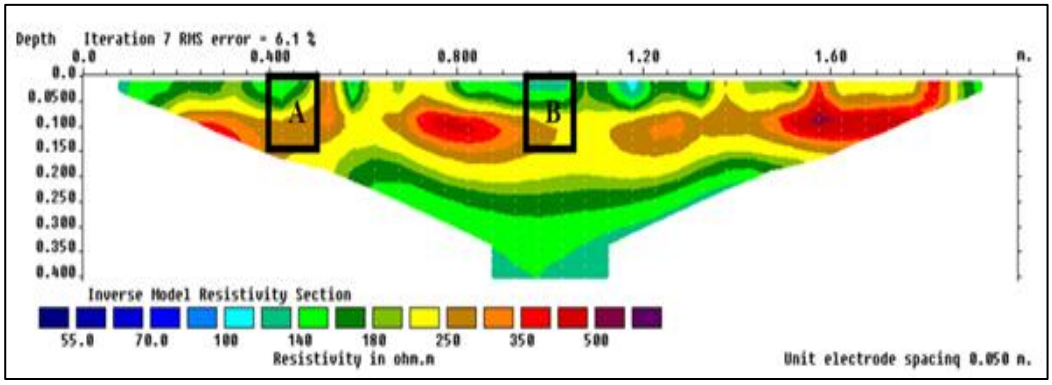

Figure 2.21 Inverted Electrical Resistivity Imaging and Localize Selected Point of ERV for Gravelly Sand. (Hazreek *et al*., 2015)

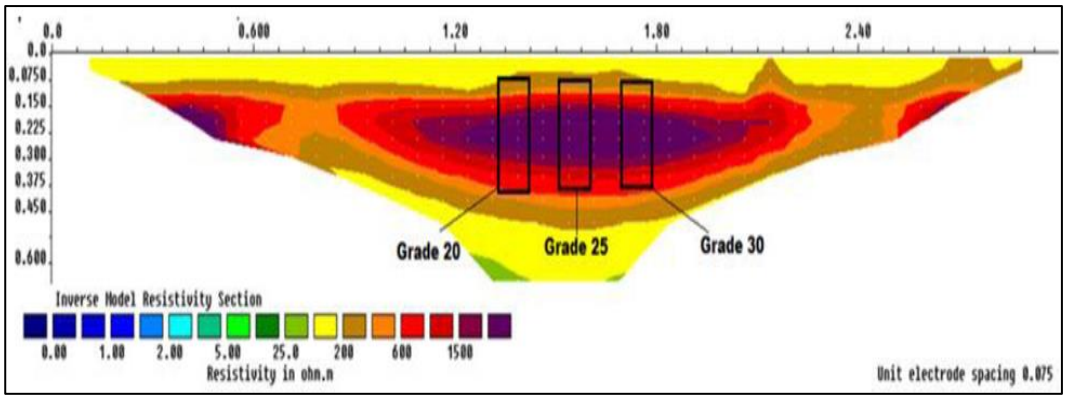

Figure 2.22 Inverted Electrical Resistivity Imaging with Buried Concrete Cube. (Hazreek *et al*., 2016)

array which has 75 mm of spacing was able to investigate the resistivity section of the soil model up to 0.6 m depth. It can be concluded that the low to moderate resistivity

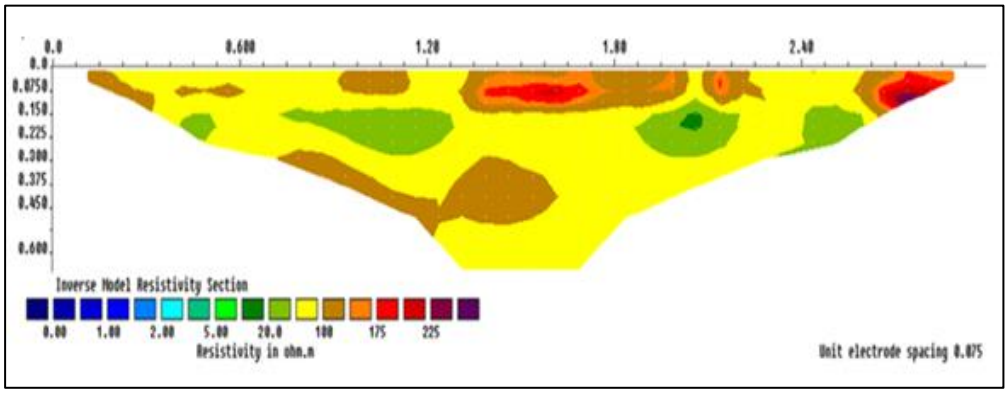

Figure 2.23 Inverted Electrical Resistivity Imaging of Homogenous Laterictic Soil. (Hazreek *et al*., 2016)

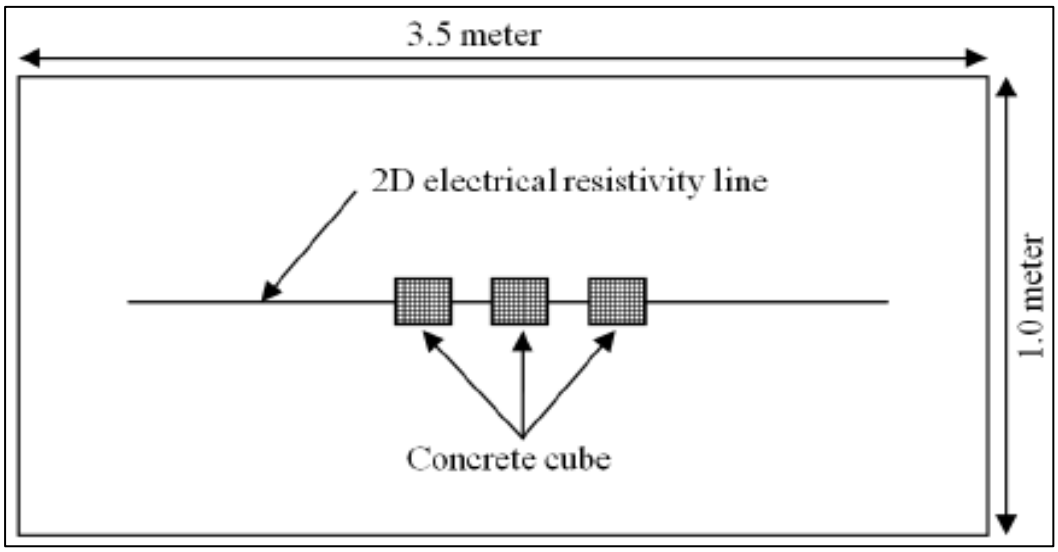

Figure 2.24 Position of the ERI and Buried Object. (Hazreek *et al*., 2016)

value (< 200 Ohm-m) represent the soil model without a buried object. The center of the resistivity profile shows the high value of the Electrical Resistivity Value (ERV) (1,000 – 2,000 Ohm-m). It means that the buried concrete cubes were able to increase the electrical resistivity value. The low to moderate electrical resistivity value (50 – 200 Ohm-m) which surrounds buried concrete cube represents lateritic soil. Therefore, this study has concluded that the electrical resistivity method was able to detect the buried object based on the variation of the electrical resistivity value.

Song *et al*. (2007) demonstrated successfully potential applicability of VES to investigate seawater intrusion area influencing in the watershed at the Byunsan

coastal area, Korea. Furthermore, 30 stations of VES, chemical analyses of groundwater from 15 monitoring wells and some exploratory core drillings were conducted as shown in Figure 2.25. Then, hydrogeological characterizations of the coastal aquifer, monitoring groundwater level and specific conductivity (SC) at a couple of chosen observation wells were studied. In their research, to investigate seawater intrusion zone, VES surveys were performed at 30 points by using Schlumberger array which the spacing of current electrode was extended from the centre while the location of potential electrodes was fixed. Typically, curves of apparent resistivity for a structure which has three layers and is determined from vertical sequence fall into one of four typical types: K, H, A, and Q. The damped least-squares technique, one of the inversion models, as shown in Figure 2.26, was selected for quantitative analysis. The groundwater samples were used to measure pH, electrical conductivity and Total Dissolved Solids (TDS) by using standard field probes. Cation analysis was filtered at 0.45 µm and preserved pH less than 2 using ultra-pure Nitric Acid (HNO3 -) in 125 ml High-density polyethene (HDPE) bottles while samples for anion analysis were filtered at 0.45 µm and kept in 60 ml HDPE. The 125 ml water samples were also collected for analysis of alkalinity. It is commonly seen the salinization of seawater is shown by the rise in TDS and major ions (i.e. Chloride ions, Cl-). Regression slope shows negative in the TDS greater than 2,000 mg/L, while the slope shows positive in the TDS less than 1,000 ml/L, as shown in Figure 2.27. This result might depict the high TDS of groundwater is enriched with Cl- because of seawater intrusion, and low TDS of groundwater is not or less affected by seawater intrusion. Hence, the plot of groundwater sample can be categorized into two groups: one group of groundwater is affected by seawater intrusion and the others are not or less affected by the seawater intrusion, as shown in Figure 2.28.

Hwang *et al*. (2004) used vertical electrical soundings (VES) and well-logging to map the seawater-freshwater interface in a more quantitative analysis in a coastal aquifer, Youngkwang-gun, Korea, as shown in Figure 2.29. The survey region extends for more than 24 km2. For investigating seawater intrusion, 60 stations of VES, with Schlumberger array and 150 m in maximum spacing of current electrode, were applied and 12 drilling wells were used to collect hydrogeological, geochemical, and geophysical well logging data. The principle objective of their research is to create a relationship between conductivity and equivalent Sodium chloride (NaCl)

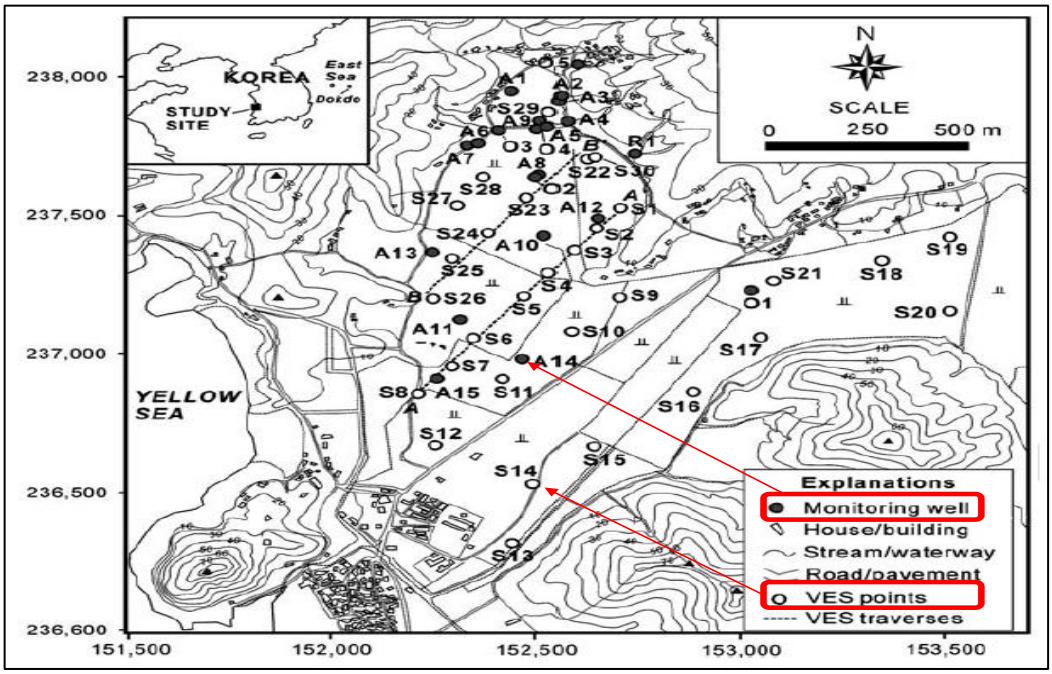

Figure 2.25 Map of the Study Area Indicating Monitoring Well and VES Points. (Song *et al*., 2007)

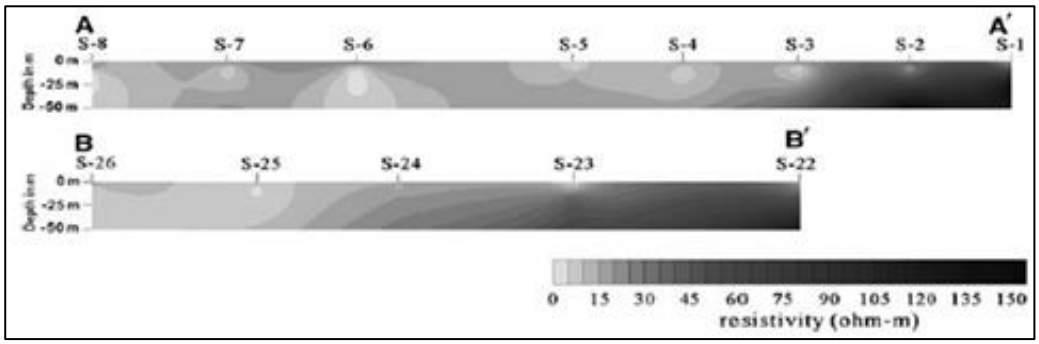

Figure 2.26 Variation of Resistivity Contour due to the Intrusion of Seawater. (Song *et al*., 2007)

concentration in groundwater from hydrological analysis result. Then the mapping the salinity in a coastal aquifer was created. They made a comparison between the drilling logs from the survey area, indicating that the thickness of mud (5-20 m), sand (25 m) and Granite bedrock (below 25m, the result of VES, as shown in Figure 2.30. Based on the comparison, they found that the thickness of the subsurface layer was insignificantly greater than the well-logging confirmation. This discrepancy is because of saturated pore water, with high electrical conductivity, in the weathered zone on the granite below

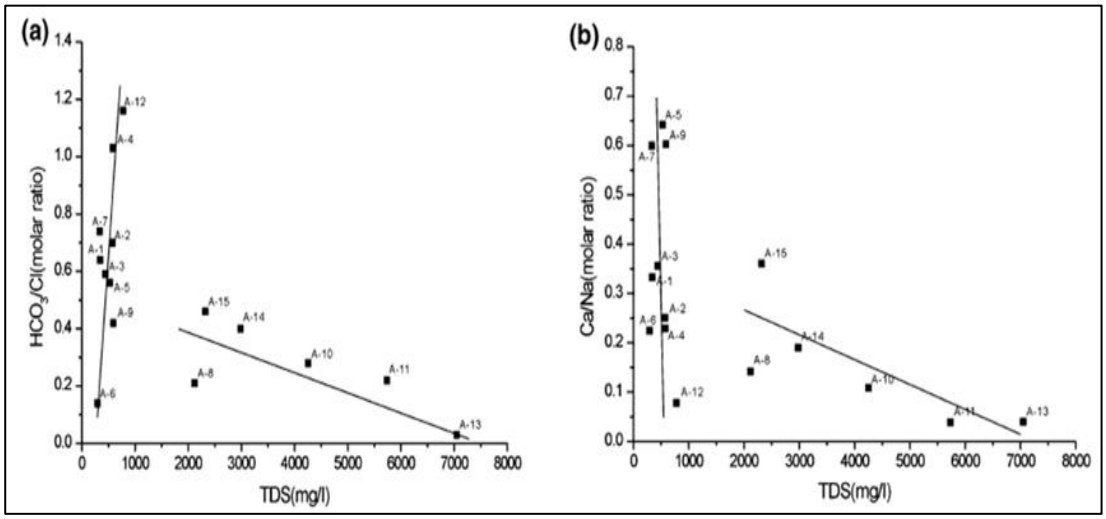

Figure 2.27 Molar Ratios of A) HCO_3^-/Cl^- and TDS Concentration and B) Ca^{2+}/Na^+ and TDS Concentration. (Song *et al*., 2007)

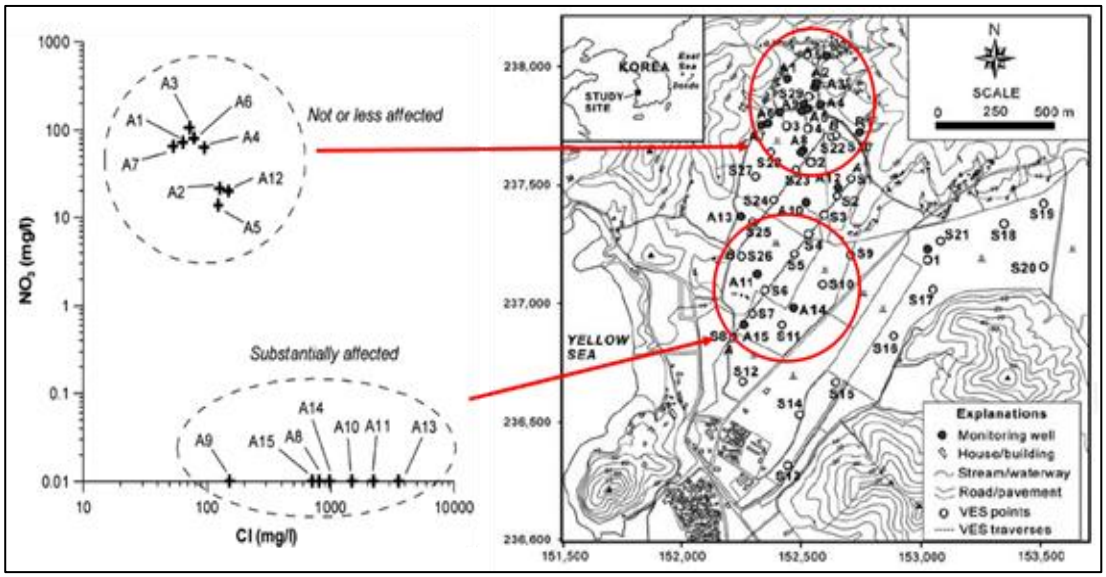

Figure 2.28 Plot of Cl^- Versus NO_3^- Concentrations. (Song *et al*., 2007)

the layer of sand. The resistivity is not much more than 10 Ohm-m, and the fluid conductivity of the borehole indicates to be more than 5,000 μS/cm. The outcome of VES was applied to create a salinity map and to investigate the seawater-freshwater in the sand layer as shown in Figure 2.31. The salinity in the layer of sand might be evaluated more quantitatively if it was demonstrated the groundwater resistivity in terms of the concentration of dissolved salts in the aquifer. Therefore, the groundwater resistivity in the main aquifer to an equivalent NaCl concentration was converted. The

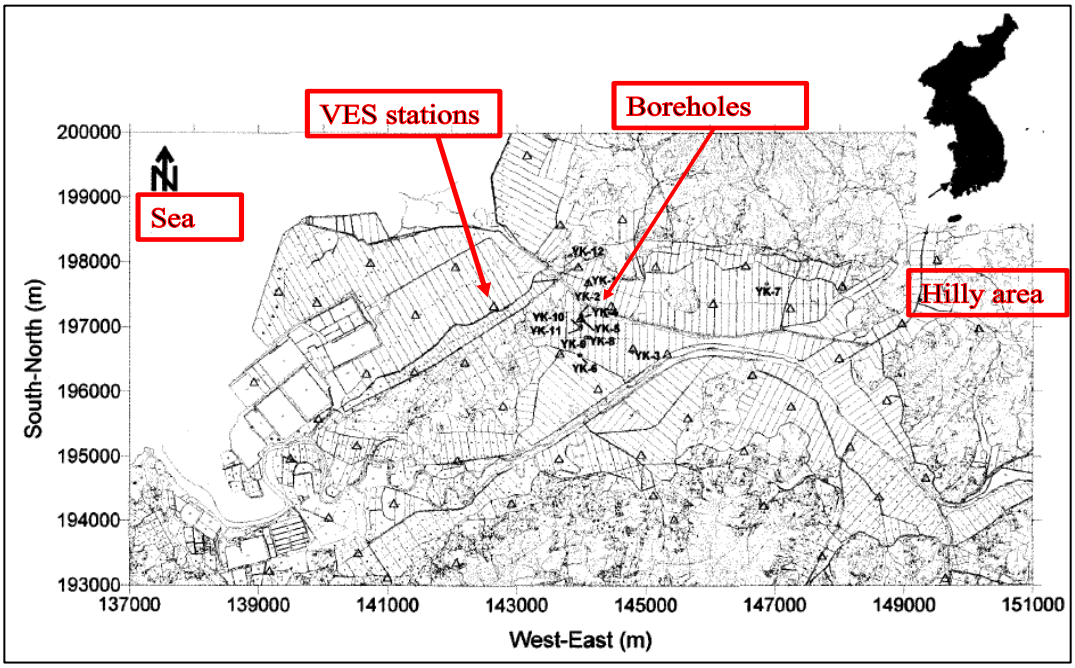

Figure 2.29 Location Map Showing Bore Hole and VES Station in the Survey Area, Youngkwang-Gun, Korea. (Hwang *et al*., 2004)

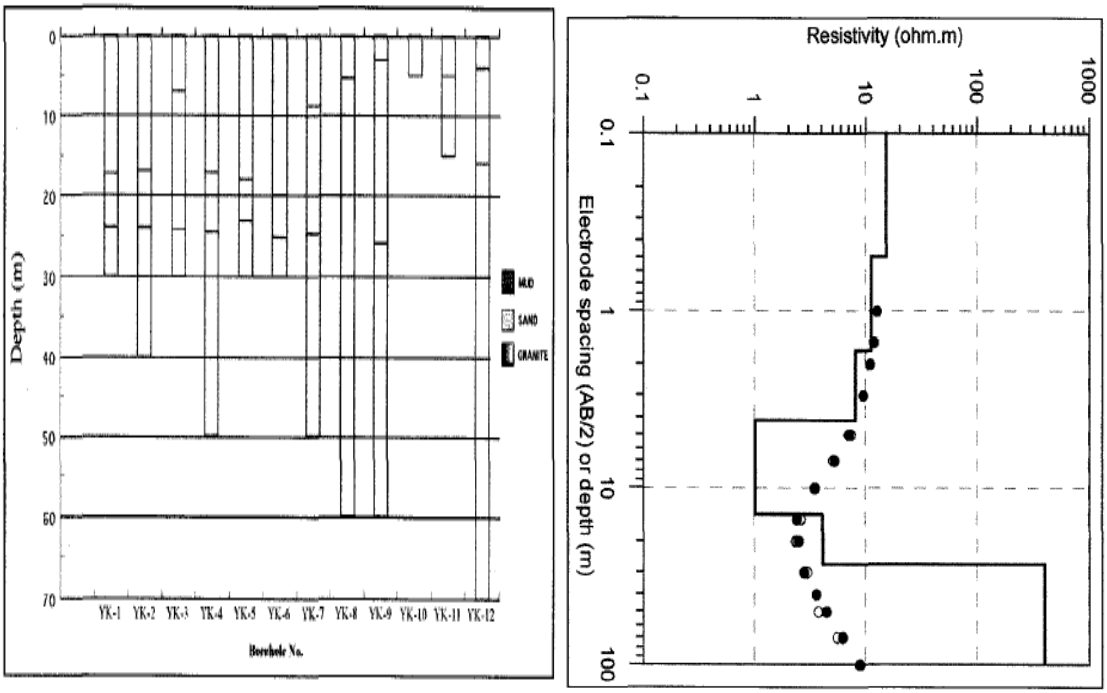

Figure 2.30 Thickness of Layers Obtaining from Logging (Left) and from VES Survey (Right) (Hwang *et al*., 2004)

equivalent NaCl concentration for the pore water in the sand layer was estimated by using the results of chemical analysis for cations and anions of the groundwater within the survey area with the verification of determination coefficient (R2) is equal to 0.98 as follows:

$$ppm_{eq} = 4612 \times R_0^{-0.98}, R^2 = 0.98 \quad (2.3)$$

Where ppm_{eq} is the equivalent NaCl concentration (ppm), R_0 is the saturated formation resistivity (Ω.m) and R^2 is the correlation coefficient in the least-squares fit.

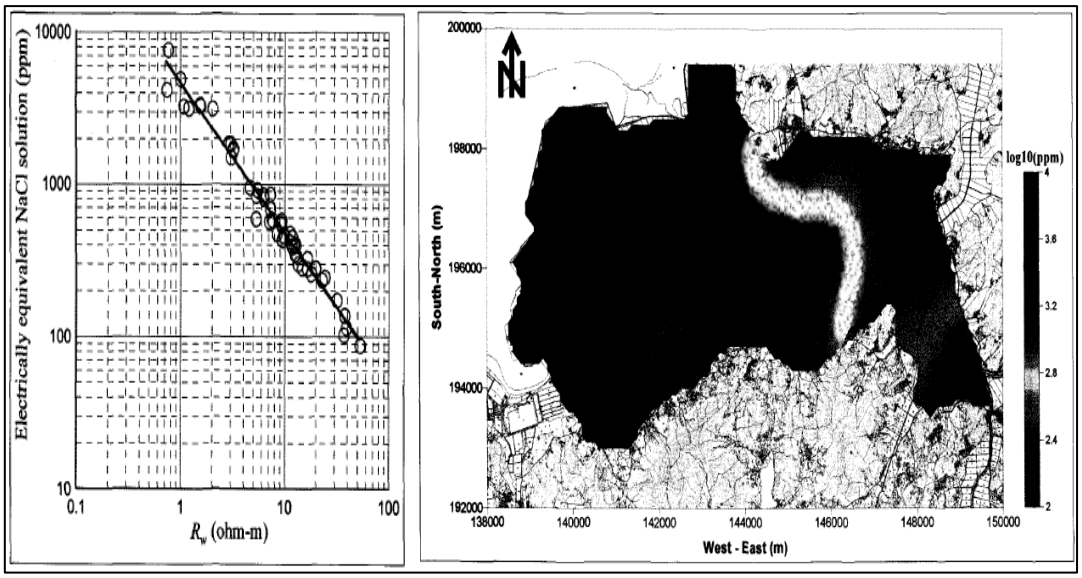

Figure 2.31 Relation between Groundwater and Nacl (Left) and Contour Map of Estimated Equivalent Nacl Concentration, in ppm, in the Sand Layer. (Right) (Hwang *et al.*, 2004)

Literature reviews for interpreting seawater intrusion based on the value of resistivity have been summarized in Table 2.2.

Table 2.2 Summary of Resistivity Value for Seawater Intrusion Interpretation

Reference	Study Area and Methodology	Resistivity value for indicating seawater intrusion
(Chafouq *et al.*, 2016)	- Ghiz-Nekor Aquifer (North Morocco)	- Low resistivity values are detected in the range of 0.5 to 4 Ohm-m and reflect the extension

Table 2.2 Summary of Resistivity Value for Seawater Intrusion Interpretation (cont.)

Reference	Study Area and Methodology	Resistivity value for indicating seawater intrusion
	- ERT (Werner Schlumberger array)	of seawater intrusion.
(Eissa *et al.*, 2016)	- Bagoush area, Northwestern coast, Egypt - ERT (Werner array) and Groundwater chemistry and isotope analyses	- Brackish water zone vary from 7.0 Ohm-m to 15.0 Ohm-m. - Saline water zone vary from 3.0 Ohm-m to 7.0 Ohm-m.
(Maury & Balaji, 2015)	- Bay of Bengal - Resistivity sounding method GPR method Borehole litho-stratigraphy Groundwater sampling	- Resistivity of 0.8 to 2.1 Ohm-m illustrates the presence of marine intrusion/deposits.
(Kura *et al.*, 2014)	ERT (Schlumberger array)	- A low resistivity of 1 to 10 Ohm-m indicates seawater intrusion - The resistivity values of 25 Ohm-m indicates the dilution of saltwater. - The resistivity values of 50 to 100 Ohm-m indicates fresh water.
(Cimino *et al.*, 2008)	- Acquedolci coastal aquifer (Northern Sicily) - Apply VES and chemical analysis of groundwater	- Intruded aquifers is lower than 5–10 Ohm-m - Values <10 Ohm-m were interpreted as high chlorine groundwater.
(Song *et al.*, 2007)	- The coastal area of Byunsan, Korea - Applying monitoring wells and VES	- High TDS groundwater vary from 0.9 to 3.0 Ohm-m, compared to 0.2 Ohm-m of seawater resistivity.

Table 2.2 Summary of Resistivity Value for Seawater Intrusion Interpretation (cont.)

Reference	Study Area and Methodology	Resistivity value for indicating seawater intrusion
(Sherif *et al*., 2006)	- Wadi Ham, UAE - Apply earth resistivity imaging methods along with water hydro-geochemistry	- The brackish and saline water zone marked with a resistivity range of 1– 30 Ohm-m.
(Hwang *et al*., 2004)	- Youngkwang-gun, Korea - Apply geophysical well logging and VES	- The electrical conductivity of brackish water is assumed to be 2000-8000 $\mu S/m$ (1.25-5 Ohm-m).

2.8 Seawater Intrusion Monitoring

Monitoring data from observation wells are regarded as essential methods for investigating seawater intrusion and the fluctuation of groundwater level. Monitoring network is normally composed of the design of field survey, sample collection, data analysis and information evaluation which is being used to detect and characterize changes in the aquifer system that might arise from human and natural influences. Monitoring network depends mainly upon the natural, the quality of existing records regarding aquifer geology, the groundwater regime, other sources of contaminants, and available financial resources. Monitoring information is needed to realize the distribution of temporal magnitude and dynamics of seawater within aquifer. It is used to present the gradients and flow velocities within the aquifer.

Melloul and Goldenberg (1997) successfully monitored on seawater intrusion by applying direct (in-situ measurement in the field and water sampling) and indirect (geophysical techniques) measurements to obtain the monitoring data of seawater intrusion. It was stated that the hydrological cross-section of aquifer is considered as one of the complicated seawater intrusion monitoring because seawater can penetrate in a different ways and to various distances from the sea based on different kinds of the aquifer. Thus, the study of seawater intrusion should be conducted a detail network of observation wells and sampling in responding to the sudden changes of

groundwater quality which is responsible for the adverse development of salinization that may occur over a relatively short period of time in the seawater intrusion area. Moreover, it is added that well data are very useful to map seawater contamination in aquifers for management of coastal aquifer systems. The scarcity of field data observation from monitoring network is undoubtedly possible to produce inaccurate outcomes and to be difficult to compare the hydrological situation between separate periods. In the case of the high well deterioration, the monitoring of seawater is supposed to require increasing use of geophysical methods (Melloul and Goldenberg, 1997).

Qahman *et al*. (2001) designed a monitoring network for seawater intrusion in the Gaza Strip by using SUTRA-ANE 3 computer code with the components of discretization and boundary conditions, selection of model parameters, set-up of the steady-state flow model, set-up of the transient model and finally calibration of the model. It is mentioned that the water head and permeability can drive the variation in the saline-freshwater interface. The clay layer can be a factor to separate the transition zones in the sub-aquifers. It was, furthermore, recommended the separate monitoring system of the chloride line of 10,000 mg/L for each sub-aquifer as the best alternative for designing seawater intrusion monitoring because the economic situation in the Gaza strip is not good which will not allow the construction of a typical seawater intrusion monitoring network. The main factor that caused seawater intrusion in the Gaza strip is due to a large amount of abstraction which is abstracted from the upper sub-aquifer. Therefore, the priority for seawater intrusion monitoring is for the upper sub-aquifer.

Giambastiani *et al*. (2007) applied the successfully numerical model to investigate seawater intrusion in the unconfined coastal aquifer of Ravenna and to discuss the present and future distributions of fresh, brackish, and saline groundwater. It is evidently proved that seawater intrusion is continuously effected owing to past anthropogenic such as industrial development and land reclamation and so on. Moreover, they used a numerical model to predict the future sea level rise and land subsidence and then confirmed that the extension of seepage owing to the heavy drainage system could be possible to cause an upcoming interface of the saline

groundwater from the bottom. Sherif *et al*. (2012) have conducted field investigations to investigate the physical conditions in the Wadi Ham, UAE and confirmed the information acquired from remote sensing images, including dam location, pumping, and observation wells. Groundwater levels were also surveyed in a number of observation wells to ensure the reliability and consistency of the historical data and other information available in the water resources. In this study, MT3D, the program function of MODFLOW, and Darcy's law equation were used to simulate the result.

CHAPTER 3

METHODOLOGY

The following is the flowchart of study (Figure 3.1) which is the main processes of study methodology, starting with data collection from Department of Groundwater Resource (DGR), between 2003 and 2016, used to analyze and assessed the most risk area of seawater intrusion in Phuket. The assessment of seawater intrusion is indicated as the output by using GIS software. Then the flowchart is ended with using ERS to delineate the distribution of seawater intrusion in the study areas. Then the resistivity data were validated by groundwater chemistry data.

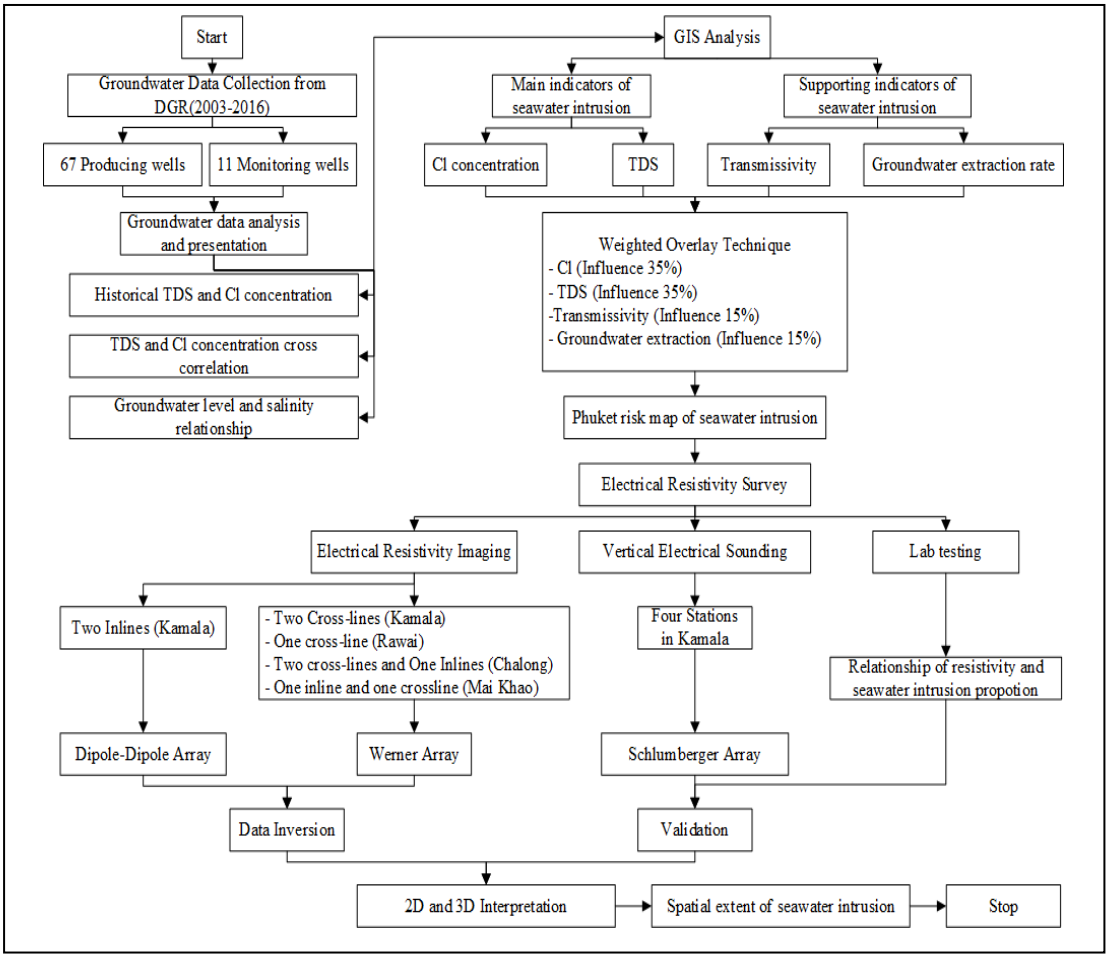

Figure 3.1 Flow Chart of Methodology

3.1 Site Description

The overview of the study area is composed of 8 areas in the western, northern and southern coast of Phuket island corresponding to a network of monitoring wells as shown in Figure 3.2. Sixty-seven of producing wells and 11 monitoring wells have been installed in the study areas including Area 1 (Chalong), Area 2 (Rawai), Area 3 (Karon), Area 4 (Kamala), Area 5 (Mai-Khao), Area 6 (Choeng-Thale), Area 7 (Sisunthorn), and Area 8 (Thep-Krasatti) with coordinate as shown in Table 3.1. In addition, this map (Figure 3.2) depicts all electrical resistivity survey lines (4 lines in Kamala, 2 lines in Chalong, 1 line in Rawai, and 2 lines in Mai Khao) and 4 VES stations in Kamala.

Table 3.1 Coordinates Of Study Area

Study Area	Latitude	Longitude
Area 1 (Chalong)	7°49'34.3"N	98°20'45.1"E
Area 2 (Rawai)	7°46'57.5"N	98°19'55.9"E
Area 3 (Karon)	7°50'17.5"N	98°18'11.4"E
Area 4 (Kamala)	7°57'14.3"N	98°17'07.9"E
Area 5 (Mai Khao)	8°11'43.4"N	98°17'28.5"E
Area 6 (Choeng Thale)	8°00'54.5"N	98°18'00.8"E
Area 7 (Sisuthon)	7°58'54.4"N	98°20'25.7"E
Area 8 (Thep Krasitti)	8°02'51.1"N	98°20'17.6"E

3.1.1 Phuket Geological Setting

Phuket, the biggest island in Thailand, located in the Andaman Sea of southern Thailand, is the place that has been developed significantly: economic improvement, social integration, industrialization, especially the expansion of tourism vision. This region is mostly covered by granite, which is hard and several meters deep, but it provides a good potential groundwater. Phuket shown in Figure 3.2 is a large-sized island with approximately 70% of its area covered by mountains stretching from North to South, and 30% of flat plain areas, mainly in the middle and eastern parts of the island. It is located in the Andaman Sea, on the West side of peninsular Thailand. Geographically, there are no main rivers, but there are nine brooks and creeks. The western coast has stretches of mountain and white sandy beaches, and the highest point

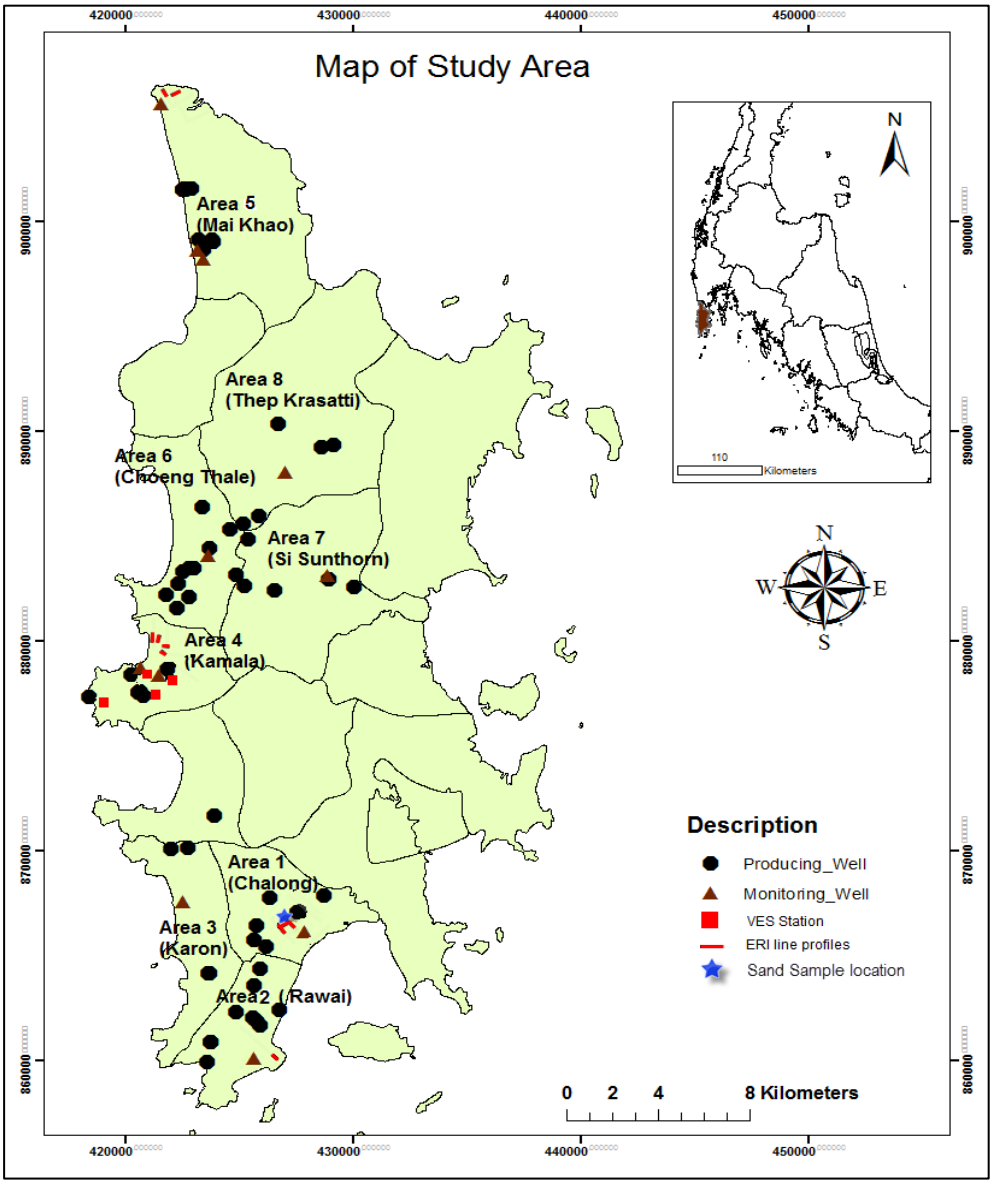

Figure 3.2 Overview Map of Study Area**.**

Is at Mai-Sip-Song, 529 m above the mean sea level (MASL). The eastern part is dominated by muddy soil and mangrove forests. The total forest area is around 307.90 km^2, contributed by 9 forests and 7 mangrove forest (192,437 Rai, 2007 – 2009). Phuket is located at 7^0 45' – 8^0 15' N and $98^0$15' – $98^0$40' E and the total area is 576 km^2 (including the province's other islands). Basically, Phuket Island is geologically composed of igneous rock (granite and granodiorite) in the western part, and of sedimentary rock (mudstone and conglomerate) in the central part (DGR, 2010; DGR, 2012). The geological setting of Phuket as shown in Figure 3.3 is naturally formed through a tectonic setting in the southern part of Thailand and has a major fold with

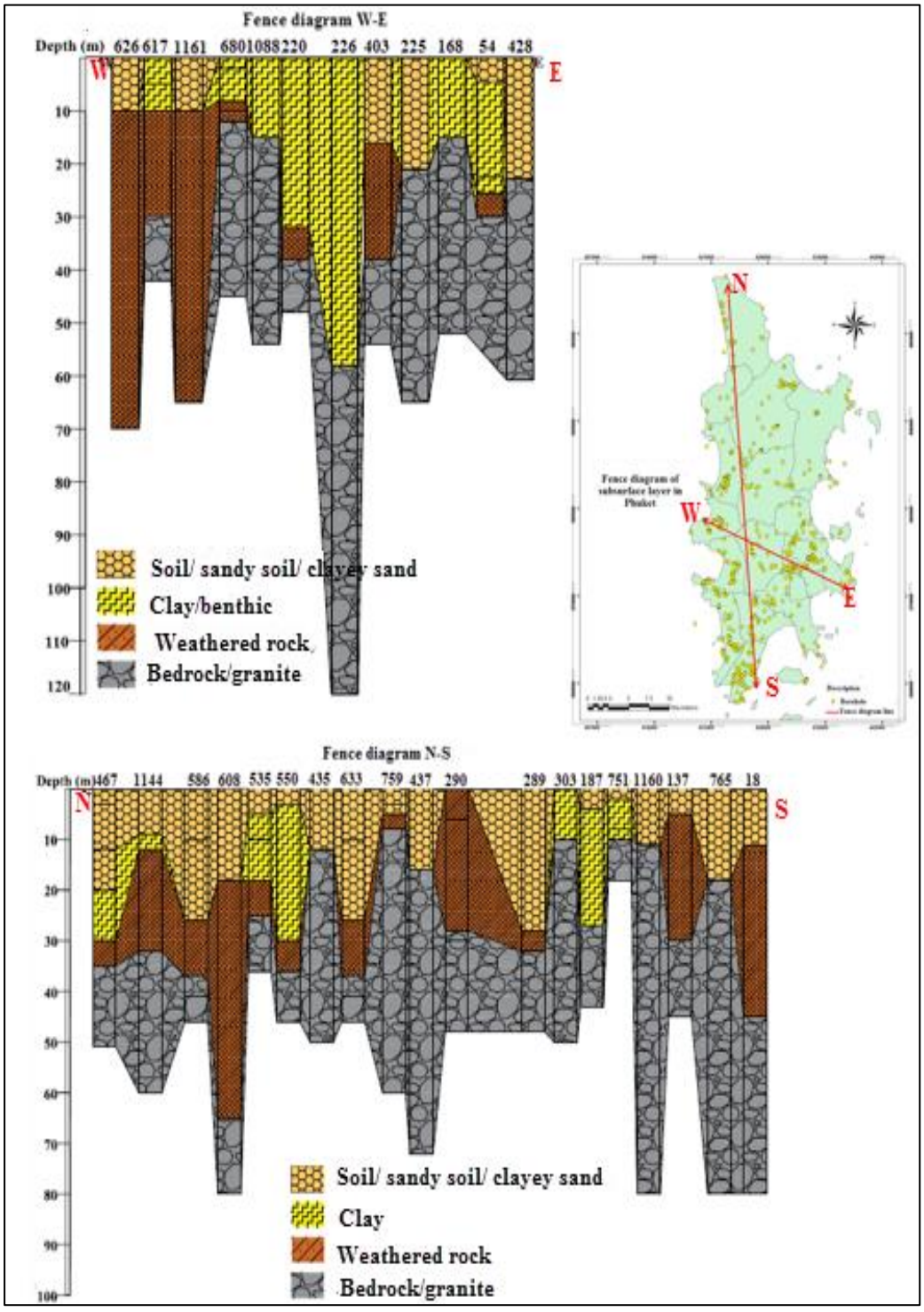

Figure 3.3 Fence Diagram of Subsurface Layer: (a) Cross-Section Line from West to East And (b) Cross-section Line from North to South.

intrusive granite in the North-South direction. Phuket Island has both a fold produced by granite intrusion in the Cretaceous age and a fault caused by the convergent boundary of a tectonic plate, creating a subduction zone in the Andaman region. Quaternary sediments in this area have accumulated unexpected geomorphology variations in the recent neo-tectonic age (DMR, 2013).

3.1.2 Phuket Hydrogeology

The groundwater is stored in several consolidated rock aquifers (47%), unconsolidated rock aquifers (24%), and intercalations between consolidated and unconsolidated rock aquifers (29%). The highest groundwater potential is located in Tepkrasattri sub-district, Thalang district, and this potential aquifer is divided into haft of sedimentary and metamorphic rock in the range of 240 – 720 m^3/day at depths from 20 to 40 m, sand beach sediment 120 – 240 m^3/day at depths from -2 to -4 m, alluvial sediment with the range of 48 – 240 m^3/day at depths -10 to -25 m, and gravel (mountain fragment) sediment with 120 – 360 m^3/day at depths -20 to -30 m, as shown in Figure 3.3. Sea level rise caused by global warming might become a root cause for seawater trying to enter the freshwater aquifers. The rise of sea level could also lift the entire aquifer and this lifting would help alleviate the overall long-term impacts of seawater intrusion. There has been a gradual rise of Andaman mean sea level from 1992 to 2016 at the rate of around 4.2 mm/year (NOAA, 2017).

3.2 Risk area assessment of seawater intrusion

This study utilized mainly groundwater chemistry data in the laboratory at the Department of Groundwater Resources (DGR), Thailand. Groundwater samples were taken from the field and were analyzed for determining key indicators of seawater including Cl and TDS concentrations in both producing wells and monitoring wells. Transmissivity and groundwater extraction data were obtained by the producing wells only. Cl and TDS concentrations are the two main chemical indicators of seawater intrusion problem. Then, mapping of seawater intrusion was done using GIS technique, as shown in the flowchart in Figure 3.1, in order to show the high-risk areas for seawater intrusion on Phuket Island. Details of the methods in this research are discussed as follows.

3.2.1 Data Collection

The groundwater data for analyzing seawater intrusion were obtained from the Department of Groundwater Resource (DGR). It is categorized into two main types of yearly datasets covering all study areas. The first dataset is groundwater producing wells (wells No. A1-67) and another dataset is the network monitoring wells (wells No. B1-11). The concentration of Cl and TDS data comes from 67 producing wells (during 2003 - 2010) and 11 network monitoring wells (during 2012 - 2016), as shown in Table 3.2. The groundwater level data in those eight areas were also gathered from 2004-2017 to use as an indicating factor of seawater intrusion. Phuket base maps of transmissivity and groundwater extraction (Kong, 2017), as shown in shown in Figures 3.4 and 3.5, respectively, have been used to be supporting factor of seawater intrusion.

Table 3.2 Groundwater Data in Different Eight Studied Areas

Location (District)	ID	Latitude	Longitude	Cl (mg/L)	TDS (mg/L)	groundwater level(m)	Year
Area 1 (Chalong)	A51	425781	866461	15	68	20	2004
	A52	427568	867053	644.8	1.13	25	2009
	A53	428732	867859	8.75	45.2	6	2009
	A54	425649	865743	11.49	106	20	2010
	A55	426193	865412	7.94	64.6	40	2010
	A56	426332	867773	14.75	203	20	2010
	A57	427559	867066	0.14	388	7	2010
	B10	427899	866122	1850	3585	2.04	2012
				1800	3495	2.19	2013
				1750	3480	2.08	2014
				1710	3325	2.42	2015
				1720	3380	2.6	2016
Area 2 (Rawai)	A58	423568	859953	43	184	30	2004
	A59	423759	860889	43	274	3.2	2005
	A60	423757	860889	41	228	9.6	2005
	A61	425682	863573	41	170	8	2005
	A62	425896	861694	180	424	6	2008
	A63	425593	862062	15.24	87.4	2	2009
	A64	426788	862424	12	58.2	6	2009
	A65	425760	861908	12.5	176.9	6	2009
	A66	424880	862315	18.49	119.2	6	2009
	A67	425905	864395	37.74	164	20	2010
	B11	425630	860102	3200	6015	3.53	2012
				3200	5910	3.55	2013
				3200	5955	3.10	2014

Table 3.2 Groundwater Data in Different Eight Studied Areas (cont.)

Location (District)	ID	Latitude	Longitude	Cl (mg/L)	TDS (mg/L)	groundwater level(m)	Year
				3200	6085	3.45	2015
Area 3 (Karon)	A47	423643	864184	29	180	7.8	2005
	A48	422757	870142	15	164.1	40	2008
	A49	423676	864139	36	252	23	2008
	A50	421984	870086	16.44	237	10	2009
	B9	422544	867537	28	151.5	6.75	2012
				26	140.5	7.62	2013
				28	151	5.44	2014
				35	179.5	6.06	2015
				23.5	177.5	9.28	2016
Area 4 (Kamala)	A35	420806	877402	13	170	22	2005
	A36	421865	878636	12	124	11	2008
	A37	420581	877566	159.95	475	60	2009
	A38	420610	877572	14.5	49.6	60	2009
	A39	423923	871698	13.75	117.5	6	2009
	A40	420646	877580	11	258	60	2009
	A41	420282	878373	26.36	270	30	2009
	A42	420610	877572	50.36	230	40	2009
	A43	420581	877566	36.24	147.1	42	2009
	A44	432496	860065	101.72	280	10	2009
	A45	420646	877582	32.49	208	45	2009
	A46	418391	877358	20.49	194.1	20	2010
	B3	420666	878738	6290	10945	2.35	2012
				5690	10525	2.38	2013
				5720	10790	2.22	2014
				5670	10850	2.38	2015
				5665	10675	2.65	2016
	B8	421464	878354	33	310.5	2.18	2013
				19	177.5	1.36	2014
				19.5	288	5.10	2015
				24	285	1.8	2016
Area 5 (Mai Khao)	A17	422555	901504	14	222	15	2008
	A18	422586	901510	13	210	14	2008
	A19	422626	901514	18	222	13	2008
	A20	422608	901513	16	212	13	2008
	A21	422554	901514	16	224	18	2008
	A22	422558	901534	29	252	18	2008
	A23	422579	901531	28	232	18	2008
	A24	422880	901549	28	258	18	2008
	A25	422610	901554	20	102	18	2008
	A26	423214	899127	304.91	672	6	2008
	A27	423869	899017	78.73	164.3	6	2008

Table 3.2 Groundwater Data in Different Eight Studied Areas (cont.)

Location (District)	ID	Latitude	Longitude	Cl (mg/L)	TDS (mg/L)	groundwater level(m)	Year
Area 5 (Mai Khao)	A27	423869	899017	78.73	164.3	6	2008
	A28	423417	898681	469.85	953	6	2008
	A29	423827	899127	9.5	176.3	6	2008
	B4	423191	898623	370	994	1.72	2012
				335	939	2.10	2013
				305	858	1.60	2014
				320	892	2.23	2015
	B5	423426	898188	320	892	2.23	2015
				305	852	2.47	2016
				65	222	0.64	2012
				47	176	1.12	2013
				1800	3790	0.59	2014
				650	1510	1.25	2015
				540	1250	1.34	2016
	B6	421559	905609	10000	18825	1.79	2012
				12200	21000	1.81	2013
				17000	29750	1.95	2014
				10200	18650	1.85	2015
				10800	20000	2.15	2016
Area 6 (Choeng Thale)	A1	422248	881567	10.49	215	60	2009
	A2	421788	882229	18.24	90.9	40	2009
	A3	422779	882098	9.5	74.2	6	2009
	A4	422551	883341	500	2240	2	2007
	A5	423026	883488	16	181	6	2008
	A6	422822	883500	286.91	618	20	2009
	A7	422329	882723	21.2	118	2	2009
	A8	423361	886367	11	122	8	2005
	A9	424864	883166	7.6	110	8	2006
	A10	423709	884423	774.76	1510	20	2010
	A11	424615	885309	48.23	247	20	2010
	B1	423630	884067	11	130	2.22	2012
				9.7	126.5	2.22	2013
				11.5	127.5	1.87	2014
				10.5	123.5	1.73	2015
				11	129	2.4	2016
Area 7 (Sisuntho -rn)	A12	430031	882595	8	173	15	2003
	A13	426529	882390	16	172	9.6	2005
	A14	425257	882632	1	0	25	2005
	A15	428936	882950	6	60	12	2006
	A16	425399	884835	7	31.4	10	2009
	B2	428895	883097	7.6	78.5	7.55	2012
				5.6	69.5	7.88	2013
				8	72.5	7.75	2014

Table 3.2 Groundwater Data in Different Eight Studied Areas (cont.)

Location (District)	ID	Latitude	Longitude	Cl (mg/L)	TDS (mg/L)	groundwater level(m)	Year
Area 8 (Thepkras -siti)				6	76	8.99	2015
				6.2	74	9.51	2016
	A30	426722	890331	12	116	16	2008
	A31	425888	885945	280	672	6	2008
	A32	428608	889229	4.49	114.8	15	2010
	A33	425200	885588	232.43	506	6	2010
	A34	429144	889348	6.99	175.1	15	2010
	B7	427056	888021	19	156	2.91	2012
				25	158.5	3.27	2013
				19	152	2.67	2014
				26.5	174.5	3.16	2015
				17.5	154.5	3.67	2016

3.2.2 Data Analysis and Presentation of Groundwater Chemistry

3.2.2.1 Historical TDS and Chloride Concentration

TDS and Cl concentration of each study area were averaged to plot with time series during 2003 – 2016. Seawater intrusion problem is here defined by thresholds: TDS and Cl concentration of the groundwater exceed 1,500 mg/L, and 600 mg/L, respectively (WEPA, 2018). In terms of studying seawater intrusion, it is very important to plot the trend of Cl and TDS concentrations because the area that has seawater intrusion problem should have the increasing trends of both Cl and TDS exceeding the threshold number. However, the increasing trend can be shown in some areas, those areas are not interpreted to be encountered the seawater intrusion problem because both concentrations are not more than the threshold number. These areas need to pay more attention to monitor seawater intrusion problem.

3.2.2.2 Correlation of TDS and Chloride Concentration

Water with TDS in the ranges 1-1,000 mg/L, 1,000-10,000 mg/L, 10,000 -100,000 mg/L and lastly above 100,000 mg/L, are generally labelled as fresh, brackish, saline, and brine water, respectively (Sherif *et al*., 2006). In case of Thailand, water with TDS in the ranges less than 500 mg/L, 500- 1,500 mg/L and higher than 1,500 mg/L, are typically labelled as fresh, brackish and seawater intrusion zone, respectively (WEPA, 2018). However, TDS is just a measurement of the combined contents of both inorganic and organic substances, contained in a liquid in molecular,

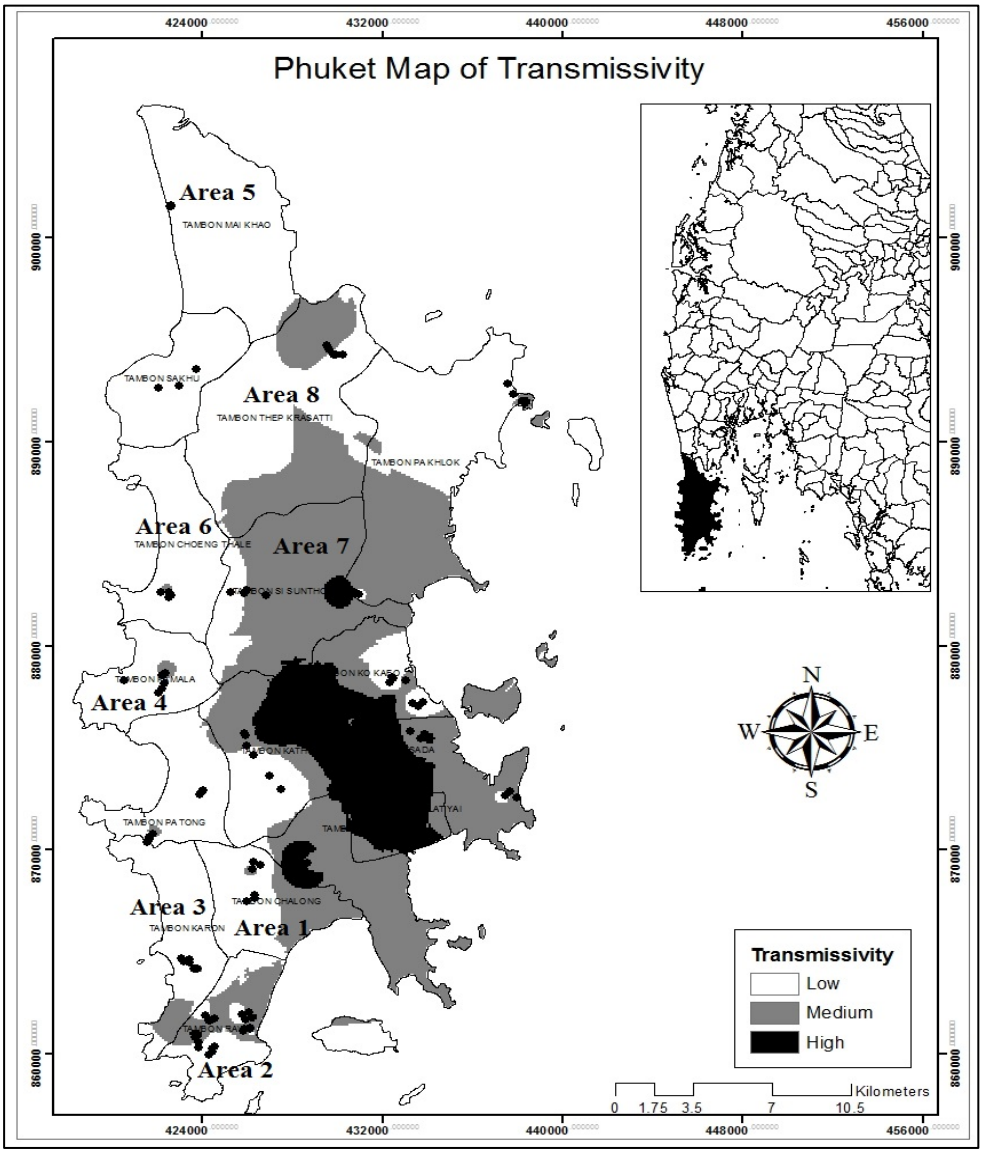

Figure 3.4 Phuket Map of Transmissivity.

ionized or micro-granular suspended from the high concentration of Cl^- contributes to high TDS, while Cl^- is selected to be a major ion of seawater. High TDS can be interpreted as contamination, but it cannot clarify a source of the contamination. Therefore, the correlation between Cl^- and TDS should be a good match in order to interpret seawater intrusion. Cross-correlation of these quantities was analyzed to better distinguish between seawater intrusion and other contaminations. The high correlation of TDS and Cl concentration indicates the area is strongly affected by seawater intrusion. Cross-plots of average TDS and Cl concentration were created for each study area representing the Phuket Island. Finally, the assessment map of Phuket seawater

intrusion was created using TDS and Cl concentration as the two main parameters. The map indicates those areas identified from cross-plots of TDS and Cl concentration.

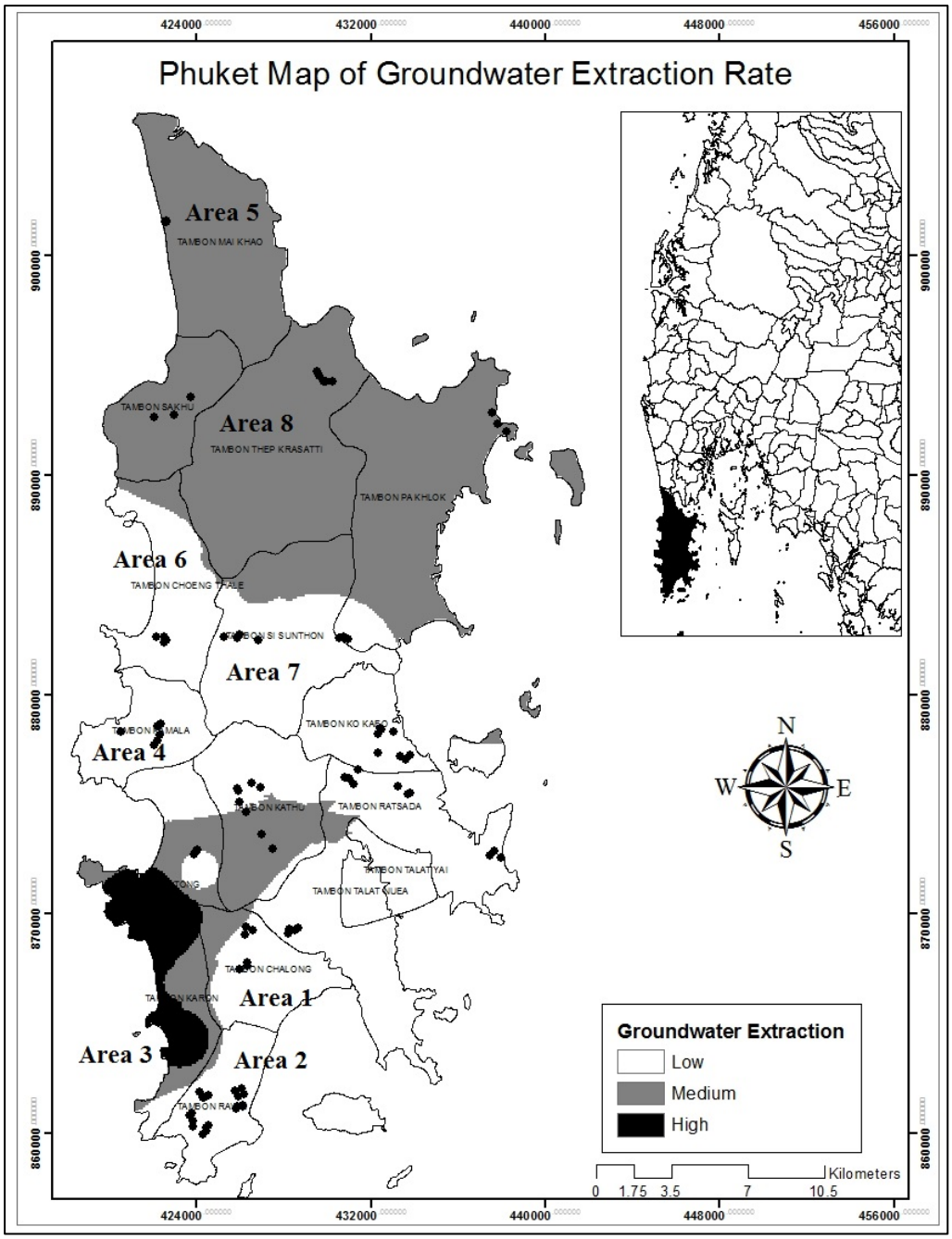

Figure 3.5 Phuket Map of Extraction Rate.

3.2.2.3 A Relationship of Groundwater Level and Ground Water Salinities (TDS and Cl Concentration)

The trends between groundwater salinities (TDS and Cl concentration) and groundwater level from 2003 to 2016 indicate that when the groundwater level

drops, the seawater can intrude into the aquifer replacing fresh water as a natural source of recharge for the coastal zones. Plots of trends in groundwater salinity (TDS and Cl concentration) and groundwater level confirm that reduction of the fresh groundwater causes seawater to move inland, intruding into the aquifer previously containing fresh water, thus the groundwater salinity shows the same trend with the groundwater level. Occasionally, groundwater level in some coastal areas increases, even though groundwater extraction rate in those areas is high. This is because of the recharge of seawater intrusion. Therefore, the increment of the groundwater level is caused by seawater intrusion in areas of coastal zones.

3.2.3 Mapping of Risk Areas for Seawater Intrusion in Phuket

Mapping seawater intrusion on Phuket Island was done using GIS method with overlaying technique. The overlaying technique in GIS provides map layers with different attributes merged into a single output map (Malczewski, 2004). The single output maps of Cl concentration, TDS concentration, transmissivity, and groundwater extraction from spatial GIS analysis were used to be the base maps for overlaying. Cl and TDS are the two main indicators of groundwater salinity; hence, both of them were used to be the main parameters to map the seawater intrusion map in Phuket. In fact, high transmissivity can cause seawater intrusion problems along coastal areas (Shammas, 2007; Qahman, 2006). Groundwater extraction is due to over-pumping of groundwater as mentioned in the previous section. Therefore, groundwater extraction and transmissivity are supported parameters enhancing the overlay map of seawater intrusion in Phuket. Groundwater extraction was used to assess seawater intrusion in this study because the exploitation of groundwater causes seawater intrusion in coastal areas. The areas with high rate of groundwater extraction tend to have elevated risk of seawater intrusion. A weighting technique was employed to overlay these maps. During the weighted overlay analysis, the ranking has been given for each individual parameter of each thematic map and the weighted were assigned by the users according to the influence of the different paramaters (Nagarajan and Singh, 2009). Hence, the two main parameters Cl and TDS concentration were given 70% weight, while the two supporting parameters were given 30% weight. This approach

integrated Cl concentration, TDS concentration, transmissivity, and groundwater extraction as indicators for areas with high tendency of seawater intrusion.

3.3 Determination of resistivity value for seawater intrusion in Phuket Island

As mentioned before, the resistivity values of seawater and freshwater are not universal standard because it varies based on the geological setting of those study area. Therefore, it is very crucial to determine the range of resistivity value for interpreting seawater intrusion in Phuket Island. To classify the resistivity values of freshwater, mixing zone and seawater zone in Phuket Island, the laboratory testing was conducted. The water sample of seawater was taken from the Andaman Sea at Kamala sub-district. Then the tap water of 250 ml (0% seawater) was used to measure the TDS and electrical conductivity in a beaker using HANNA HI 9813-6 portable pH/EC/TDS/Temperature meter. Every 1% of seawater proportion was added into the beaker by volume starting from 1% up to 7% (Seawater) for measuring the changes of TDS and electrical conductivity, the water temperature was kept constant at 27°C. The reason why the measurement must be stopped at 7% of seawater because HANNA HI 9813-6 is capable to measure 2,000 ppm of TDS value in maximum. The electrical resistivity was calculated as measurements of reciprocal conductivity (Table 3.3).

Table 3.3 Relationship between resistivity and TDS based on seawater proportion

No	Seawater		Tap water		Conductivity (mS/cm)	Resistivity (Ohm-m)	TDS
	Proportion (%)	Volume (mL)	Proportion (%)	Volume (mL)			
1	0	0.00	100	250.00	0.17	58.82	121
2	1	2.50	99	247.50	0.48	20.83	463
3	2	5.00	98	245.00	0.71	14.08	502
4	3	7.50	97	242.50	1.22	8.19	875
5	4	10.00	96	240.00	1.74	5.74	1265
6	5	12.50	95	237.50	1.81	5.52	1322
7	6	15.00	94	235.00	2.50	4.00	1673
8	7	17.50	93	232.50	2.70	3.70	2000

3.4 Electrical Resistivity Survey of Phuket Seawater Intrusion

3.4.1. Electrical Resistivity Imaging (ERI) Survey

3.4.1.1 ERI Acquisition

Ten ERI profile lines, as shown in Figure 3.6, have been generated in four risk sub-districts (Kamala, Chalong, Rawai and Mai Khao) according to the risk map of seawater intrusion in Phuket as mentioned in the previous section. Two ERI inline profiles (Line A-A' and Line B-B') which were parallel to the coastline in Kamala sub-districts were surveyed by using a Dipole-Dipole array. Despite the Signal to the noise level of this Dipole-Dipole is relatively low compared to that of other configurations; it is very good for interpreting complex structures or small-scale anomalies because of its high-resolution data (Park *et al*., 2016). However other 7 ERI inline profiles (Line F-F'and Line I-I') and cross-line profiles (Line C-C', Line D-D', Line E-E', Line G-G' and Line H-H') were surveyed by applying Werner array which is usually applied for good vertical resolution whereas it may generate appropriate horizontal resolution (Afshar *et al*., 2015). Werner array is an attractive choice due to its high signal strength and better signal to noise ratio and is also useful if a good vertical resolution is required. Those ten profiles were extended in different lengths, the spacing of configuration and distance from the beach, but the same number of electrodes (56 stainless-steel electrodes). Stainless steel electrodes were used to avoid corrosion problems. The distribution of the profile line survey has been explained in Table 3.4.

Table 3.4 Electrical Resistivity Survey Lines in Phuket Island

Profile lines	Total length (m)	Spacing (m)	Number of Electrodes	Configuration	Location
Line A-A'	220	4	56	Dipole-Dipole	Kamala
Line B-B'	165	3	56	Dipole-Dipole	Kamala
Line C-C'	137.5	2.5	56	Werner	Kamala
Line D-D'	165	3	56	Werner	Kamala
Line E-E'	137.5	5	56	Werner	Chalong
Line F-F'	275	5	56	Werner	Chalong
Line J-J'	275	5	56	Werner	Chalong
Line G-G'	275	5	56	Werner	Rawai

Table 3.4 Electrical Resistivity Survey Lines in Phuket Island (cont.)

Profile lines	Total length (m)	Spacing (m)	Number of Electrodes	Configuration	Location
Line H-H'	275	5	56	Werner	Mai Khao
Line I-I'	275	5	56	Werner	Mai Khao

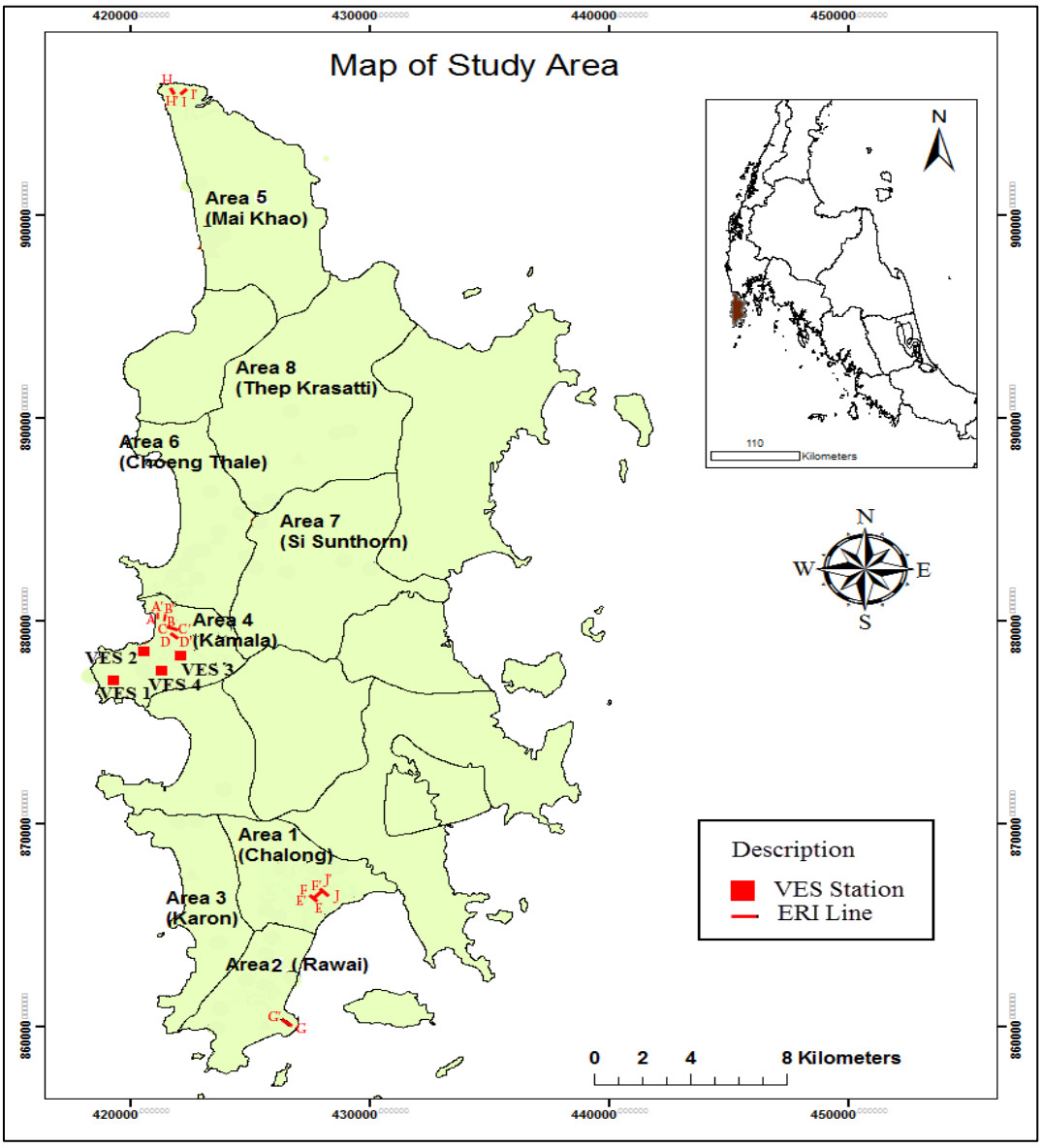

Figure 3.6 Map of ERI Survey and VES Stations.

3.4.1.2 Data Inversion

All data files (.stg files) getting from each ERI profile were input in licensed EarthImager2D and EarthImager3D software in order to get the inverted

resistivity model. In the case of 2D and 3D inversion, smooth model inversion was used in the inversion method. The underdetermined and ill-posed nature of 2D resistivity inverse problems makes the inverse solution inherently non-unique. Additional constraints, or regularization, must be imposed on the model to single out one optimal solution. The smooth model inversion, also known as Occam's inversion, finds the smoothest possible model whose response fits the data to a-priori Chi-squared statistic. The true model must be at least as, but never less complex than, the smooth model obtained through smooth model inversion. Smooth model inversion is based on the assumption of Gaussian distribution of data errors (AGI, 2014). The terrain file (.trn files) was read in order to do data inversion based on the elevation.

3.4.2 Vertical Electrical Sounding Survey

Vertical Electrical Sounding (VES) were generated in the western part (Kamala sub-district) of Phuket Island as shown in Figure 3.6. Four stations (VES1, VES2, VES3 and VES4) which were done using Schlumberger array with current electrode spacing kept between 2 m and 5 m and up to 150 m in total length were done near to producing wells (A35, A40, A41, A42, A43 and A45) and monitoring wells (B3 and B8) in Kamala sub-district. At the site, Supersting R2 and four electrodes were mainly used for data collection in this survey. Four stainless steel electrodes were used to avoid corrosion problems. The purpose of running VES survey near either producing wells or monitoring wells in Kamala sub-district was to determine the empirical model of resistivity (ρ) and groundwater salinity (Cl^- and TDS) in the same depth in each well.

3.5 Resistivity Validation

3.5.1 Correlation between resistivity and groundwater chemistry concentration (Cl and TDS)

The purpose of doing correlation between groundwater salinity (Cl^- and TDS) and apparent resistivity obtaining from VES survey was to verify that the apparent resistivity indicates the low value (< 100 Ohm m) in the area having high rate of Cl- and TDS concentration (higher than 600 mg/L and 1,500 mg/L respectively), while the value of apparent resistivity gets high (> 1,000 Ohm-m) in the area having low rate of Cl^- and TDS. Evidentially, seawater intrusion might be interpreted in one

area when it shows high groundwater salinity and low resistivity. Also, it can be concluded the groundwater data and resistivity data are reliable even though it was provided from different sources. Four stations of VES survey is designed to carry out near the groundwater wells producing wells (A35, A40, A41, A42, A43, and A45) and monitoring wells (B3 and B8) as shown in Figure 3.2, for taking the apparent resistivity data in the different depth. The resistivity data obtained from VES are validated to the groundwater salinities (Cl concentration and TDS) taken from groundwater data using data cross-plot, the high correlation between the resistivity and groundwater salinities helps to confirm whether or not the results of 2D and 3D-ERI are reliable. According to the cross-plot, the empirical model between resistivity versus Cl^- and TDS was determined. This method is useful to validate your resistivity data whether or not they are reliable for your work. In fact, resistivity validation has been done only in Kamala sub-district, however, it would be recommended to represent in other coastal areas such as Chalong, Rawai, and Mai Khao.

3.5.2 Laboratory Testing

3.5.2.1 Relationship between seawater and soil resistivity

Initial moisture sand samples collecting from Chalong sub-district as shown in Figure 3.2 by using Hand-Auger was used to test the resistance and then convert to resistivity. This sample was separated into 10 samples with 232 cm^3 in the volume of each sample. They were saturated proportionally with different solution rate of distilling water and seawater (taking from the sea at Chalong sub-district) and filled in the soil model in the plastic cylinder as shown in Figure 3.7. The solution of seawater and distilled water were measured in 80mL-beaker. The percentage of seawater and distilled water were converted to volume (e.g. 75% of seawater equals 60 ml, while 25% of distil water equals 20 ml). The plastic cylinder which is attached at both end-side with copper slice connecting with copper wires to be acted as electrodes of A and B for injecting the current while other two electrodes are put at 3.5 cm from both end-side to be an electrode of M and N (MN=3.5 cm) for measuring the voltage. The soil model has dimensions of 5.29 cm in diameter and 10.58 cm in length as shown in Figure 3.7. The proportion of distilling water and seawater mixed up initial moisture sand has been listed in Table 3.5. AGI SuperStingR2 resistivity meter was used to measure the

Figure 3.7 Plastic Cylinder for Soil Model

Table 3.5 Soil Sample Preparation

Soil Sample	Seawater	Distill water
1	100%	0%
2	75%	25%
3	50%	50%
4	40%	60%
5	20%	80%
6	10%	90%
7	8%	92%
8	6%	94%
9	4%	96%
Initial condition	0%	0%

the resistance of each proportional sample. Resistance measurement has been done three times in order to average of the resistance value for getting more accurate results. Not only the resistance (R) of material is influenced by material properties, but also it can be affected by its dimensions. Resistance behaviours of materials depend on the length and cross-sectional area of material that the electrical current is flowing through. In addition, it can also be affected by a constant value which is the ability to permit electrical current to flow through. Eq. 3.1 discuss material resistance (R) which is influenced by resistivity (ρ) and its dimensions (Morris *et al.*,1996), therefore, the resistivity can be defined as follows:

$$\rho = \pi \frac{d^2}{4L} R \tag{3.1}$$

Where d is the diameter of cylinder and L is the length of the cylinder.

Consequently, it would be useful to compare it with the inversion result of electrical resistivity survey which was run on the field. The resistivity value decreased when soil model was mixed up seawater. Likewise, the resistivity measured at the field was very low, unless those areas had been intruded by seawater. The aim of this work is to assist for accurate interpretation of seawater intrusion based on electrical resistivity value getting from field data inversion of electrical resistivity survey. After getting resistivity (ρ) value from laboratory testing, those data were used to plot versus proportional seawater filled in soil model. All resistivity data might be reliable if the resistivity value decreases when the proportion of seawater has been increased. The resistivity value of the initial moisture sand sample was used to be threshold value to determine whether or not the resistivity decreases when seawater increase.

3.5.2.2 Relationship between seawater and water resistivity

The relationship between electrical resistivity and seawater was validated by laboratory testing in order to demonstrate the geo-electrical method using 2D and 3D ERI is an effective tool for delineating seawater intrusion problem. The laboratory testing was conducted based on the concept that the water resistivity decreases corresponding to the presence of seawater proportion increasing, the water sample of seawater was taken from the Andaman Sea at Kamala sub-district. Then the

tap water of 250 ml (0% seawater) was used to measure the initial electrical conductivity in a beaker using HANNA HI 9813-6 portable pH/EC/TDS/Temperature meter. Every 5% of seawater proportion was added into the beaker by volume starting from 5% up to 100% (Seawater) for measuring the changes of the electrical conductivity, the water temperature was kept constant at 27°C. The electrical resistivity was calculated as measurements of reciprocal conductivity (Table 3.6).

Table 3.6 Proportion of seawater and resistivity

No	Seawater		Tap water		Conductivity (mS/cm)	Resistivity (Ohm-m)	Temperature (℃)
	Proportion (%)	Volume (mL)	Proportion (%)	Volume (mL)			
1	0	0.00	100	250.00	0.17	58.82	27
2	5	12.50	95	237.50	2.16	4.63	27
3	10	25.00	90	225.00	4.79	2.09	27
4	15	37.50	85	212.50	6.02	1.66	27
5	20	50.00	80	200.00	6.82	1.47	27
6	25	62.50	75	187.50	7.43	1.35	27
7	30	75.00	70	175.00	7.70	1.30	27
8	35	87.50	65	162.50	7.92	1.26	27
9	40	100.00	60	150.00	8.08	1.24	27
10	45	112.50	55	137.50	8.41	1.19	27
11	50	125.00	50	125.00	8.48	1.18	27
12	55	137.50	45	112.50	8.68	1.15	27
13	60	150.00	40	100.00	8.78	1.14	27
14	65	162.50	35	87.50	8.90	1.12	27
15	70	175.00	30	75.00	8.99	1.11	27
16	75	187.50	25	62.50	9.04	1.11	27
17	80	200.00	20	50.00	9.14	1.09	27
18	85	212.50	15	37.50	9.16	1.09	27

Table 3.6 Proportion of seawater and resistivity (cont.)

No	Seawater		Tap water		Conductivity (mS/cm)	Resistivity (Ohm-m)	Temperature (℃)
	Proportion (%)	Volume (mL)	Proportion (%)	Volume (mL)			
19	90	225.00	10	25.00	9.26	1.08	27
20	95	237.50	5	12.50	9.30	1.08	27
21	100	250.00	0	0.00	9.31	1.07	27

CHAPTER 4

RESULTS

4.1 Assessment of Phuket Seawater Intrusion

4.1.1 Historical Trends of Cl^- and TDS

The historical groundwater salinity (Cl concentration and TDS) in all study areas shows increasing trends from 2003 -2016, as shown in Figure 4.1a and 4.1b. The increasing groundwater salinity may imply seawater intrusion problems present in the coastal areas. The areas with rapidly increasing salinity are Area 5 (Mai-Khao), Area 4 (Kamala), Area 1 (Chalong) and Area 2 (Rawai). These areas also have TDS and Cl concentration above the respective thresholds: the TDS exceeds 1,500 mg/L and the Cl concentration is above 600 mg/L. In terms of TDS trend, it is clear from the chart that the TDS trend of above four areas increased dramatically in 2012 with the rate approximately 2,000 mg/L, 3,500 mg/L, 3,500 mg/L, and 4,000 mg/L for Area 1, Area 4, Area 2 and Area 5 respectively compared to lower than 500 mg/L for all areas in 2010. The trend of TDS for Area 1, Area 2 and Area 4 remained stable until 2016, while that for Area 5 reached a peak in 2014 with the rate nearly 12,000 mg/L. Likewise, the Cl trend of above four areas rose significantly in 2012 with the rate around 2,000 mg/L, 3,500 mg/L, 3,500 mg/L and just under 4,000 mg/L for Area 1, Area 4, Area 2 and Area 5 respectively. The trend of Cl for Area 1, Area 2 and Area 4 remained constant until 2016. However, Area 5 reached a peak with the rate more than 6,000 mg/L in 2014. Overall, both historical Cl and TDS have been shown in a similar increasing trend from 2010 to 2016.

4.1.2 Cross-plot of Chloride Concentration and TDS

The cross-plots of these average concentration of Cl and TDS indicate a high correlation in most study areas except Area 3 (Karon) and Area 7 (Sisunthorn), as

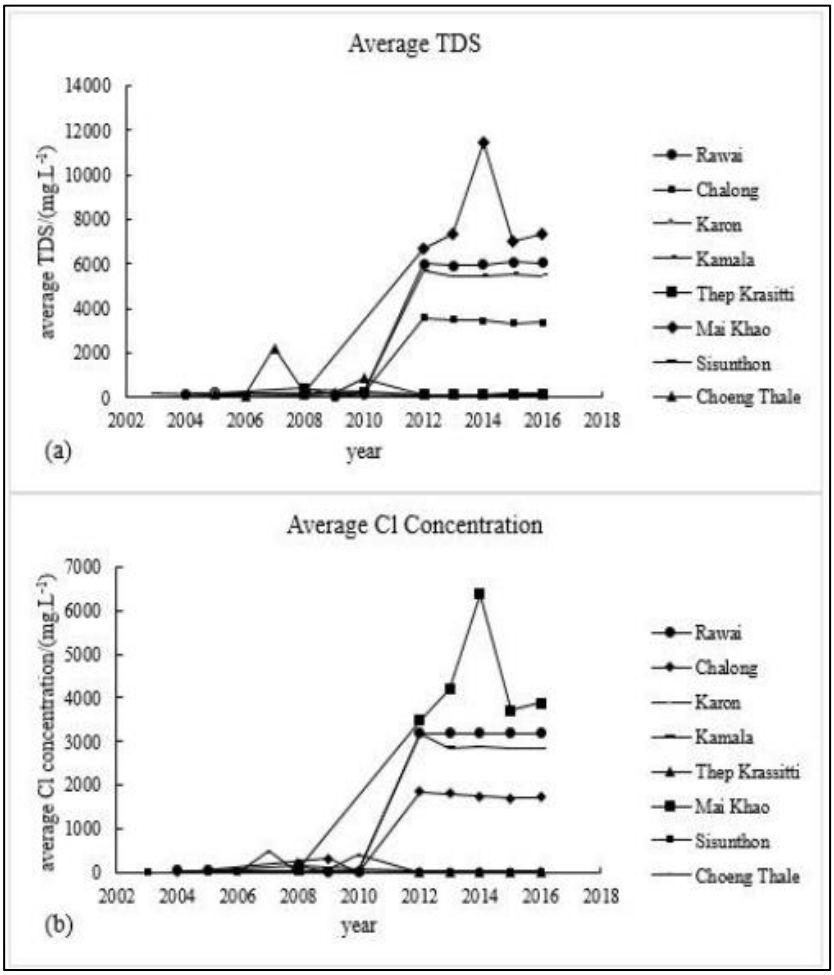

Figure 4.1 Trends of Average TDS And Cl Concentration From 2002 To 2016 In 8 Sub-Districts: (a) Average TDS And (b) Average Cl Concentration.

Shown in Figure 4.2. The areas which have seawater intrusion problem, show a high correlation between average Cl concentration and TDS concentration, and the average Cl concentration and TDS are also higher than the thresholds 600 and 1,500 $mg.L^{-1}$, respectively. The maximum average Cl concentration and TDS are approximately 7,000 mg/L and 12,000 mg/L as shown in Figure 4.2f, which is in Area 5 (Mai Khao). Therefore, it can be evaluated that the area where has severe seawater intrusion problem is Area 5 (Mai-Khao). Apart from Area 5 (Mai Khao), other three areas- Area 1 (Chalong), Area 2 (Rawai) and Area 4(Kamala) are likely to meet seawater intrusion because their correlation between Cl concentration and TDS show high as shown in Figure 4.2b, 4.2c, and 4.2e, and the average Cl concentration and TDS are also higher

than the thresholds. On the other hand, Area 3 (Karon) and Area 7 (Sisunthorn) districts are unlikely to encounter seawater intrusion, since the average TDS and Cl concentration are very low compared to the other districts, and the cross-plots of average Cl concentration and TDS are very scattered (Figure. 4.2d and 4.2h). In case of Area 6 (Choeng Thale) and Area 8 (Thep Krasitti), these two areas cannot be evaluated to have seawater intrusion problem even though they have high correlation because the average Cl concentration and TDS are also lower than the threshold numbers as shown in Figure 4.2g and 4.2i.

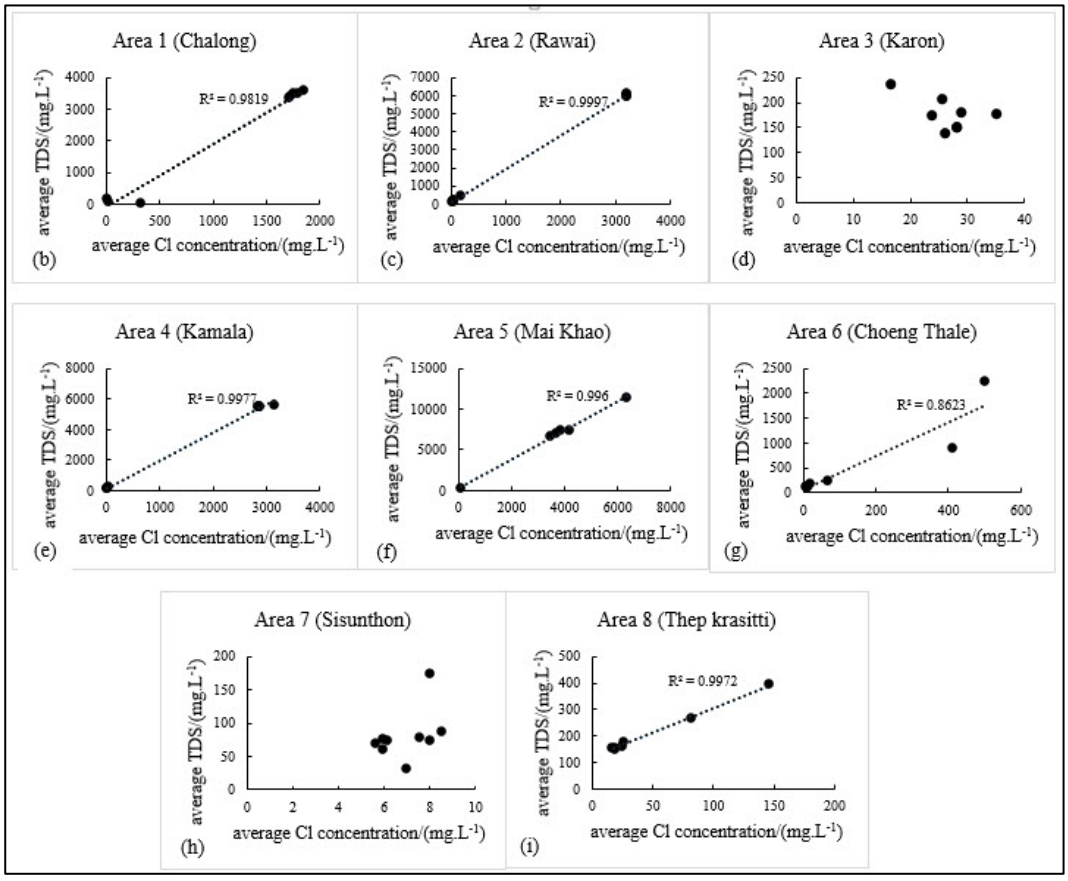

Figure 4.2 Cross-Plots Of Average TDS And Cl Concentration By Study Area: (a) Phuket Map Of Groundwater Wells And Network Monitoring Wells, (b) Chalong, (c) Rawai, (d) Karon, (e) Kamala, (f) Mai-Khao, (g) Choeng-Thale, (h) Sisunthon And (i) Thep-Krasatti.

4.1.3 Groundwater Level Trends versus Groundwater Salinity Trends

It is commonly known that the trends of groundwater salinities (Cl concentration and TDS) are opposite to those of the groundwater level, i.e., when groundwater level drops, the seawater will intrude into the fresh water resulting in the salinity increase. However, the seawater intrusion can act as natural recharge in the coastal area, the groundwater level in coastal zones might be increased due to seawater intrusion. According to the graph, as shown in Figure 4.3, the groundwater level tends to increase with increasing groundwater salinities, as seen in the cross-plots. The Areas 1, 2, 4, and 5 (Chalong, Rawai, Kamala, and Mai-Khao districts) can be seen that both groundwater level and groundwater salinity, which are higher than thresholds, increase simultaneously. Those areas are here identified as seawater intrusion areas from the cross-plots shown in Figure 4.3. In contrast, Areas 3, 6, 7, and 8 (Karon, Choeng-Thale, Sisunthorn, and Thep-Krasatti districts) cannot be interpreted as seawater problem areas because the average Cl concentration and TDS are also lower than the thresholds.

4.1.4 Mapping of Seawater Intrusion of Phuket Island

Mapping of TDS and Cl concentration, transmissivity, and groundwater extraction in single maps was done by GIS techniques. All the single output maps were used for overlaying process to get the Phuket seawater intrusion map shown in Figure 4.4. The map shows that the coastal areas of Mai-Khao sub-district in the northern part of Phuket island is the most risk area for seawater intrusion, while Kamala, Chalong, Rawai sub-district which are attractive beaches, are risked to be moderate seawater problems.

4.2 Determination of resistivity value for seawater intrusion in Phuket Island

According to Drinking Water Quality Standard in Thailand (DWQST), it can be interpreted as freshwater (TDS<500mg/L), mixing zone (500<TDS<1,500mg/L) and saline zone (1,500mg/L<TDS) (WEPA, 2018). The laboratory test of the changing resistivity with seawater indicates that the water resistivity is reduced by the proportions

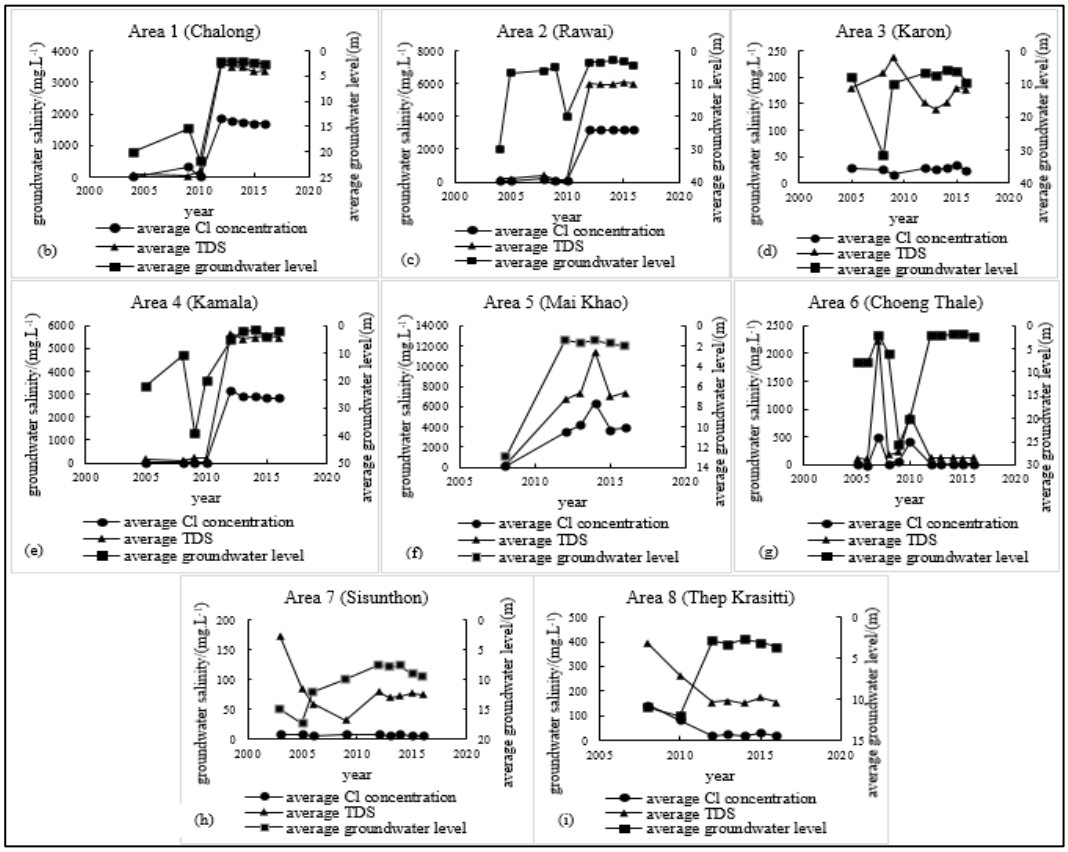

Figure 4.3 Comparison Of Trends In Groundwater Salinities (TDS And Cl Concentration) And Groundwater Level: (a) Phuket Map Of Groundwater Wells And Network Monitoring Wells, (b) Chalong, (c) Rawai, (d) Karon, (e) Kamala, (f) Mai-Khao, (g) Choeng-Thale, (h) Sisunthon And (i) Thep-Krasatti.

of the seawater. A trend of changing water resistivity was decreased dramatically in small amounts of seawater (0% – 3%), then the water resistivity was slightly dropped with increments of seawater proportion (3% - 7%) as shown in Figure 4.5. The initial resistivity (tap water) of 58 Ohm-m was reduced to 3.7 Ohm-m with the 7% of seawater. Therefore, it can be classified that saline zone, mixing zone, and freshwater zone has resistivity value with smaller than 5 Ohm-m, 5-15 Ohm-m and 15-100 Ohm-m, respectively.

4.3 Electrical Resistivity Imaging (ERI)

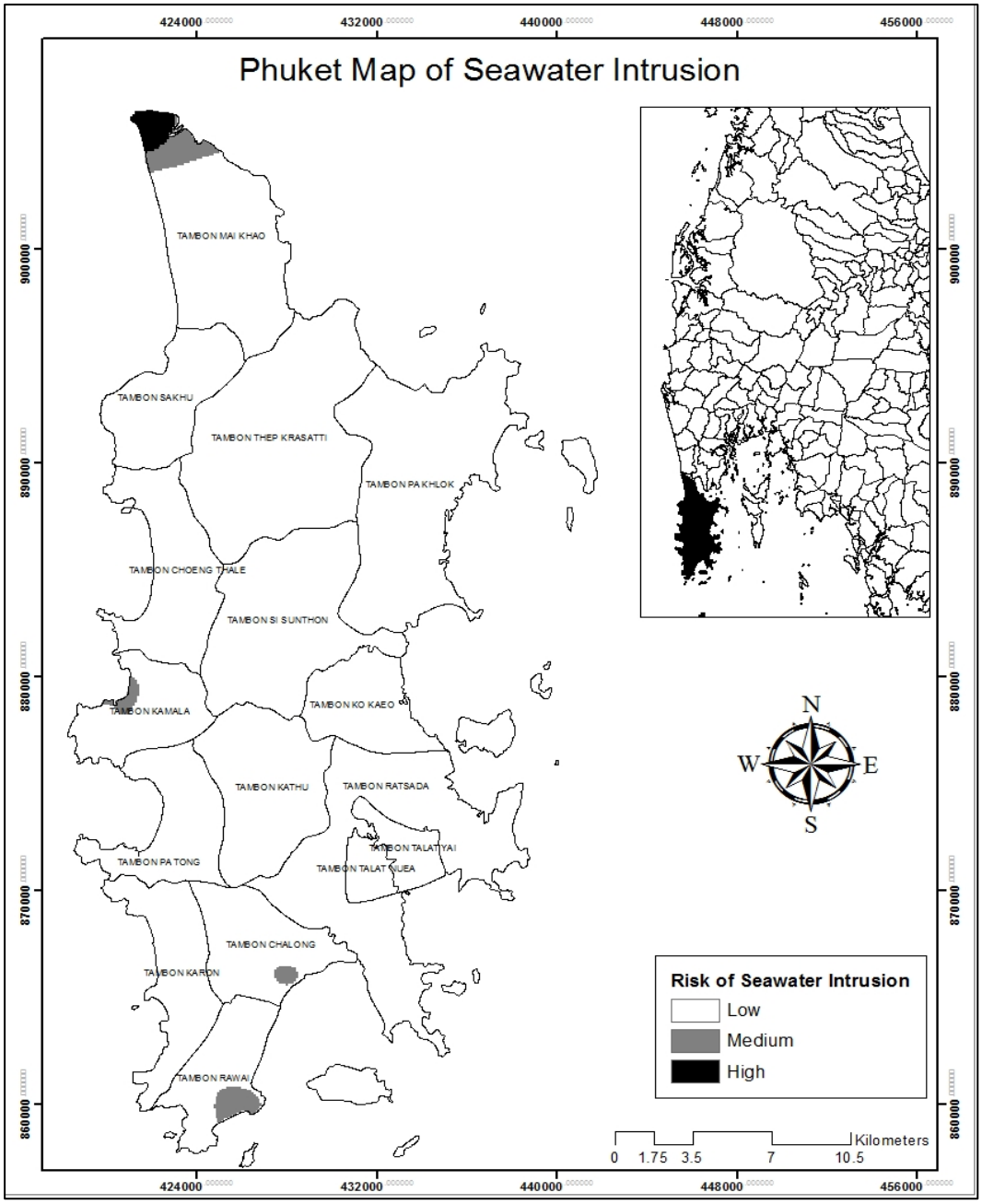

Figure 4.4 Phuket Map of Risk of Seawater Intrusion.

4.3.1 2D ERI of Kamala

The sub-surface layer of Kamala sub-district as shown in Figure 4.6 is categorized into 4 layers: topsoil (the top layer with the depth up to 20 m below the surface), clay (the second layer with the depth up to 30 m), weathered or fractured rock

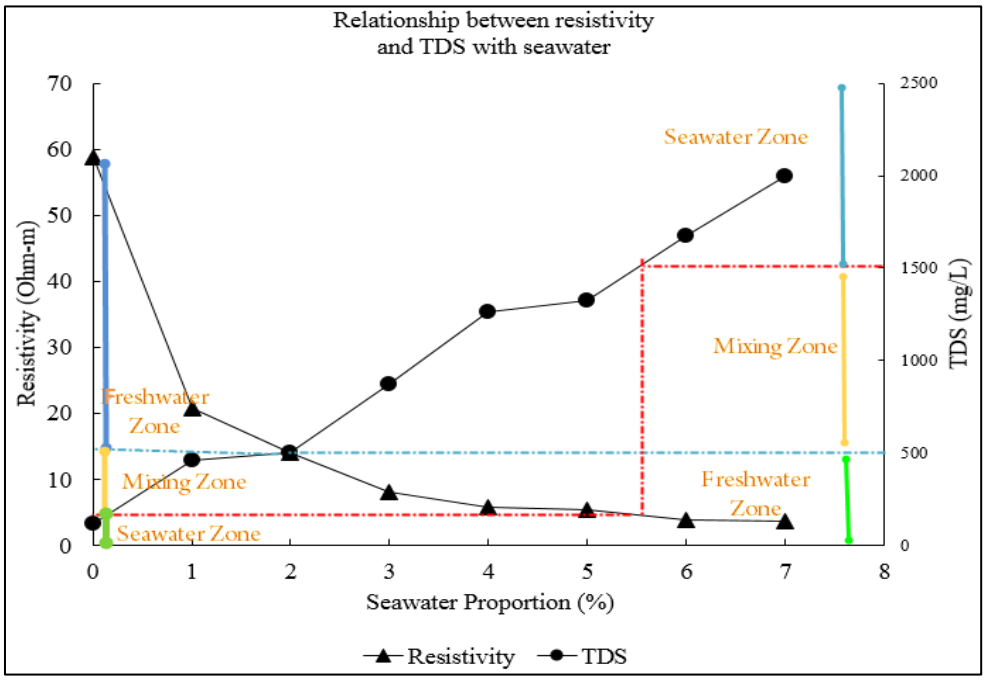

Figure 4.5 Determination of resistivity value for seawater intrusion in Phuket Island.

(the third layer with the depth ranging from 10 m to nearly 50 m) and base rock or granite layer (the fourth layer with the depth ranging from 10 m to more than 100 m below the soil surface). In-Line A-A' (Figure 4.7a) which has the total length of 220 m, is located at elevation 6 m above mean sea level (abms). The depth of penetration is approximately 49 m. The cross-section model of inverted resistivity (synthesized by measured and calculated resistivity) beneath Line A-A' illustrates the contrast in the lithology and degree of saturation of clayey sand and weathered or fractured layer as well as groundwater quality. The depth to water level which is underlain by the topsoil layer is shown in the very light green colour is around 5 m below the soil surface as shown in Figure 4.7a. Its inverted resistivity is ranging from 30 to 100 Ohm-m. The saline water zone which is underlain by bedrock(resistivity value is higher than 300 Ohm-m) is shown in the dark blue coloured layer in the depth ranging from 7 m to 35 m below the surface with the inverted resistivity ranging from 3 Ohm-m to lower than 5 Ohm-m. The saline water zone can be seen that it is surrounded by a brackish zone which is illustrated in a light blue coloured layer (the inverted resistivity value is ranging from 5 to 15 Ohm-m. Based on Line A-A', the subsurface model clearly

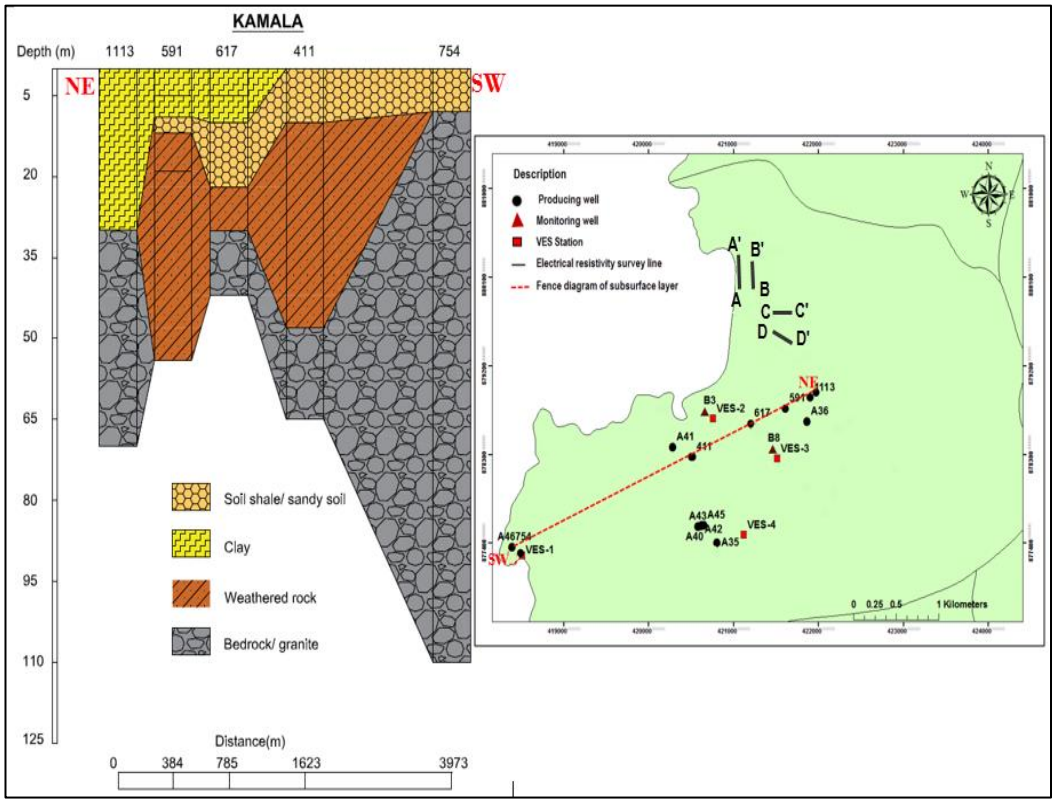

Figure 4.6 Fence Diagram of Subsurface Layer in Kamala Sub-District.

shows a plume of the direction of seawater intrusion into inland. Line B-B' (165 m in total length and around 39 m in the penetration depth), as shown in Figure 4.7b, is situated 120 m to the east of Line A-A' and is parallel to it. The subsurface result indicates the expansion of plume of seawater intrusion moving to inland decreases, compared to Line A-A'. The inverted result of this profile illustrates that the saline water zone shown in dark blue colour is located at the left-hand side (southern part) and right-hand side (northern part) of the profile in the depth ranging from approximately 10 m to 29 m below subsurface (0.2 to 19 m below mean sea level). Its inverted resistivity ranges from 2 Ohm-m to less than 5 Ohm-m. Apparently, the result shows that the saline water zone can be seen as a small plume in the centre of the profile and it is surrounded by the cylindrical zone of brackish water in depth around 10 m below the surface with the average value of resistivity 10 Ohm-m. Like Line A-A', Line B-B', the brackish and saline water zone show as the cylindrical shape indicating as the plume of seawater intrusion direction moving to the freshwater aquifer inland. Both

plumes of the saline zone are likely to expand to connect with each other from one side to another side in the short-term period.

Line C-C', Figure 4.7c, is located approximately 350 m to the east of Kamala beach and 344 m to the south of Line B-B' and perpendicular to it. This profile can get the data in depth of penetration around 25 m below subsurface (15 m abms) and 137.5 m in total length. Based on this profile, it can be seen that the mixing zone (light blue color) which has the resistivity value in the range from 8 Ωm to lover than 15 Ωm can be encountered in the depth around 12 m below the sub-surface (around 3 m bmsl) and extend to the whole of total length of this profile, while freshwater zone (light green colour) can be seen that it is quite thick with thickness around 7 m upper the zone of mixing. Similarly, Line D-D' (Figure 4.7d) is located approximately 520 m to the east of Kamala beach and is perpendicular to it. This profile is also situated at 9 m abms of elevation and just over 600 m to the southern part of Line B-B'. This profile gets the data along the total length of 165 m and the maximum of the penetration depth of around 30 m. The interpretation result of this profile illustrates that along the length from beginning to 45 m at the left-hand side of this profile and the penetration depth which is about 5 m below surface (equal to around 7 m abms) the saline water zone is encountered. This profile shows clearly the saline water zone indicating in dark blue coloured zone intrudes inland. The mixing zone (moderated blue colour zone) can be seen from 45 m in length to around 100 m. Also, the thickness of the saline zone is around 5 m. Because this profile is located more than 300 m to the beach, it can be concluded that now seawater intrudes freshwater aquifer inland in the distance approximately 400 m (Interface location) in the Kamala sub-district.

4.3.2 3D ERI of Kamala

A 3D ERI result from Figure 4.8 is consistent with 2D ERI results of Line A-A' and Line B-B', the 3D model provides additional information indicating the brackish plume in the subsurface cube. A layer of the coastal aquifer layer is at the depth between 15.8 and 40.0 m from the surface (thickness of about 24 m), the brackish plume is high accumulation near the sea and decreases eastward toward the inland area.

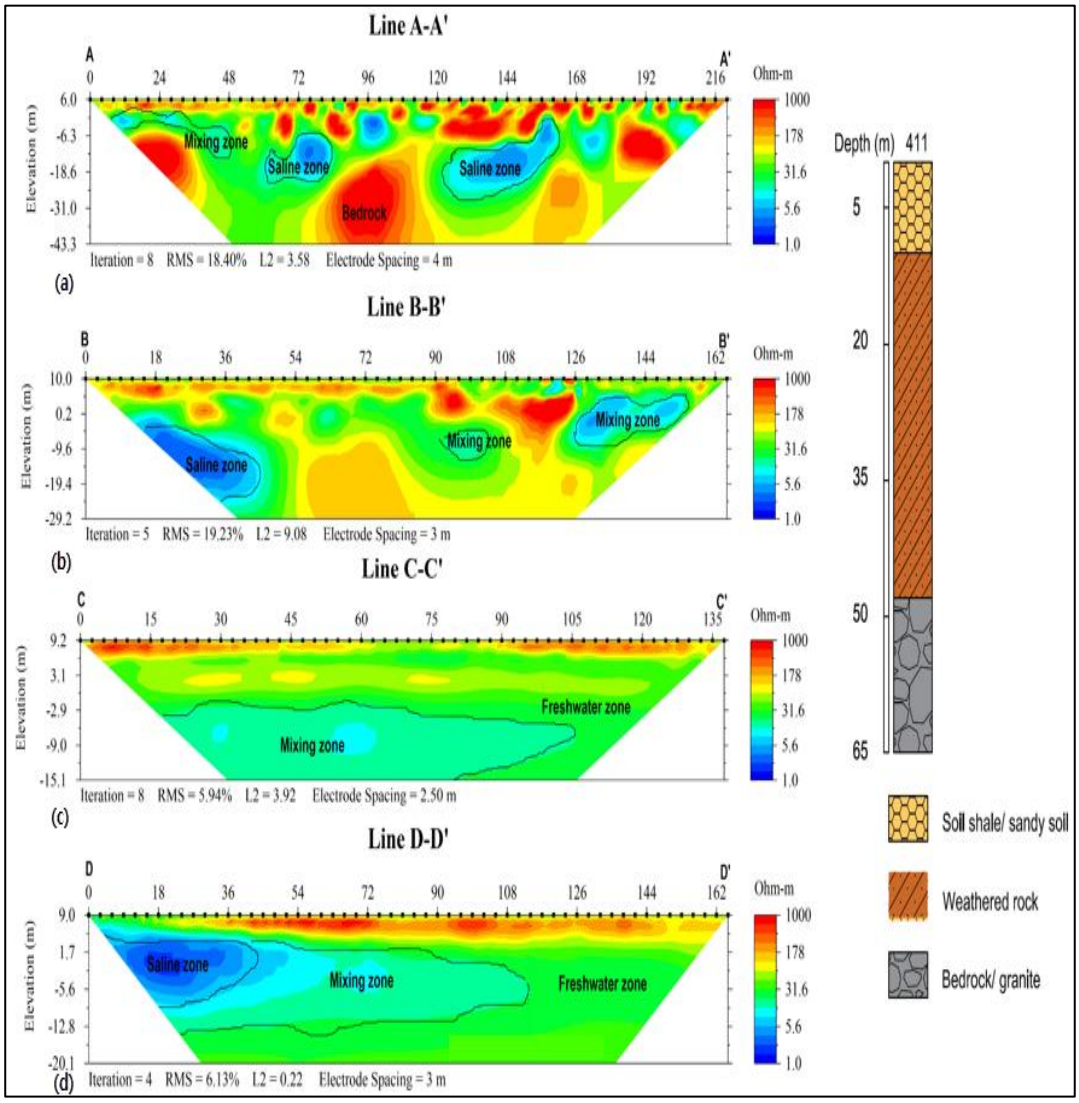

Figure 4.7 Inverted Resistivity (a) Line A-A', (b) Line B-B', (c) Line C-C' and (d) Line D-D'

4.3.3 2D ERI of Chalong

The subsurface layer of Chalong sub-district as shown in Figure 4.9 is naturally divided into 4 layers: topsoil (the depth up to 20 m below the ground surface), clay layer (the depth ranging from 5 m to around 30 m), weathered or fractured rock (the depth ranging from 5 m to just under 90 m) and bedrock or granite layer (the depth

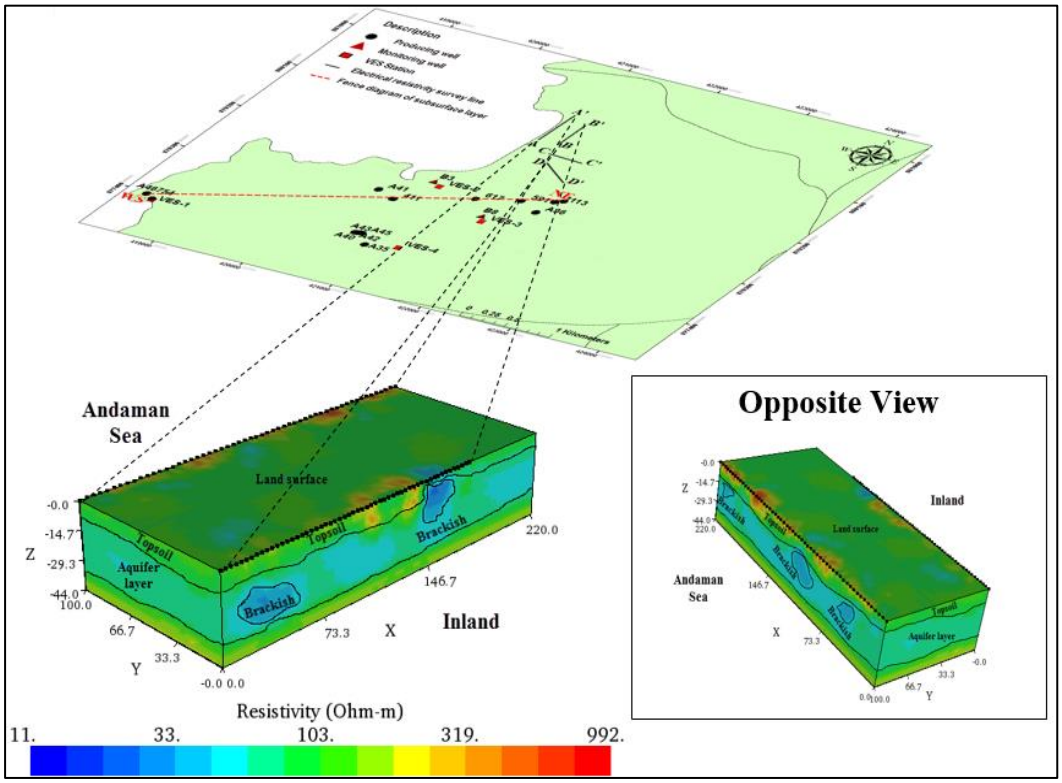

Figure 4.8 3D Inverted Resistivity Integrating Line A-A' and Line B-B'

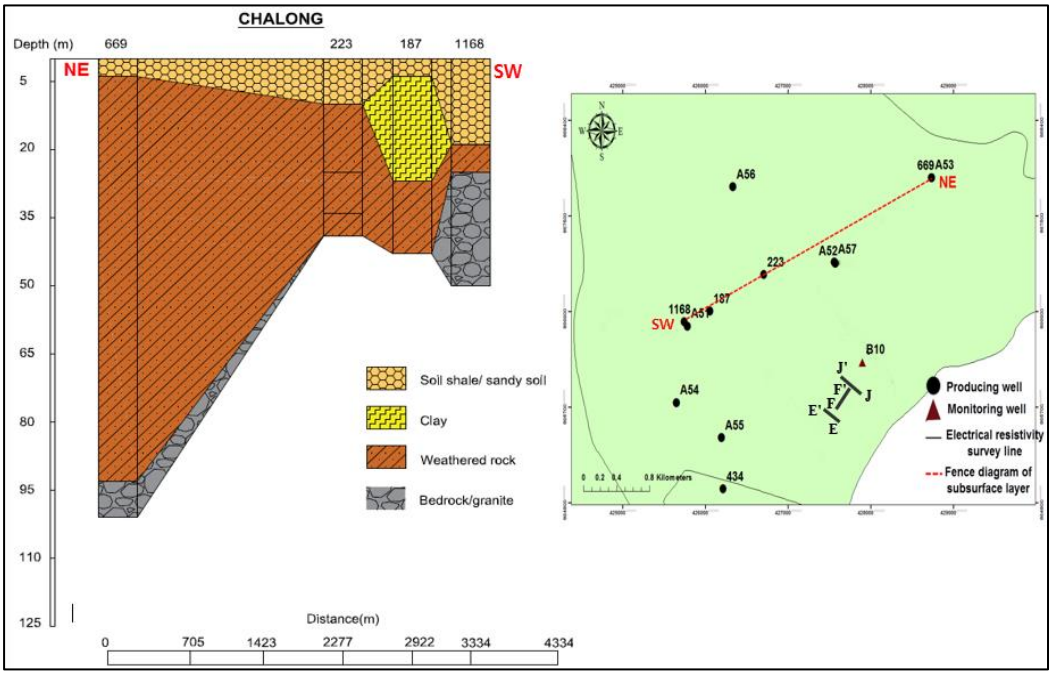

Figure 4.9 Fence Diagram of Subsurface Layer in Chalong Sub-District.

ranging from 30 m to around 100 m below the soil surface). Line E-E' (Figure 4.10a) is located approximately 80 m to the north of beach and perpendicular to it. This profile can get the data in depth of penetration around 25 m below subsurface (6.5 m abms) and 137.5 m in total length. Based on this profile, it can be seen that the brackish water zone (light blue color) which has the resistivity value in the range from 5.6 to around 15 Ohm-m can be encountered in the depth around 3 m below the sub-surface and extend inland to the haft of total length of this profile. The seawater/freshwater interface can be seen at around 150 m from the beach. Line F-F' (275 m in total length and around 50 m in the penetration depth), as shown in Figure 4.10b, is situated 20 m to the east of Line E-E' and is parallel to the beach. The subsurface result indicates the plume of seawater intrusion can be seen in the depth 2 m with the resistivity around 5 Ohm-m to 10 Ohm-m. The inverted result of this profile illustrates that the mixing zone shown in light blue colour is located at the left-hand side (western part) and right-hand side (eastern part) of the profile in the depth ranging from approximately 2 m to 12 m below subsurface. Its inverted resistivity ranges from 8.2 Ohm-m to less than 15 Ohm-m. Like Line B-B', the brackish and saline water zone for Line F-F' show as the cylindrical shape indicating as the plume of seawater intrusion direction moving to freshwater aquifer inland. Both plumes of the brackish zone are likely to expand to connect with each other from one side to another side in the short-term period. Line J-J' (Figure 4.10c) which has the total length 275 m, is located at elevation 9 m above mean sea level (abms) and perpendicular to the beach. The depth of penetration is approximately 50 m. The saline water zone is shown in the light blue coloured layer in the depth ranging from 2 m to just over 20 m below the surface with the inverted resistivity ranging from 5 Ohm-m to lower than 15 Ohm-m. The mixing zone can be seen that it is surrounded by a freshwater zone which is illustrated in light green coloured layer.

4.3.4 3D ERI of Chalong

A 3D ERI result from Figure 4.11 is consistent with 2D ERI results of Line E-E' and Line J-J'. Because the distance between Line E-E' and Line J-J' is so far (around 300 m), the result of 3D is not likely to be visually perfect for interpretation. The 3D model provides additional information indicating the brackish plume in the subsurface cube. A layer of the coastal aquifer layer is at the depth between 5

and 30.0 m from the surface (thickness of about 20 m), the brackish plume is high accumulation near the sea and decreases toward the inland area.

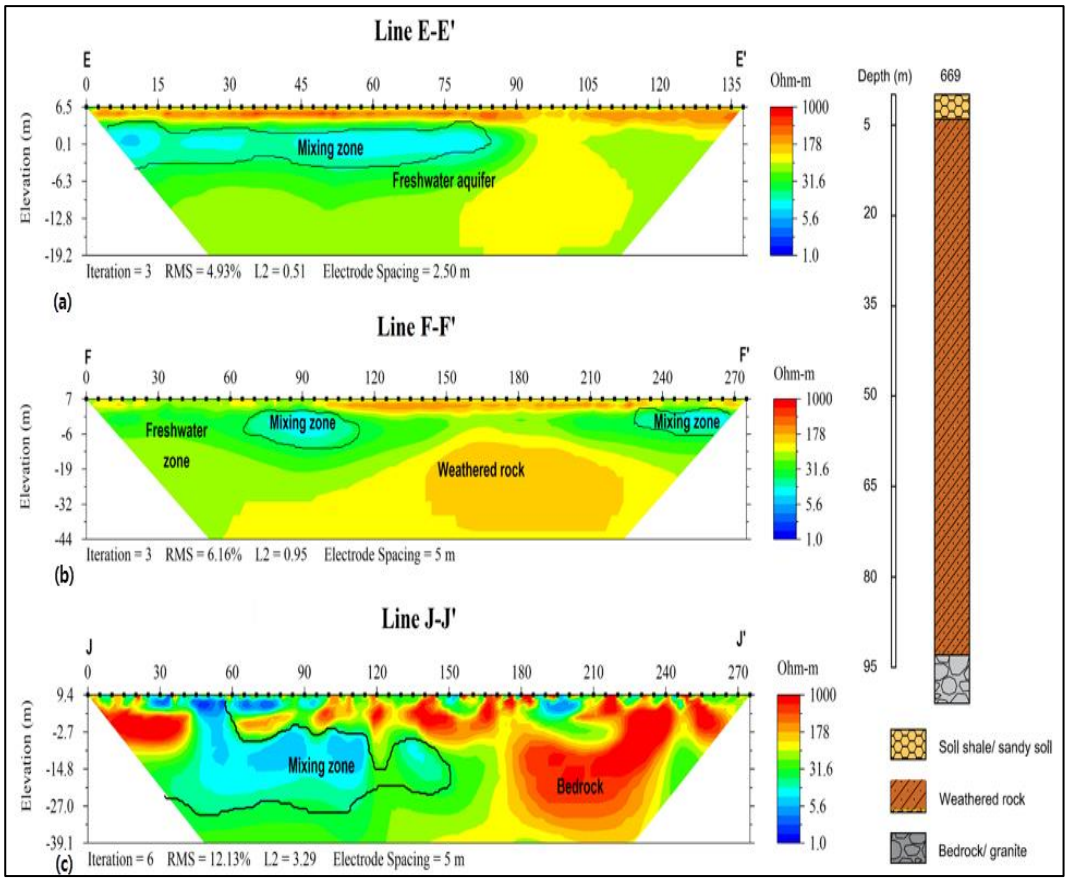

Figure 4.10 2D Inverted Resistivity (a) Line E-E', (b) Line F-F' and (c) Line J-J'

4.2.5 2D ERI of Rawai

Similar to the subsurface layer of Chalong sub-districts, the lithology of Rawai sub-district (Figure 4.12) is naturally categorized to three layers: topsoil/shale soil/ sandy soil (the top layer with the depth up to 15 m below the surface), weathered or fractured rock (the second layer with the depth ranging from 15 m to nearly 65 m) and bedrock or granite layer (the third layer with the depth more than 55 m below the soil surface). However, according to Line G-G', as shown in Figure 4.13, the bedrock zone (indicated in dark red colour) which has high resistivity value can be found in

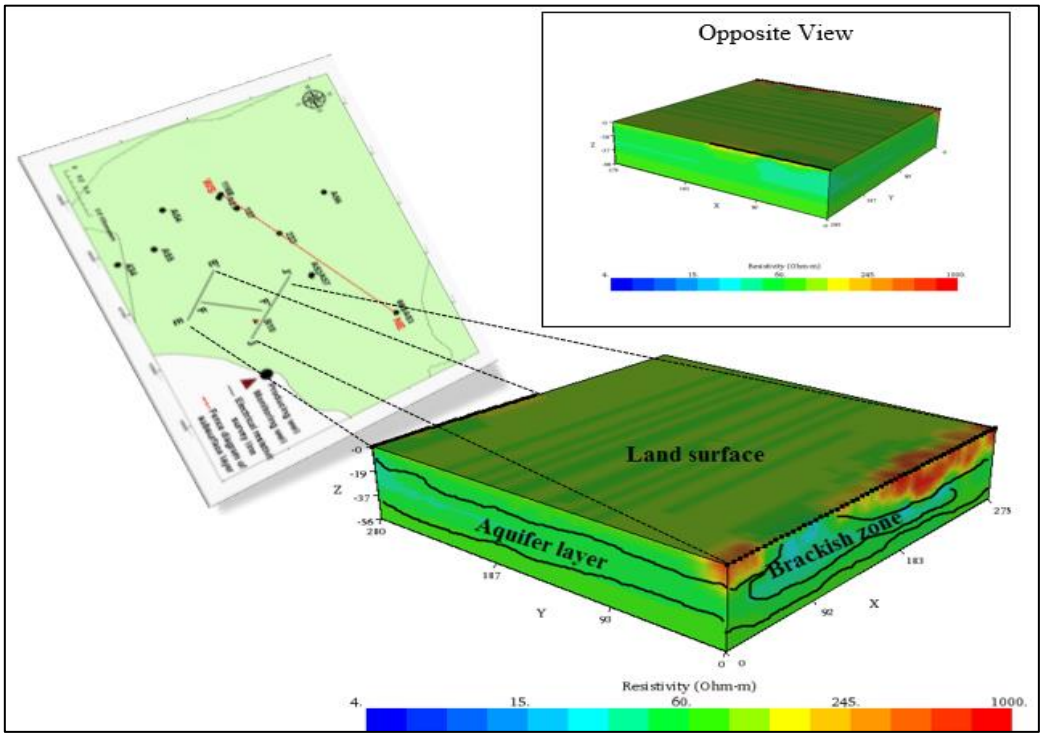

Figure 4.11 3D Inverted Resistivity Integrating Line E-E' and Line J-J'

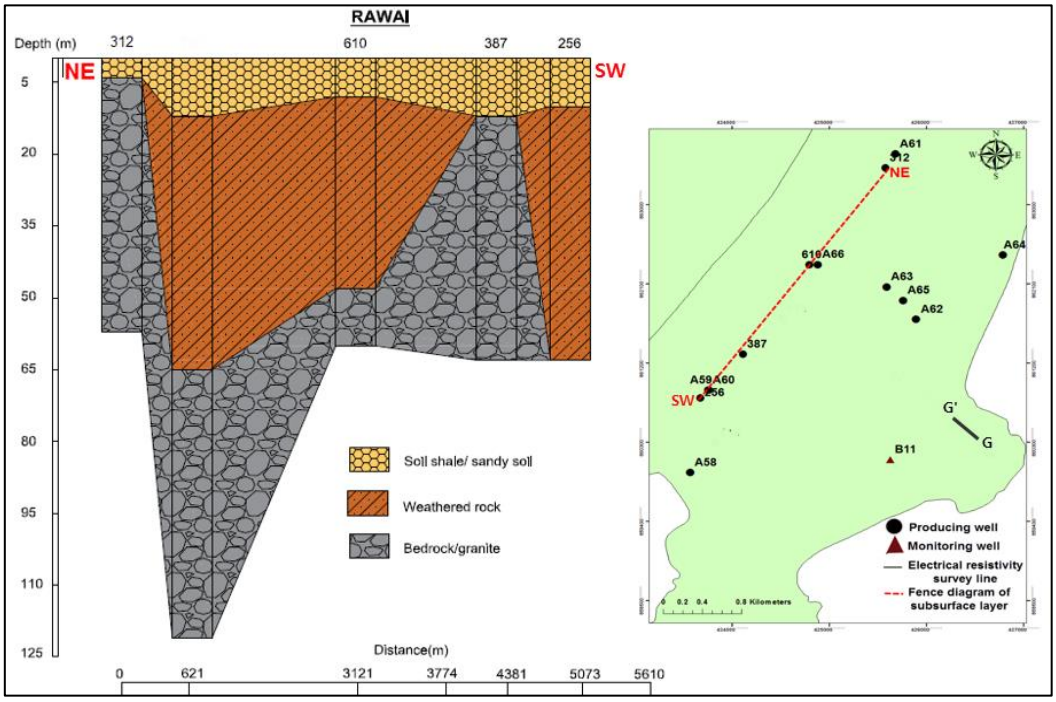

Figure 4.12 Fence Diagram of Subsurface Layer In Rawai Sub-District.

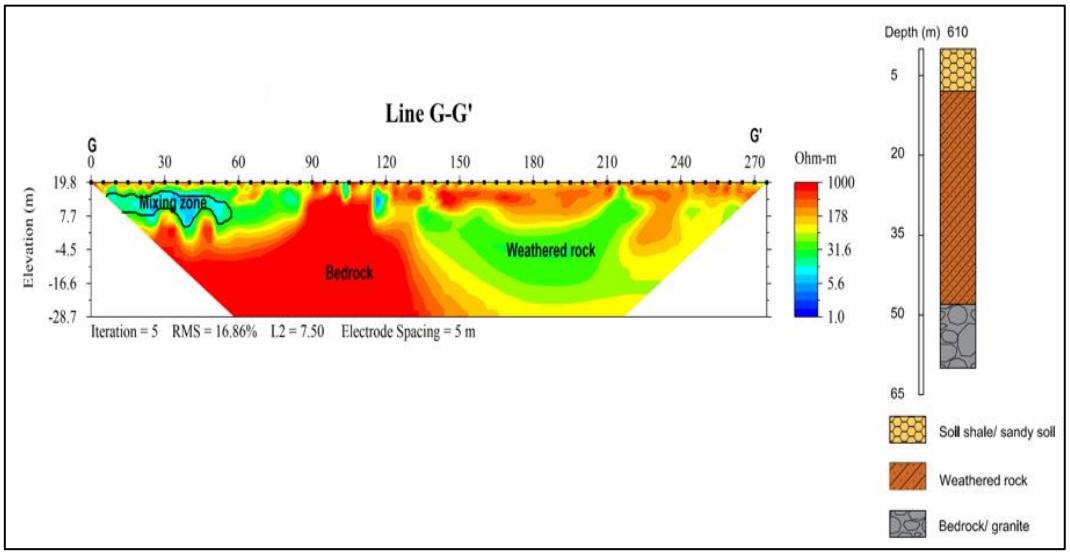

Figure 4.13 2D Inverted Resistivity of Line G-G'

the range of 3 m to deeper than 28 m which seem to be a contrary reference to the subsurface layer as mentioned above. In fact, this appearance is likely to be an outcrop of that area which locates around 450 m from the sea. Moreover, the light blue (5 – 15 Ohm-m) which is projected to be mixing zone can be seen in the shallow depth (5 to 10 m).

4.2.6 2D ERI of Mai Khao

The subsurface layer of Mai Khao sub-district as shown in Figure 4.14 is naturally divided into 4 layers: topsoil/shale soil/ sandy soil (the depth up to 20 m below the ground surface), clay layer (the depth ranging from 5 m to around 20 m), weathered or fractured rock (the depth ranging from 10 m to just under 70 m) and bedrock or granite layer (the depth ranging 30 m to around 90 m below the soil surface). Line H-H' (Figure 4.15a) is located approximately 30 m to the north of the beach and perpendicular to it. This profile can get the data in depth of penetration around 51 m below subsurface (6 m abms) and 275 m in total length. Based on this profile, it can be seen that the saline water zone (dark blue colour) is very thick around 30 m in thickness and underlain by brackish zone (moderate blue colour) which have the resistivity value in the range from approximately 6 to 15 Ohm-m. Freshwater zone in this line is very thin above the saline zone. Line I-I' (275 m in total length and around 50 m in the penetration depth), as shown in Figure 4.14b, is situated to the east of Line H-H' and is

perpendicular to it. The subsurface result indicates that the thick plume of seawater intrusion can be seen in the depth 3 m with the resistivity around 3 Ohm-m to 10 Ohm-m which is connected by brackish water zone.

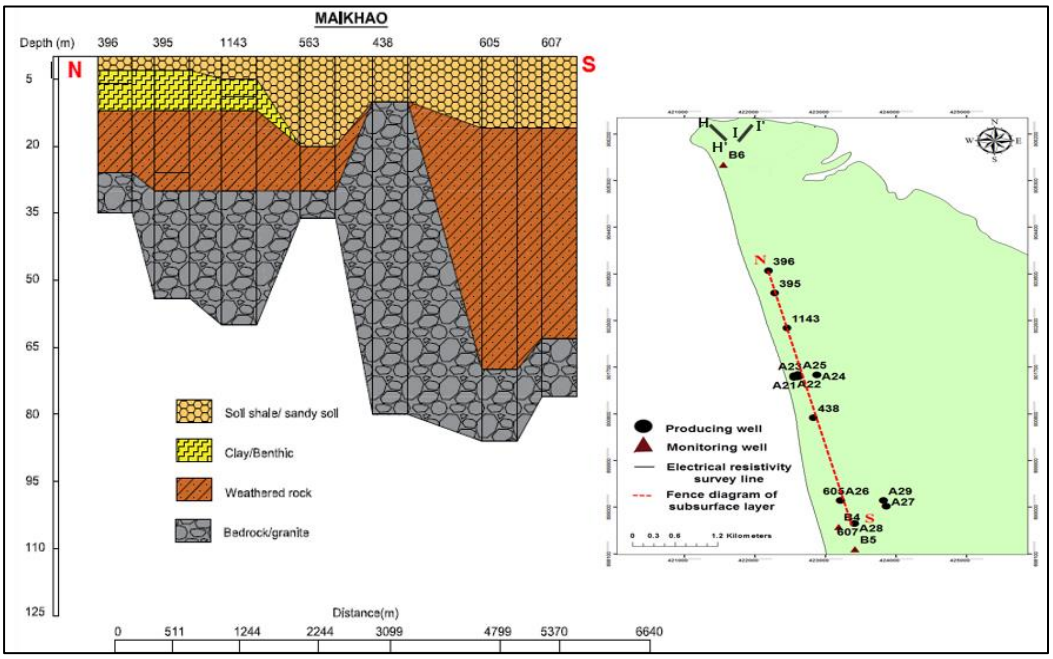

Figure 4.14 Fence Diagram of Subsurface Layer in Mai Khao sub-district.

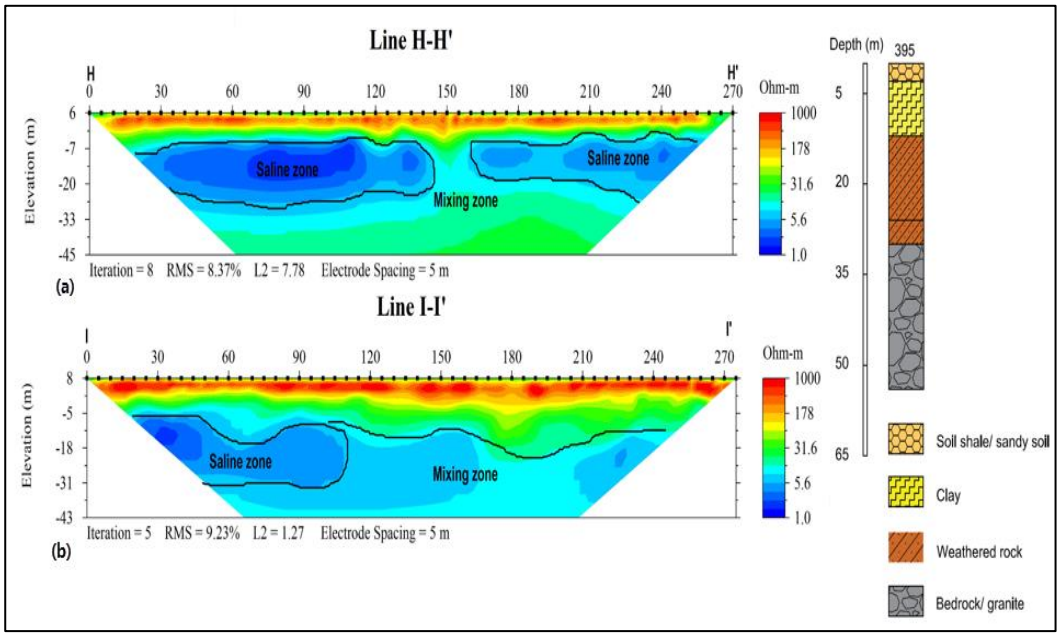

Figure 4.15 2D Inverted Resistivity (a) Line H-H’ and (b) Line I-I’

4.3 Resistivity Validation

4.3.1 A Relationship between resistivity (ρ) and groundwater salinities

Data cross-plot in logarithm scale showing the correlations between resistivity value and groundwater salinity (Cl and TDS) are a clear correlative similarity between the high amounts of Cl^- and TDS and a low electrical resistivity at similar depths. Therefore, the inverse relationship between electrical resistivity and metal content is qualitatively illustrated by cross-plots in Figure. 4.16a and 4.16b. Moreover, the high correlation of TDS and Cl with soil resistivity is indicated by a correlation coefficient (R) of 0.8 and 0.9 respectively, thus the empirical model with a determination coefficient (R^2) of 0.7 and 0.8 between resistivity and TDS and Cl^- concentration in this study area are established as shown in Eq. 4.2 and Eq 4.3 respectively. The Cl concentration and TDS concentration increases with the decreasing resistivity (ρ) based on exponential function as follows.

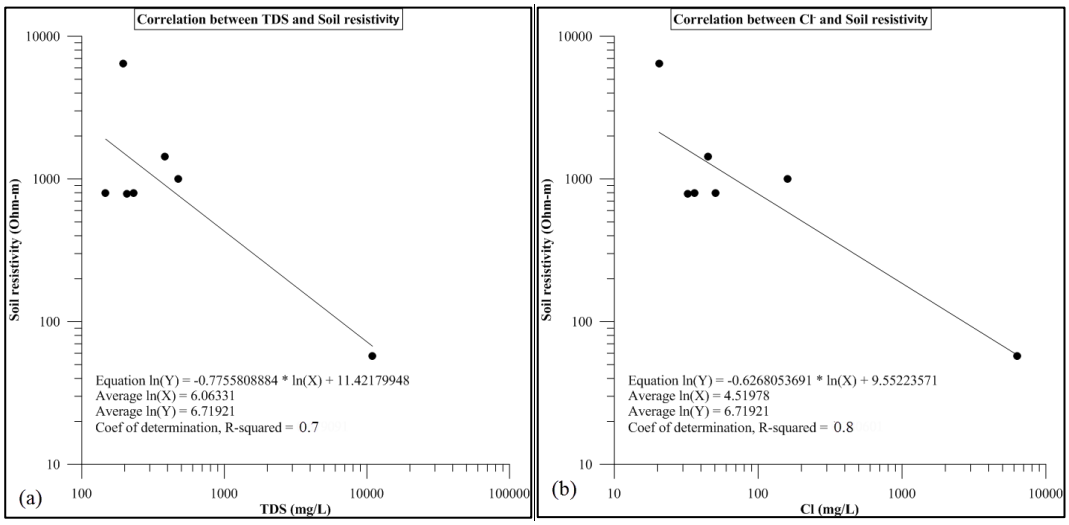

Figure 4.16 Correlation between Soil Resistivity with (a) TDS and (b) Cl^-

$$\ln(\rho) = -0.77 \times ln(TDS) + 11.42 \quad (4.2)$$

$$\ln(\rho) = -0.62 \times ln(Cl) + 9.55 \quad (4.3)$$

4.3.2 Laboratory Testing of Proportional Seawater and Soil Resistivity (ρ)

The resistivity value of initial moisture sand (condition before adding seawater and distilled water) is around 216 Ohm-m as shown in Table 4.1. According

to the result, as shown in Table 4.2, the resistivity decreases with increasing the quantity of seawater in wet sand. It is clear from the graph, as shown in Figure 4.17, that resistivity value of sand saturated with 100% of seawater is just under 4 Ωm, compared to approximately 150 Ohm-m of sand saturated with 0% of seawater.

Table 4.1 Resistance and Resistivity Value of Initial Condition of Sand Sample

Moisture Sand Sample	R (Ohm)	ρ (Ohm-m)
Initial condition	3266.26	216.21
Initial condition	3270.42	216.47
Initial condition	3269.18	216.41
Average	***3268.88***	***216.36***

Table 4.2 Resistance and Resistivity Value of Sand Sample saturated with a solution of Distill water and Seawater

Seawater Concentration (mg/L)	R (Ohm)	ρ (Ohm-m)
100%	55.48	3.67
100%	55.35	3.66
100%	55.55	3.68
Average	***55.46***	***3.67***
75%	75.84	5.02
75%	76.22	5.05
75%	76.44	5.06
Average	***76.17***	***5.04***
50%	100.00	6.62
50%	100.50	6.65
50%	101.30	6.71
Average	***100.60***	***6.66***
40%	148.30	9.82
40%	148.90	9.86
40%	149.00	9.86
Average	***148.73***	***9.85***

Table 4.2 Resistance and Resistivity Value of Sand Sample saturated with a solution of Distill water and Seawater (cont.)

Seawater Concentration (mg/L)	R (Ohm)	ρ (Ohm-m)
20%	390.00	25.82
20%	391.20	25.90
20%	392.10	25.96
Average	***391.10***	***25.89***
10%	642.40	42.53
10%	626.70	41.49
10%	625.80	41.43
Average	***631.63***	***41.81***
8%	746.20	49.40
8%	751.80	49.77
8%	760.00	50.31
Average	***752.67***	***49.83***
6%	828.80	54.87
6%	832.00	55.08
6%	836.00	55.34
Average	***832.27***	***55.10***
4%	1086.00	71.89
4%	1089.00	72.09
4%	1094.00	72.42
Average	1089.67	72.14

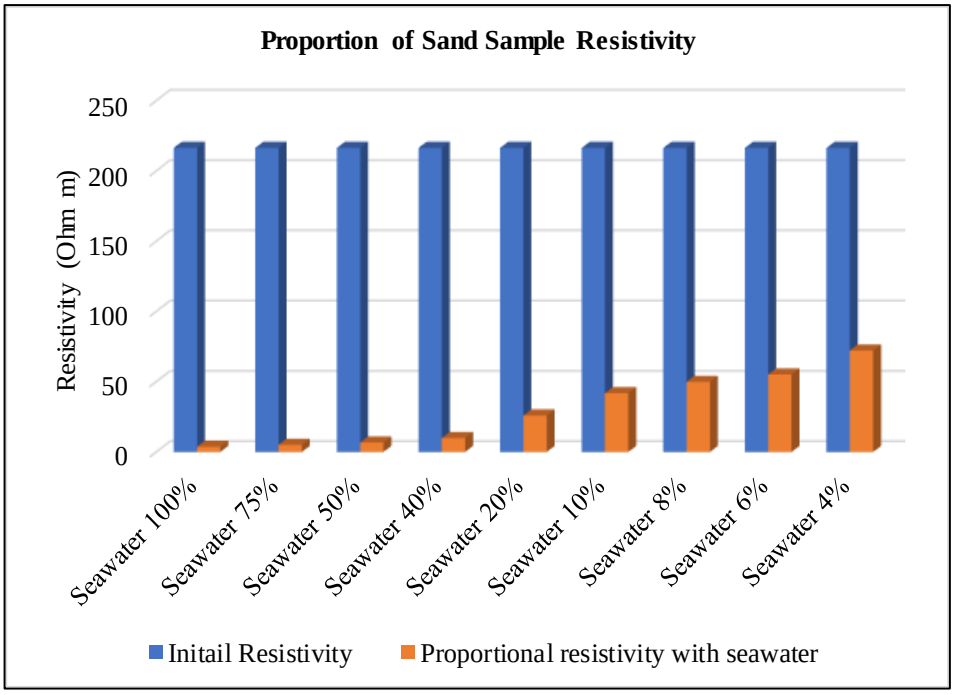

Figure 4.17 Proportion of Sand Sample Resistivity.

4.3.3 Relationship between seawater and water resistivity

The laboratory test of the changing resistivity with seawater shows that the water resistivity is decreased by the proportions of the seawater. A trend of changing water resistivity was dropped sharply in small amounts of seawater (5% – 10%), then the water resistivity was slightly decreased with increments of seawater proportion (15% - 100%) as shown in Figure 4.18. The initial resistivity (tap water) of 58 Ohm-m (resistivity of freshwater is about 50-100 Ohm-m) was reduced to 1.07 Ohm-m with the seawater proportion of 100.

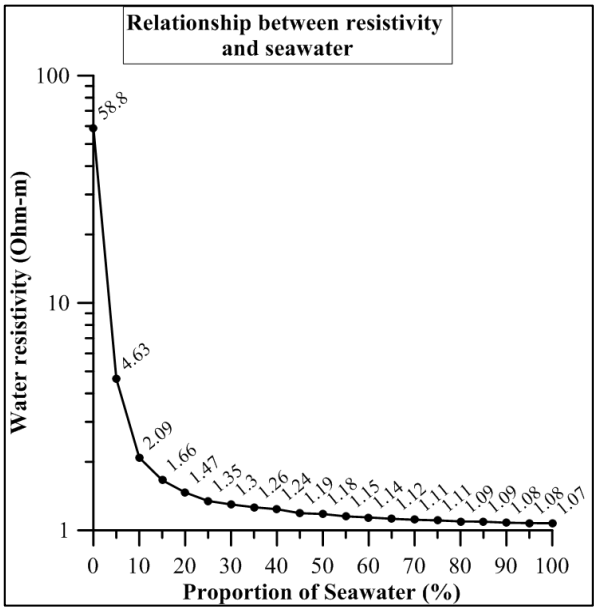

Figure 4.18 Relationship between resistivity and seawater.

CHAPTER 5

DISCUSSION AND CONCLUSIONS

5.1 Assessment of Phuket Seawater Intrusion

Phuket Island has a high risk of seawater intrusion due to the surrounding Andaman Sea with saline water, the increased groundwater exploitation, and the sea level rise. The current study sought to assess the seawater intrusion situation in that potentially high-risk area. TDS and Cl concentration can be used as the two main indicators in an analysis of seawater intrusion risks. When these indicators are concordant with high correlation and exceed some threshold levels (here 500 and 1,000 mg/L for Cl concentration and TDS, respectively), the groundwater has been intruded. It is commonly known that the trends of groundwater salinities (Cl concentration and TDS) are opposite to those of the groundwater level, i.e., when groundwater level drops, the seawater will intrude into the fresh water resulting in the salinity increase. However, the seawater intrusion can act as natural recharge in the coastal area, the groundwater level in coastal zones might be increased due to seawater intrusion. In addition, the groundwater level trend was used to confirm the seawater intrusion, by its level increasing while TDS and Cl concentration increased. An assessment map of seawater intrusion on Phuket Island was created by GIS techniques. The areas with the highest risk of seawater intrusion on Phuket is the coastal areas of Mai-Khao sub-district (northern part of Phuket), while Kamala (western part of Phuket), Rawai and Chalong sub-districts (southern part of Phuket) which are attractive beaches, are risked to be moderate seawater problems. However, the eastern part of Phuket has not been done the data analysis because no monitoring wells have been installed in those areas. According to the trend of historical Cl and TDS concentration data (unpublished producing wells during 1998- 2009) in Pa Khlok and Ratsada sub-district as shown in Figure 5.1a and Figure 5.1b respectively, it can be concluded that the risk of seawater intrusion in the eastern part is likely to be very low. Because the eastern part is encountering the low risk of seawater intrusion compared to western and northern part, the government has not taken into account to install the monitoring wells.

5.2 Delineation of Seawater Intrusion Using Electrical Resistivity Method in the Coastal Aquifer of Phuket Island, Thailand

Seawater intrusion in the western part of Phuket, Kamala sub-district, can be seen to intrude in the freshwater aquifer in both top layer (clayey sand) and a second layer (weathered and fractured rock layer) with the expansion approximately

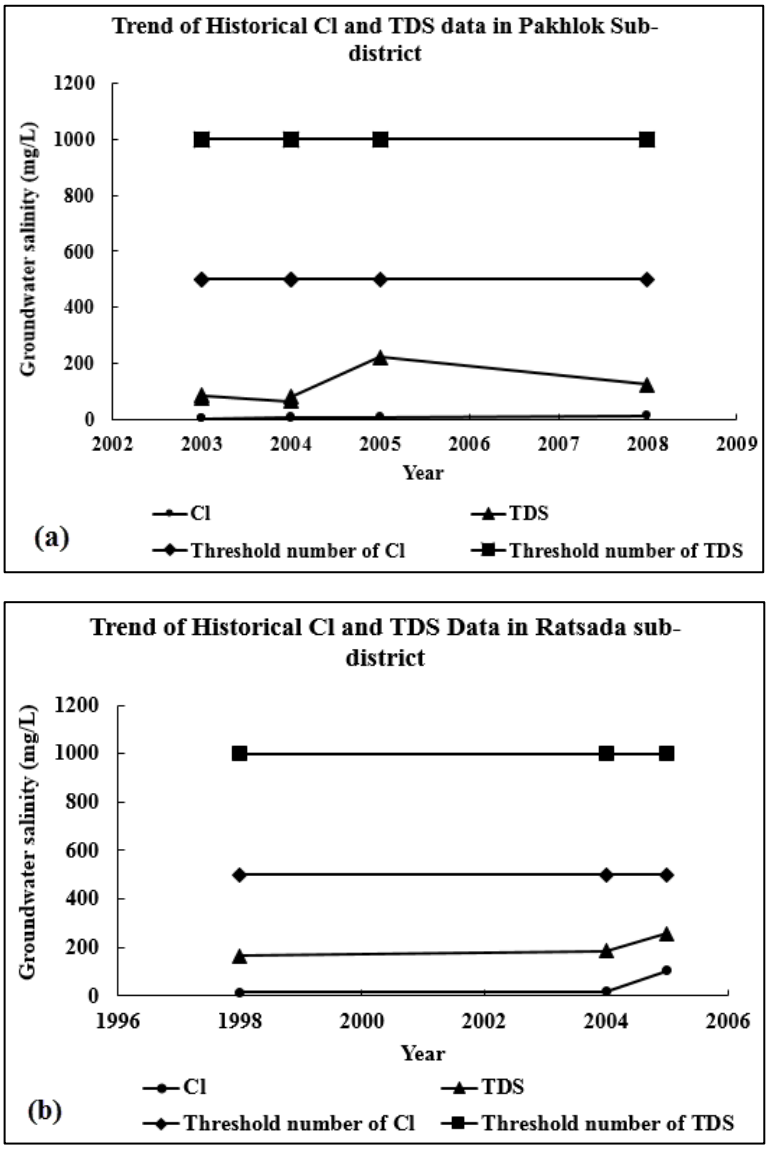

Figure 5.1 Trend of Historical Cl and TDS data in (a) Paklok sub-district and (b) Ratsada sub-district.

400 m inland and in the depth around 4 m below land surface. Like Kamala, Chalong sub-district, seawater intrudes in the freshwater aquifer in the clayey sand and

weathered rock layer with the expansion approximately 150 m inland and in the depth around 3 m above below the land surface. In terms of Rawai, bedrock zone has been found in the shallow depth around 3 m above mean sea level and the saline zone has been found near the bedrock zone in shallow depth as well. Regarding Mai Khao, the area which is located about 500 m from the beach is completely covered by seawater intrusion. An integration between geo-electrical surveys (electrical resistivity imaging and vertical electric sounding methods) and groundwater chemistry data has proved to be an effective tool for delineating the spatial extent and interface between freshwater and seawater of seawater intrusion. The resistivity represents a feasible and an efficient parameter for quantitative and qualitative studies with respect to seawater intrusion problem in a coastal aquifer. The inversion model for both 2D and 3D show the usefulness of seawater intrusion in the freshwater aquifer. Based on the cross-plot between salinity indicators (Cl^- and TDS) and apparent earth resistivity, the earth resistivity value decreases in the area that has a high rate of Cl^- and TDS while the high value of resistivity can be seen in the area having a low rate of Cl^- and TDS. An empirical relationship between the resistivity and groundwater chemistry (TDS and Cl concentrations) in Kamala was obtained by cross-plot of seawater indicators (Cl- and TDS) and apparent resistivity. This empirical model can be used to estimate the fresh, brackish, and saline zone of seawater intrusion problem in the other parts of Phuket Island using ERI method. This study will be worthwhile for further research in this study area to study a modelling of seawater intrusion in order to determine and predict the effects of different pumping scenarios. Finally, this research findings can help to know the capability of the aquifer as the warning threshold level of groundwater exploitation at a time for sustainability.

5.3 Further Research

Seawater intrusion in coastal aquifers has been indicated to be mainly affected by the spatial variability of hydraulic properties in geological formations. Hence, the heterogeneity optimization should be selected to solve density-dependent flow or seawater intrusion modelling processes. Because seawater intrusion is a relatively complex and nonlinear process, coastal aquifer management should be done

carefully with the planning of withdrawal strategies to successfully control seawater intrusion. Therefore, prediction and control future seawater intrusion in a coastal aquifer might be effectively done by mathematical model simulation called SEAWAT program (Nofal *et al*., 2015). The SEAWAT program was originally developed to simulate three-dimensional variable-density, transient ground-water flow in porous media by Guo and Bennett (1998). The source code for SEAWAT was developed by combining MODFLOW and MT3DMS into a single program that solves the coupled flow and solute-transport equations.

REFERENCES

Advanced Geosciences, Inc. (2014). Instruction manual for Earthimager2D version 2.4.2 Resistivity and IP inversion software. 2121 Geoscience Drive, Austin, Texas 78726.

Advanced Geosciences, Inc. (2014). Instruction manual for Earthimager3D version 1.5.3 Resistivityinversion software. 2121 Geoscience Drive, Austin, Texas 78726.

Afshar, A., Abedi, M., Norouzi, G. H., and Riahi, M. A. (2015). Geophysical Investigation of Underground Water Content Zones Using Electrical Resistivity Tomography and Ground Penetrating Radar: A Case Study in Hesarak-Karaj, Iran. Engineering Geology, 196, 183-193.

Ataie-Ashtiani, B., Volker, R. E. E. and Lockington, D. A. a. (1999). Tidal Effects on Sea Water Intrusion in Unconfined Aquifers. Journal of Hydrology, 216, 17–31.

Calvache, M. L. and Pulido-Bosch, A. (1997). Effects of Geology and Human Activity On the Dynamics of Salt-water Intrusion in Three Coastal Aquifers in Southern Spain. Environmental Geology, 30(3–4), 215–223.

Chafouq, D., Mandour, A. E., Elgettafi, M., Himi, M., Bengamra, S., Lagfid, Y. and Casas, A. (2016). Assessing of Saltwater Intrusion in Ghiz-Nekor Aquifer (North Morocco) Using Electrical Resistivity Tomography. Near Surface Geoscience, 1-6.
DOI: 10.3997/2214-4609.201602066

Chang, S. W., Clement, T. P., Simpson, M. J. and Lee, K. K. (2011). Does Sea-level Rise Have An Impact on Saltwater Intrusion? Advances in Water Resources, 34(10), 1283–1291.

Chen, K. P. and Jiao, J. J. (2007). Seawater Intrusion and Aquifer Freshening Near Reclaimed Coastal Area of Shenzhen. Water Science and Technology: Water Supply, 7(2), 137–145.

Chenini, I., Mammou, A. B. and May, M. Y. (2010). Groundwater Recharge Zone

Mapping Using GIS-based Multi-criteria Analysis: A Case Study in Central Tunisia (Maknassy Basin). Water Resour Manag, 24, 921– 939. Doi:10.1007/s11269-009-9479-1

Cimino, A., Cosentino, C., Oieni, A. and Tranchina, I. (2008). A geophysical and geochemical approach for seawater intrusion assessment in the Acquedolci coastal aquifer (Northern Sicily). Environ Geol, 55, 1473-1482. DOI 10.1007/s00254-007-1097-8

Department of Groundwater Resources (DGR). (2010). Completed Report: Groundwater Well Observation, Study of Specific Network Groundwater Well, and Groundwater Consumption Evaluation for Groundwater Management. D.M. Printing Co., LTD, Bangkok

Department of Groundwater Resources (DGR). (2012). Final Report: Groundwater Conservation and Recovery from Summer Flooding in Southern Thailand. Groundwater Conservation and Recovery Institution, Bangkok

Department of Mineral Resources (DMR). (2013). Geological and Geo-resources Classification for Management in Phuket. Onpa Co., LTD., Bangkok.

DGR (Department of Groundwater Resource). (2015).Annual Report: Thailand Groundwater Situation in 2015., Groundwater Conservation and Recovery Institution, Bangkok.

Eissa, M. S., Mahmoud, H. H. and Orfan, S. S. (2016). Geophysical and Geochemical Studies to Delineate Seawater Intrusion in Bagoush Area, Northwestern coast, Egypt. Journal of African Earth Science, 121, 365-381.

Giambastiani, B. M. S., Antonellini, M., Oude Essink, G. H. P. and Stuurman, R. J. (2007). Saltwater Intrusion in the Unconfined Coastal Aquifer of Ravenna (Italy): A Numerical Model. Journal of Hydrology, 340(1–2), 91–104.

Hazreek, Z. A. M., Rosli, S., Chitral, W. D., Fauziah, A., Azhar, A. T. S., Aziman, M. and Ismail, B. (2015). Soil Identification using Field Electrical Resistivity Method. Journal of Physics: Conference Series, 622(October).

Hazreek, Z. A. M., Nizam, Z. M., Azhar, A. T. S., Aziman, M. and Shaylinda, M. Z. N. (2016). Physical Modelling on Detecting Buried Object Using Electrical Resistivity Imaging (ERI). IOP Conference Series: Materials Science and Engineering, 136(1).

Healey, R. G. (1991). Database Management Systems. In: Maguire D J, Goodchild M F, Rhind D W (eds.) Geographical Information Systems: principles and applications. Longman, London, 1, 251-267

Hwang, S., Shin, J., Park, I. and Lee, S. (2004). Assessment of Seawater Intrusion Using Geophysical Well Logging and Electrical Soundings in a Coastal Aquifer, Youngkwang-gun, Korea. Exploration Geophysics, 35, 99-104.

Irénée, K., Théophile, M., Dieu, N. J. De, Placide, U. and Jeanne, M. (2016). An Integrated Study on Seawater Intrusion Using Geoelectrical Resistivity and GIS Techniques in Part of Pondicherry, South-East Coast of India An Integrated Study on Seawater Intrusion Using Geoelectrical Resistivity and GIS Techniques in Part of Pondich. International Journal of Innovative Research in Science,5, 1-9

Institute for Social and Environmental Transition-International (ISET), Thailand Environmental Institute (TEI), Vietnam National Institute for Science and Technology Policy and Strategy Studies (VNISTPSS). (2014). Urban Vulnerability in Southeast Asia: Summary of Vulnerability Assessments in Mekong-Building Climate Resillience in Asian Cities (M-BRACE). Bangkok. Thailand. Institute for Social and Environmental Transition-international, 1-58.

Institute for Social and Environmental Transition-International (ISET), Thailand Environmental Institute (TEI), Vietnam National Institute for Science and Technology Policy and Strategy Studies (VNISTPSS). (2013). Urban Vulnerability in Southeast Asia: Summary of Vulnerability Assessments in Mekong-Building Climate Resilience in Asian Cities (M-BRACE). Bangkok. Thailand. Institute for Social and Environmental Transition-international, 1-98

Jatau, B. S., Patrick, N. O. and Baba, A. (2013). The Use of Vertical Electrical Sounding (VES) for Subsurface Geophysical Investigation around Bomo Area, Kaduna State, Nigeria. IOSR Journal of Engineering (IOSRJEN), 3(1), 10–15. www.iosrjen.org

Kearey, P., Brooks, M. and Hill, I. (2002). An Introduction to Geophysical Exploration. Blackshell Science, 183-207.

Kong, S.O. (2017). Hydrogeological Characterization and Groundwater Analysis with Reference to (urban, tourists, and economic) Development of Phuket areas,

Thailand. Unpublished master's thesis, Prince of Songkla University (PSU), Phuket Campus, Phuket.

Kura, N. U., Ramli, M. F., Ibrahim, S., Sulaiman, W. N. A., Zaudi, M. A., and Aris, A. Z. (2014). A Preliminary Appraisal of the Effect of Pumping on Seawater Intrusion and Upconing in a Small Tropical Island Using 2D Resistivity Technique. The Scientific World Journal, 2014, 1-12.

Mahesha, A. (1996). Effect of Natural Recharge on Sea Water Intrusion in Coastal Aquifers. Journal of Hydrology, 174, 211–220.

Malczewski, J. 2004. GIS-based land-use suitability analysis: a critical overview. Progress in Planning 62: 3–65.

Martínez, J., Benavente, J., García-Aróstegui, J. L., Hidalgo, M. C. and Rey, J. (2009). Contribution of Electrical Resistivity Tomography to the Study of Detrital Aquifers Affected by Seawater Intrusion-extrusion Effects: The River Vélez Delta (Vélez-Málaga, southern Spain). Engineering Geology, 108(3–4), 161–168.

Maury, S. and Balaji, S.; Application of resistivity and GPR techniques for the characterization of the coastal litho-stratigraphy and aquifer vulnerability due to seawater intrusion. Estuarine, Coastal and Shelf Science.; 2015, 165, 104- 116.

Millett, N. G. and Evans, S. (2009). Hydrographic Data Management using GIS Technologies. Environmental Systems Research Institute, Inc., 380 New York St., Redlands, CA 92373-8100

Nagarajan, M. and Singh, S. (2009). Assessment of Groundwater Potential Zones using GIS Technique. J. Indian Soc. Remote Sens, 37, 69-77

NOAA, (2016). Andaman Sea level rising during 1992 – 2016. Available online, https://www.star.nesdis.noaa.gov/sod/lsa/SeaLevelRise/LSA_SLR_timeseries_regional.php

Park, S., Yi, M. J., Kim, J. H. and Shin, S. W. (2016). Electrical Resistivity Imaging (ERI) Monitoring for Groundwater Contamination in An Uncontrolled Landfill, South Korea. Journal of Applied Geophysics, 135, 1-7.

Qahman, K. A. and Zhou, Y. (2001). Monitoring of Seawater Intrusion in the Gaza Strip, Palestine. First International Conference on Saltwater Intrusion and Coastal Aquifers: Monitoring, Modeling, and Management,1-23.

Saowanee, C., Chanida, S. and Pun, T. Impacts of Interpolation Techniques on Groundwater Potential Modeling Using GIS in Phuket Province, Thailand. The 33th Asian Conference on Remote Sensing, 1-7.

Shammas, M. I. and Jacks, G. (2007). Seawater Intrusion in the Salalah Plain Aquifer, Oman. Environmental Geology, 53(3), 575–587.

Sherif, M., Kacimov, A., Javadi, A. and Ebraheem, A. A. (2012). Modelling Groundwater Flow and Seawater Intrusion in the Coastal Aquifer of Wadi Ham, UAE. Water Resources Management, 26(3), 751–774.

Sherif, M., Mahmoudi, a. El, Garamoon, H., Kacimov, A., Akram, S., Ebraheem, A. and Shetty, A. (2006). Geoelectrical and Hydrogeochemical Studies for Delineating Seawater Intrusion in the Outlet of Wadi Ham, UAE. Environmental Geology, 49(4), 536–551.

Sivan, O., Yechieli, Y., Herut, B. and Lazar, B. (2005). Geochemical Evolution and Timescale of Seawater Intrusion into the Coastal Aquifer of Israel. Geochimica et Cosmochimica Acta, 69(3), 579–592.

Song, S. H., Lee, J. Y. and Park, N. (2007). Use of Vertical Electrical Soundings to Delineate Seawater Intrusion In a Coastal Area of Byunsan, Korea. Environmental Geology, 52(6), 1207–1219.

Steele, R., Thongkraung, L., Panton, Sean., Anthony, N., Homcha-aim, K., Mather, R. and Vorratnchaiphan, C. (2013). Phuket Sustainability Indicator Report. Society Environmental Economy Knowledge (SEEK Phuket), 8-36

U.S.Geological Survey. (2000). Atlantic Coastal Zone. U.S. Department of the Interior, 1-4

Vafidis, A., Soupios, P., Economou, N., Hamdan, H., Andronikidis, N. and Kritikakis, G. (2014). Seawater Intrusion Imaging at Tybaki, Crete, Using Geophysical Data and Joint Inversion of Electrical and Seismic Data. European Association of Geoscientists and Engineers, 32, 1-9.
www.firstbreak.org

Werner, A. D., Bakker, M., Post, V. E. A., Vandenbohede, A., Lu, C., Ataie-Ashtiani, B. and Barry, D. A. (2013). Seawater Intrusion Processes, Investigation and Management: Recent advances and Future Challenges. Advances in Water Resources, 51, 3–26.

Werner, A. D. and Simmons, C. T. (2009). Impact of Sea-level Rise on Sea Water Intrusion in Coastal Aquifers. Ground Water, 47(2), 197–204.

WEPA, (2018). Drinking Water Quality Standard in Thailand. Available online, http://www.wepa-db.net/policies/law/thailand/std_drinking.htm

Zhou, X., Chen, M. and Liang, C. (2003). Optimal Schemes of Groundwater Exploitation for Prevention of Seawater Intrusion in the Leizhou Peninsula in Southern China. Environmental Geology, 43(8), 978–985.

VITAE

Name Sakanann VANN

Student ID 5930421003

Educational Attainment

Degree	Name of Institute	Year of Graduation
Master of Science (Earth System Science)	Prince of Songkla University Phuket Campus	2017

Scholarship and Awards during Enrolment

Apr 25, 2018: "The First Runner-up" in Research Poster Presentation Award 2018 in Prince of Songkla University (PSU) Phuket

Research Poster Title: *"Assessment of Seawater Intrusion Using Electrical Resistivity Method in a Coastal Aquifer of Western part of Phuket Island, Thailand"*

Apr 25, 2018: "The First Runner-up" in 3 Minute Thesis (3MT) Award 2018 in Prince of Songkla University, Phuket Campus, Thailand.

Title of 3MT Presentation: *"Preliminary Assessment of Seawater Intrusion in Coastal Area of Phuket Island, Thailand"*

Apr 26, 2017: "The First Prize Winner" of Prince of Songkla University (PSU) Phuket Best Research Poster Presentation Award 2017

Research Poster Title: *"Evaluation of Risky Area on Seawater Intrusion in Phuket Island using Groundwater Data Analysis"*

Dec 20, 2015: Thai Royal Scholarship under Her Royal Highness Princess Maha Chakri Sirindhorn Education Project to the Kingdom of Cambodia to pursue Master program at Prince of Songkla University (PSU)

VITAE (cont.)

List of Publication and Proceeding

Puttiwongrak, A., **Sakanann, V**. (2018). Delineation of Seawater Intrusion Using 2D and 3D Electrical Resistivity Imaging in a Coastal Aquifer of Kamala Beach, Phuket, Thailand. Frontier of Environmental Science & Engineering, Submitted: September 29, 2018.

Puttiwongrak, A., Suteerasak, T., Mai, K.P., Tesfaldet, Y.T., Ratha, M., Htwe, N.N., **Sakanann, V.**, Gonzalez, J.C., Rattanakom, R., and Prueksakorn, K. (2018). Application of Multi-Monitoring Methods to Investigate the Contamination Levels and Dispersion of Heavy Metals from Tin Mining in Coastal Sediments at Saphan Hin, Phuket, Thailand. Journal of Clean Production, Submitted: April 30, 2018.

Puttiwongrak, A. and **Sakanann, V.** (2018). Preliminary Assessment of Seawater Intrusion in Phuket Island using Groundwater Data Analysis and GIS Techniques, GMSARN International Journal. Submitted: January 15, 2018.

Puttiwongrak, A.; Samol, K.; and **Sakanann, V**. (2018). Groundwater recharge estimation in Kathu, Phuket using groundwater modelling. Geotechnical Engineering Journal of SEAGS and AGSSEA, In press.

Puttiwongrak, A. and **Sakanann, V. (2018).** Using 2D & 3D Electrical Resistivity Imaging for Spatial Extent of Seawater Intrusion in Phuket Island, Thailand. Proceeding of the Vietnam International Water Week - VACI2018, 4-8 March 2018, Hanoi, Vietnam.

Puttiwongrak, A., and **Sakanann, V. (2017).** "Preliminary Assessment of Seawater Intrusion on Phuket Island using Groundwater Data Analysis and Geographic Information System (GIS) Techniques." Proceeding of GMSARN Int. Conf. on Energy Connectivity, Environment, and Development in GMS, Da-Nang City, Vietnam: 28-30 November 2017.

Puttiwongrak, A., Giao, P.H., Sam Ol, K., and **Sakanann, V.** (2017). "Hydrogeological Characterization and Groundwater Analysis with Reference to Development of Kathu, Phuket Island, Thailand." Proceeding of 2017 International Conference on 5th ASIA-PACIFIC COASTAL AQUIFER MANAGEMENT MEETING, University of Da Nang, Da Nang city in Vietnam: 17-19 July 2017.

Puttiwongrak, A., Sam Ol, K., Rattanakom, R., and **Sakanann, V.** (2017). "Groundwater Modelling of Natural Recharge Estimation in Phuket Island, Thailand." Proceeding of 2017 International Conference on International Symposium on Flood Pulse Ecosystem (ISFE 2017), HOTEL SOMADEVI ANGKOR RESORT & SPA in Siem Reap, Cambodia: 24-27 July 2017.